Appendix A

UT inspection of tanker J3857

T.T.S.

Topping Test Services Ltd.

Report: **Ultrasonic Inspection of Welding on 10-Banded Fuel Tanker.**

Prepared by: H.Topping MinstNDT.

Issued by: T.T.S. Ltd.
84 Aldreth Road
Haddenham
Ely
Cambs
CB6 3PN

Prepared for: TWI Limited,
Granta Park,
Gt Abington,
Cambs
CB1 6AL

FAO: Mr. Alan Day.

Date: 24th April 2014

Report No: 14/1946/TTS

Introduction:

Our inspector visited the Pullman Fleet Services depot at West -Thurrock on the 24th April 2014.
The purpose of the visit was to conduct ultrasonic inspections of the internal fillet welds between adjoining sections of a 10-banded fuel tanker.
The objective of the inspections was to provide information of the fillet weld geometry and location in order that strain gauges could be attached at specific locations throughout the tanker structure.
Please refer to the appended ultrasonic inspection report and photographs for full details of the inspection results:

Inspections:

The tanker was identified as a 45000 litre capacity aluminium shell fuel tanker, manufactured in South Africa by GRW Engineering on 26-10-2010.
VIN No. AC 9433AA60CCU1857.

All 10 seams were ultrasonically inspected and identified as M-10 A/10 to M-1 MJ/10 as per the tanker band naming convention – (copy appended).

Results:

It was noted that bands C, D, E, F & G were continuously welded on the outer edge on the internal side of the joining band in the lower half of the tank – positions 3 to 9 o-clock – and 'stitched' (typically 100mm weld 600mm gap) over the upper – 9 to 3 o-clock – portion of the tank.
Bands A, B, H, I & J were noted to be 'stitched' over their full circumference.
Note: The 100mm weld, 600mm gap weld pattern was noted to be irregular and varied considerably throughout the 10 bands of the tanker.
The location and toes of each internal fillet weld were marked with indelible ink on the outer face of the tanker shell to facilitate the accurate positioning of the strain gauges relative to the weld toes.
Each band was then photographed for reference – refer to photographs for further information.

ULTRASONIC INSPECTION REPORT

CLIENT: TWI Ltd. PROJECT: Tanker internal weld inspection
Report No. 14-1946 Sheet 3 of 5

DATE OF TEST(S) 24th April 2014	TEST VENUE: Pullman Fleet Services Depot, West – Thurrock, Essex.			
COMPONENT IDENTIFICATION: Fuel tanker No. 5587.	SURFACE CONDITION AND WELD DETAILS: As welded MIG fillet welds.			
MATERIAL: Aluminium. TEMPERATURE 0 - 40 C [✓]	STAGE OF MANUFACTURE: On completion of welding + 48 Hrs.			
FLAW DETECTOR(S): SITESCAN D10+ SERIAL NO:1007527	PROBES USED (TYPE)	ANGLE	FREQUENCY (MHz)	SIZE (mm)
CALIBRATION/REFERENCE BLOCKS: TYPE SERIAL NO. A2 44558 A4 77403 DAC PF001	Twin CD 10	0	5	10
COUPLANT: UCA-7 Dry Powder Couplant.				
INSPECTION STANDARD: BSEN 1714 EXAMINATION LEVEL: B	ACCEPTANCE STANDARD: Report findings.			
TECHNIQUE/PROCEDURE: BSEN1714 section 12	TIME BASE RANGE: 0 – 100mm			
TEST SENSITIVITY: COMPRESSION: DAC +14dbs SHEAR: DAC +14dbs ATTENUATION/TRANSFER: +2dBs	TEST RESTRICTIONS: Yes [ ] No [✓] If yes state details			
CALIBRATION: Equipment calibrated in accordance with BS EN 12668-1:2000				

AREA TESTED AND RESULTS:

The internal fillet welds in the identified bands were inspected to determine their geometry and location

RESULTS: The weld dimensions were marked on the out shell of the tanker and each band photographed.

Please refer to the attached photographs for further information on the internal fillet weld locations.

Signed:

PCN
H.T. TOPPING
111082
UT Level 2 • MT Level 2
PT Level 2
TWI

INSPECTOR(S) : H.Topping CERTIFICATION STATUS: PCN Level 2 No. 111082

Photographs of Tanker.

Figure No.1 – Showing general view of Tanker with inspected band locations arrowed.

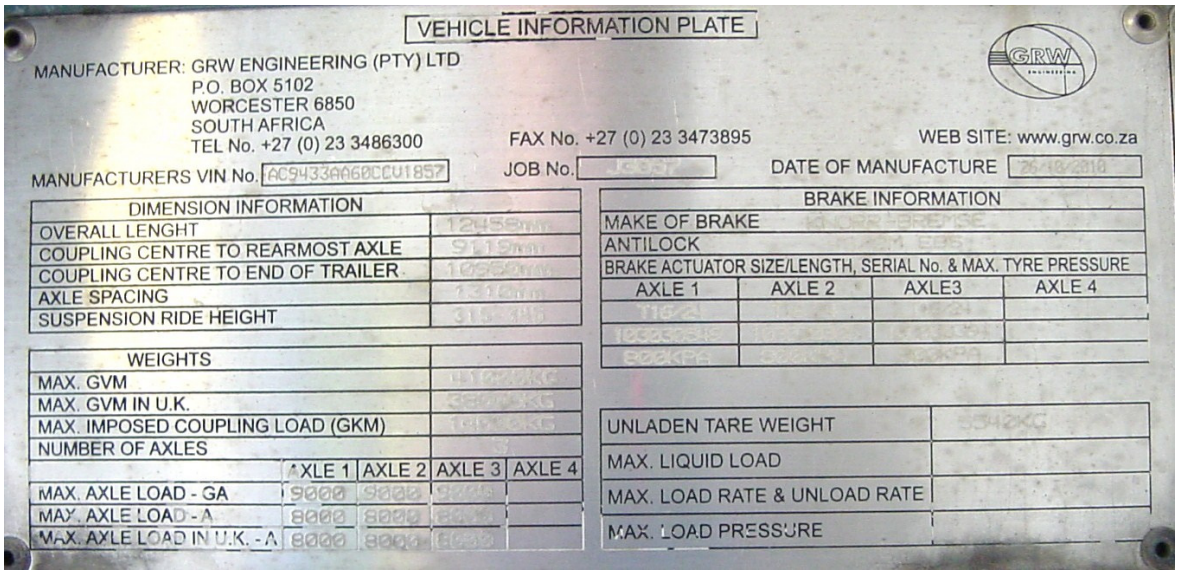
VEHICLE INFORMATION PLATE

MANUFACTURER: GRW ENGINEERING (PTY) LTD
P.O. BOX 5102
WORCESTER 6850
SOUTH AFRICA
TEL No. +27 (0) 23 3486300

FAX No. +27 (0) 23 3473895

WEB SITE: www.grw.co.za

MANUFACTURERS VIN No. AC9433AA60CCU1857

JOB No.

DATE OF MANUFACTURE

DIMENSION INFORMATION	
OVERALL LENGHT	12455mm
COUPLING CENTRE TO REARMOST AXLE	9119mm
COUPLING CENTRE TO END OF TRAILER	10950mm
AXLE SPACING	1310mm
SUSPENSION RIDE HEIGHT	315-415

WEIGHTS				
MAX. GVM				
MAX. GVM IN U.K.				
MAX. IMPOSED COUPLING LOAD (GKM)				
NUMBER OF AXLES				
	AXLE 1	AXLE 2	AXLE 3	AXLE 4
MAX. AXLE LOAD - GA	9000	9000	9000	
MAX. AXLE LOAD - A	8000	8000	8000	
MAX. AXLE LOAD IN U.K. - A	8000	8000	8000	

BRAKE INFORMATION			
MAKE OF BRAKE			
ANTILOCK			
BRAKE ACTUATOR SIZE/LENGTH, SERIAL No. & MAX. TYRE PRESSURE			
AXLE 1	AXLE 2	AXLE3	AXLE 4
T16/24			

UNLADEN TARE WEIGHT	
MAX. LIQUID LOAD	
MAX. LOAD RATE & UNLOAD RATE	
MAX. LOAD PRESSURE	

Figure No.2 – showing tanker ID plate.

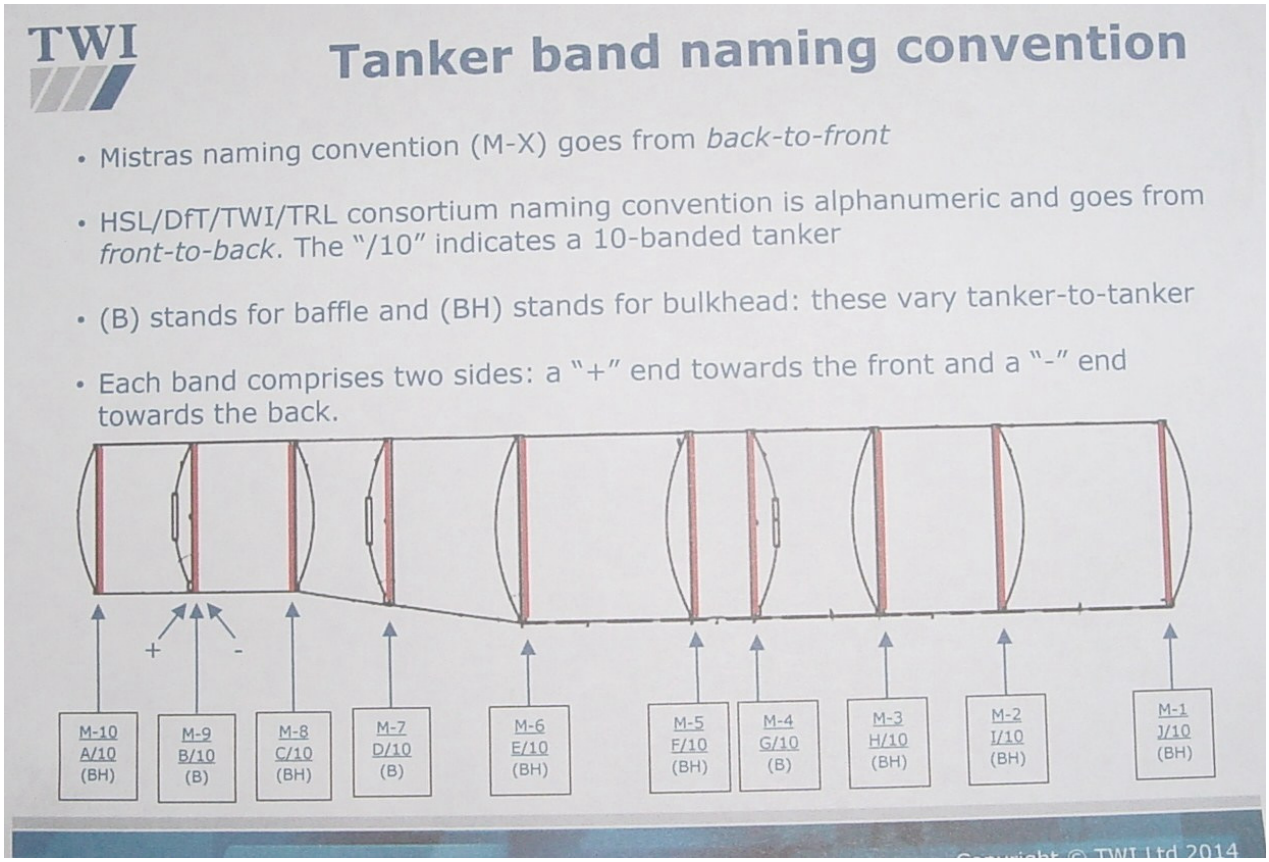

Figure No.3 – showing tanker band naming convention.

The main objective of the UT inspection of the tanker was to determine the position and extent of internal fillet welds between the extrusion band toe and the tanker shell inner surface to ensure the appropriate placement of the strain gauges. For this reason, the tanker was marked up with approximate positions of the internal fillet welds for each band and each side of the band (ie positive side and negative side). Below, Figures A1-A20 are taken of the nearside and Figures A21-A40 are taken of the offside. Figures A41-A50 are 'fillet weld map' diagrams. Each figure represents an idealised cross-section of a tanker band. The left hand side shows the negative side of the band and the right hand side shows the positive side of the band. Based on the images provided by the UT inspector, informative lengths (dark, bold lines) have been drawn on the cross-section diagrams to indicate the positions of the fillet welds. As noted previously, the objective during this phase of work was not to exactly map the fillet welds, but was to ensure that strain gauges were not placed on top of fillet welds, thereby resulting in inaccurate or unrepresentative readings. Therefore, the lengths of the dark lines on the fillet weld map diagrams should be taken to be indicative and not precise. Moreover, locations that were not necessarily fully inspected (ie underneath the tanker) are not marked up with dark bold lines to indicate fillet welds, but this does not mean that they may not be present.

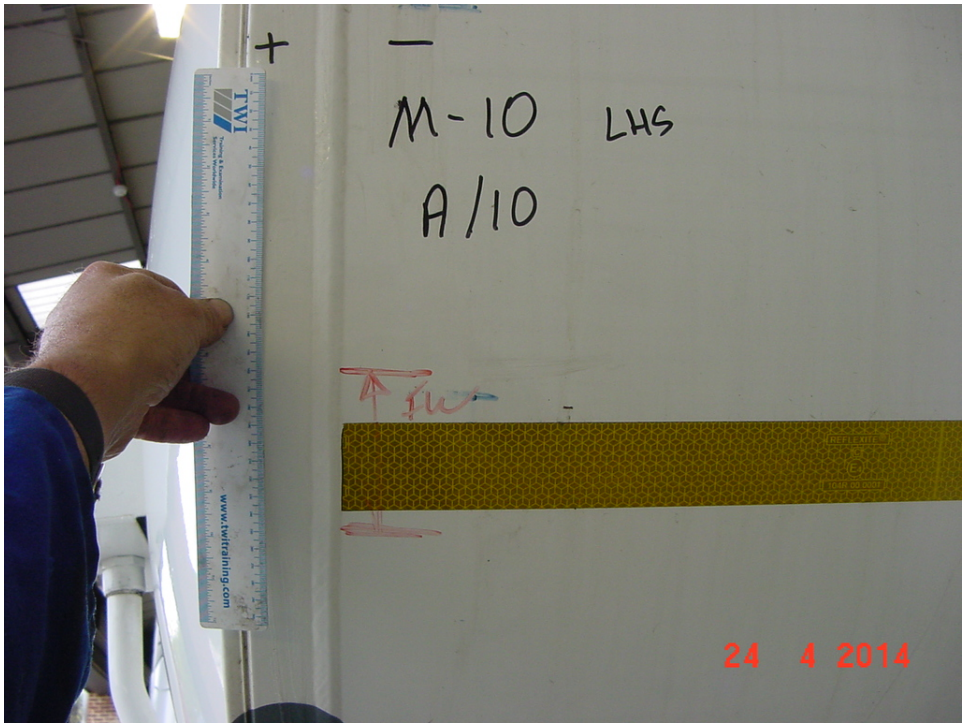

Figure A1 Nearside (labelled left-hand side, LHS), Band A.

Figure A2 Nearside (labelled left-hand side, LHS), Band A.

Figure A3 Nearside (labelled left-hand side, LHS), Band A.

Figure A4 Nearside (labelled left-hand side, LHS), Band B.

Figure A5 Nearside (labelled left-hand side, LHS), Band B.

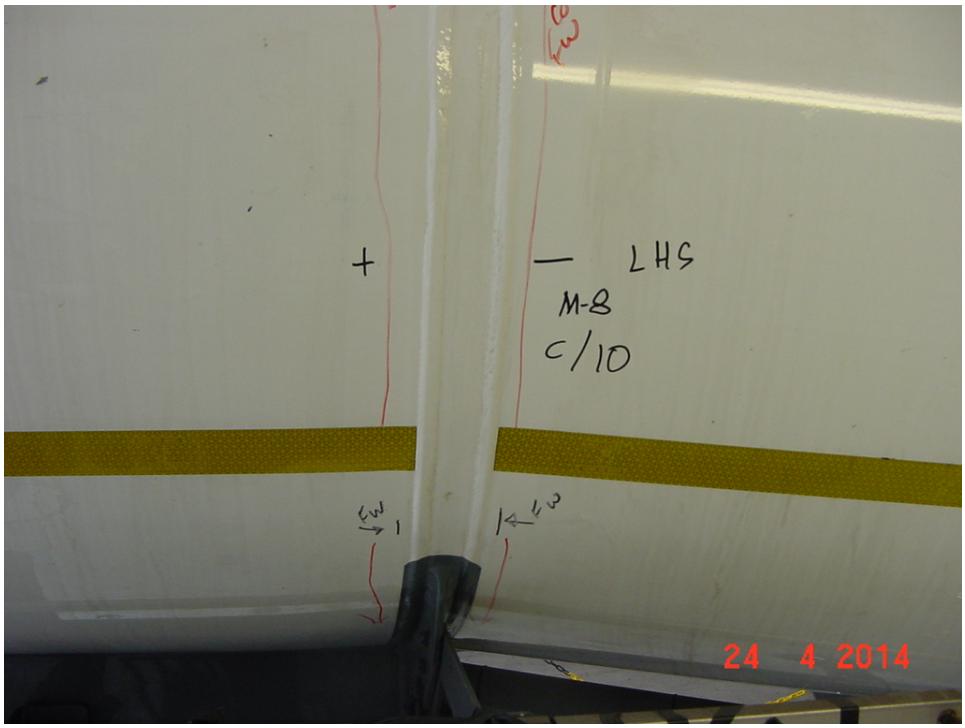

Figure A6 Nearside (labelled left-hand side, LHS), Band C.

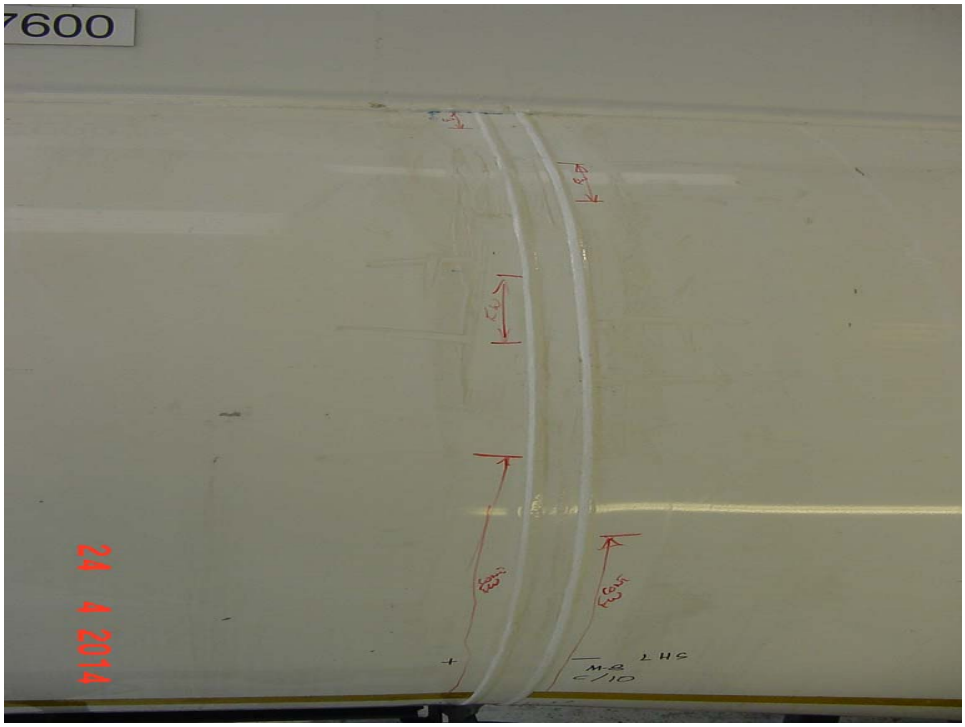

Figure A7 Nearside (labelled left-hand side, LHS), Band C.

Figure A8 Nearside (labelled left-hand side, LHS), Band D.

Figure A9 Nearside (labelled left-hand side, LHS), Band D.

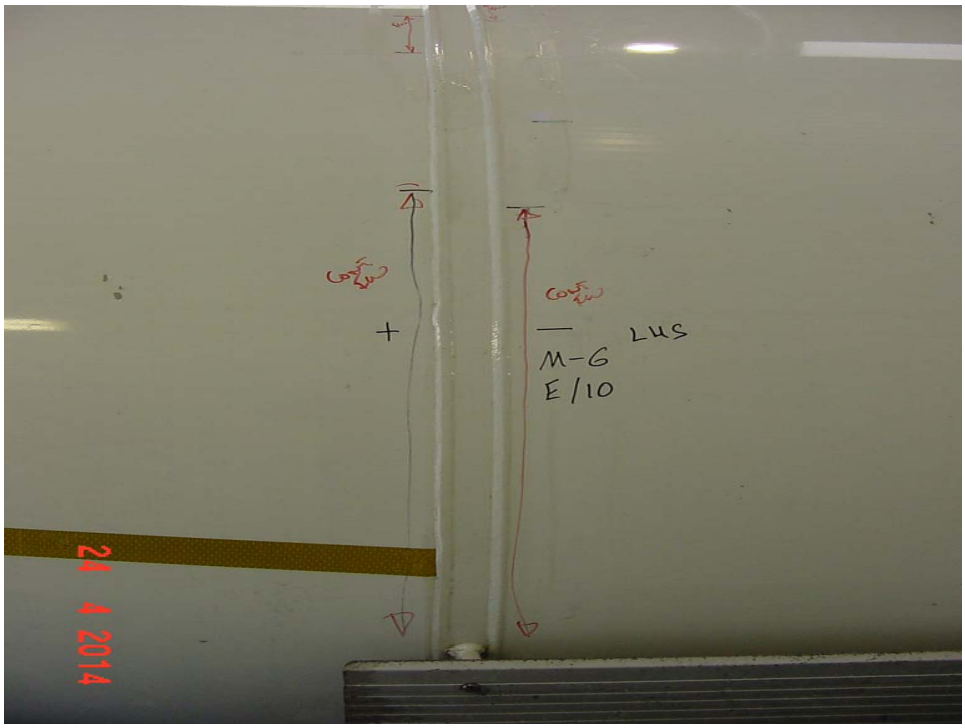

Figure A10 Nearside (labelled left-hand side, LHS), Band E.

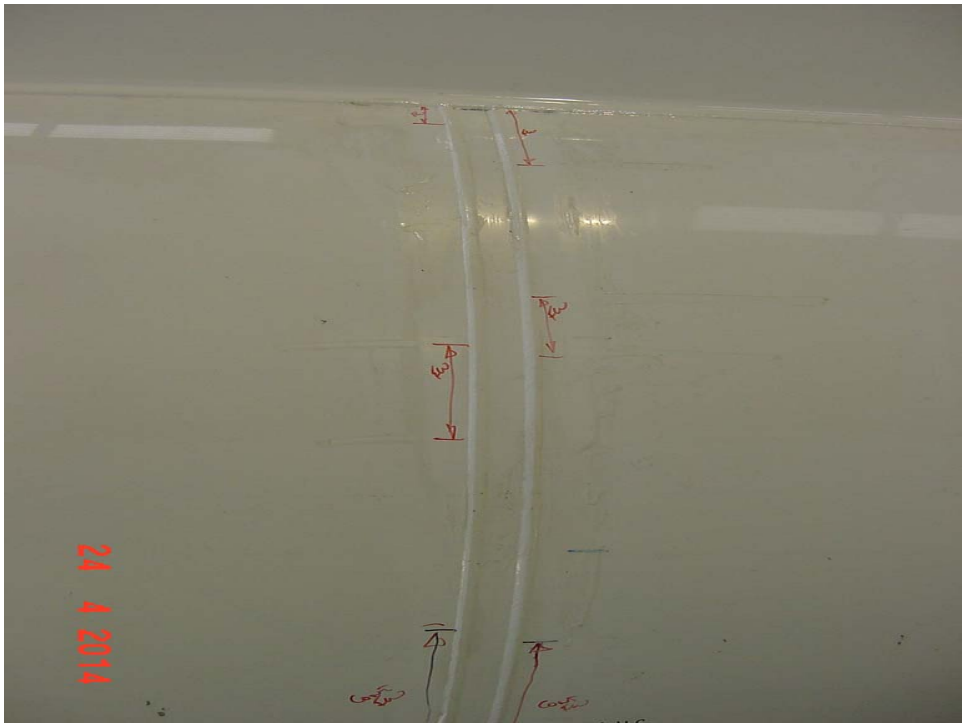

Figure A11 Nearside (labelled left-hand side, LHS), Band E.

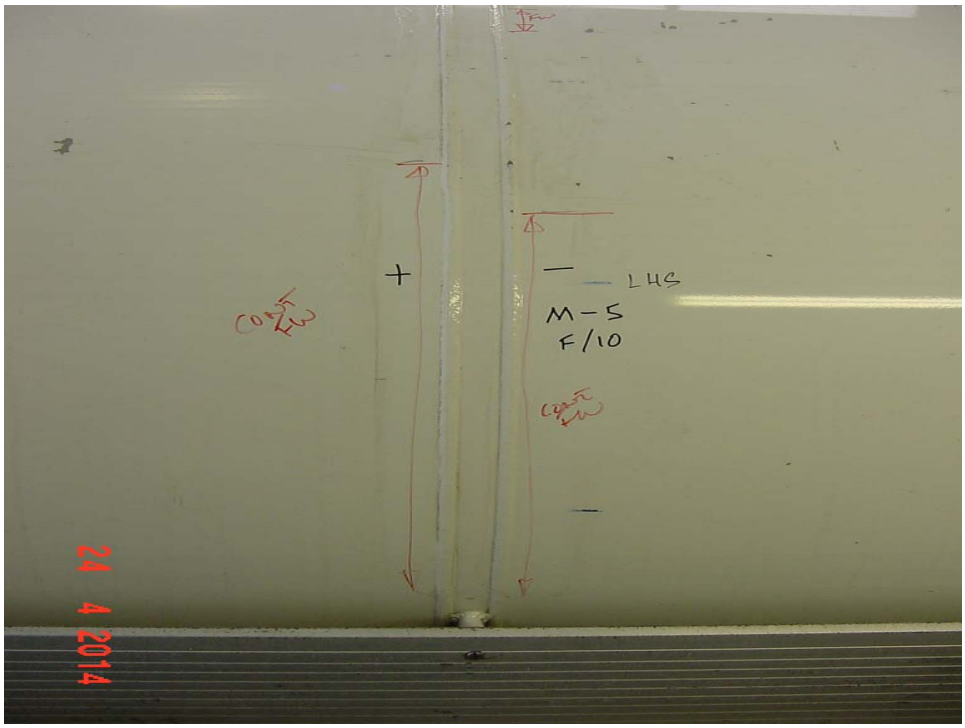

Figure A12 Nearside (labelled left-hand side, LHS), Band F.

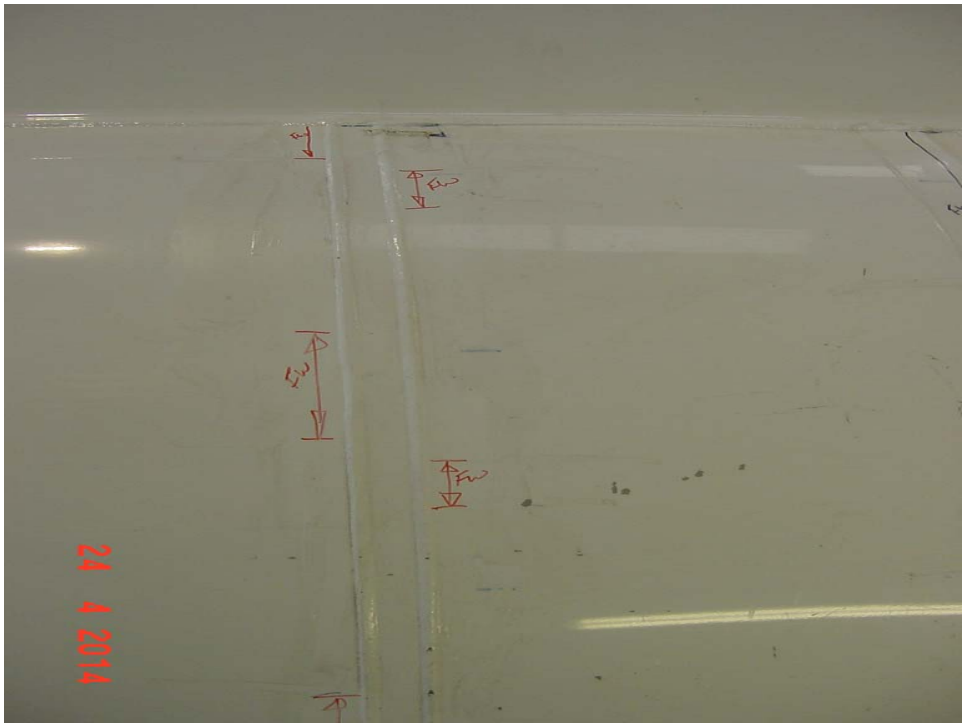

Figure A13 Nearside (labelled left-hand side, LHS), Band F.

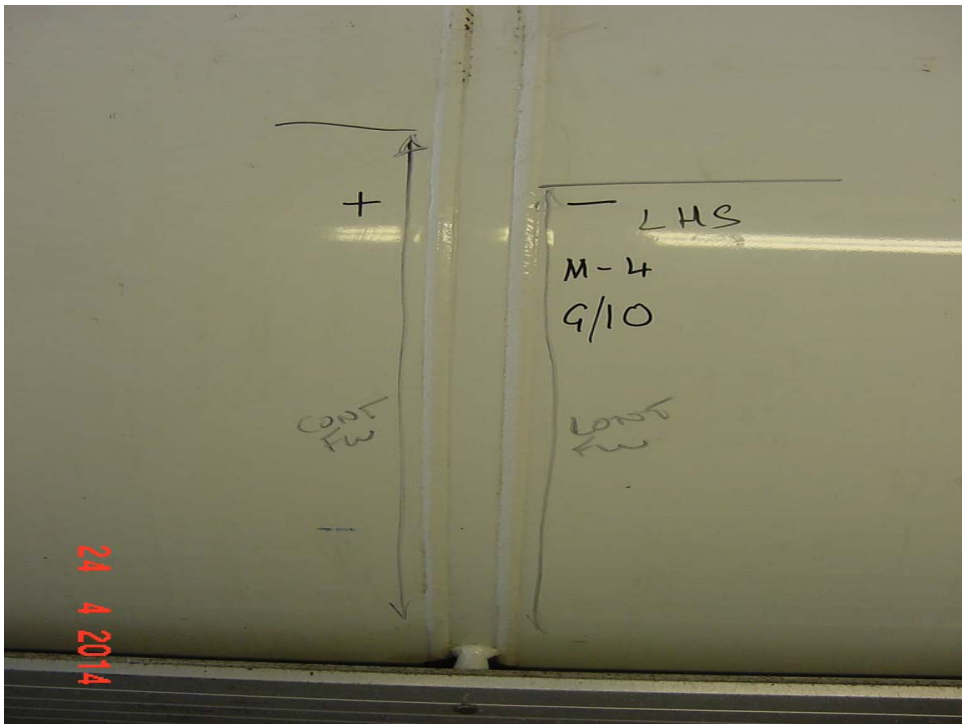

Figure A14 Nearside (labelled left-hand side, LHS), Band G.

Figure A15 Nearside (labelled left-hand side, LHS), Band G.

Figure A16 Nearside (labelled left-hand side, LHS), Band H.

Figure A17 Nearside (labelled left-hand side, LHS), Band H.

Figure A18 Nearside (labelled left-hand side, LHS), Band I.

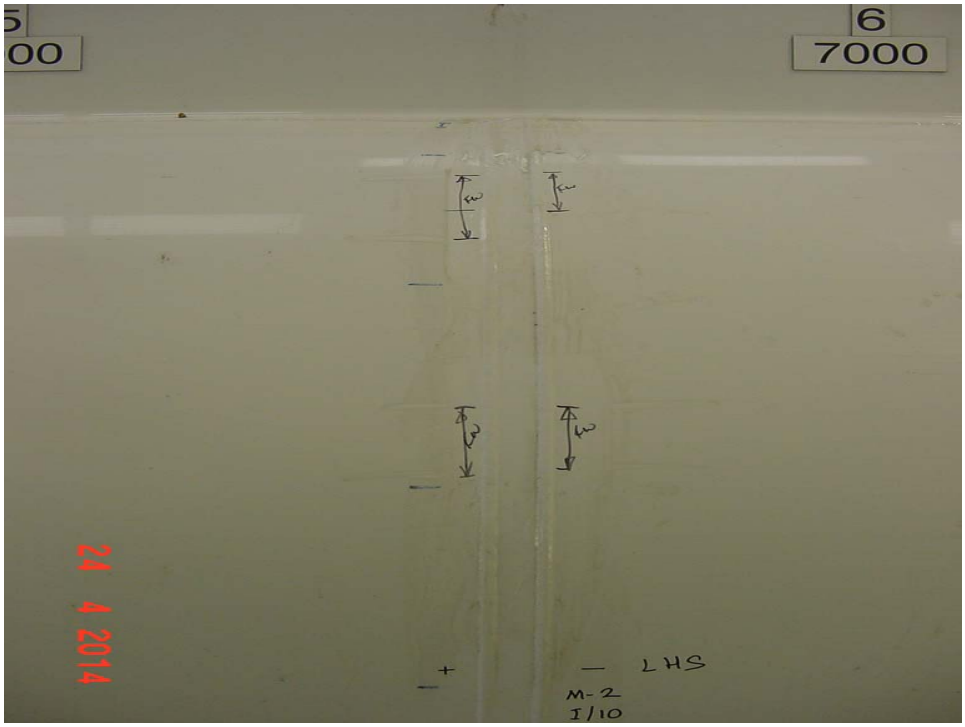

Figure A19 Nearside (labelled left-hand side, LHS), Band I.

Figure A20 Nearside (labelled left-hand side, LHS), Band J.

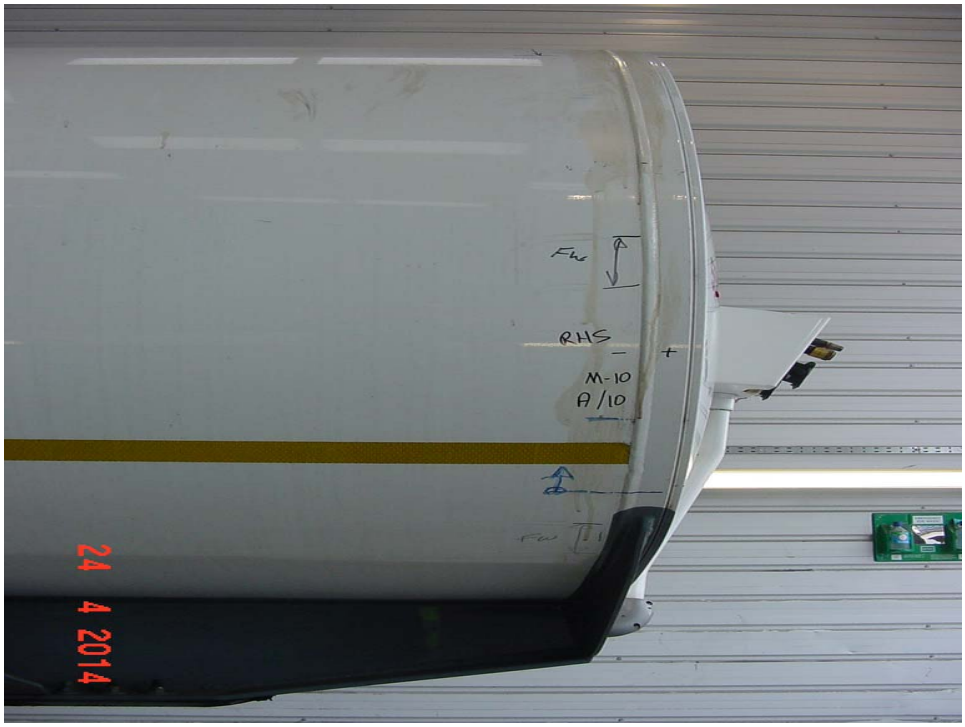

Figure A21 Offside (labelled right-hand side, RHS), Band A.

Figure A22 Offside (labelled right-hand side, RHS), Band A.

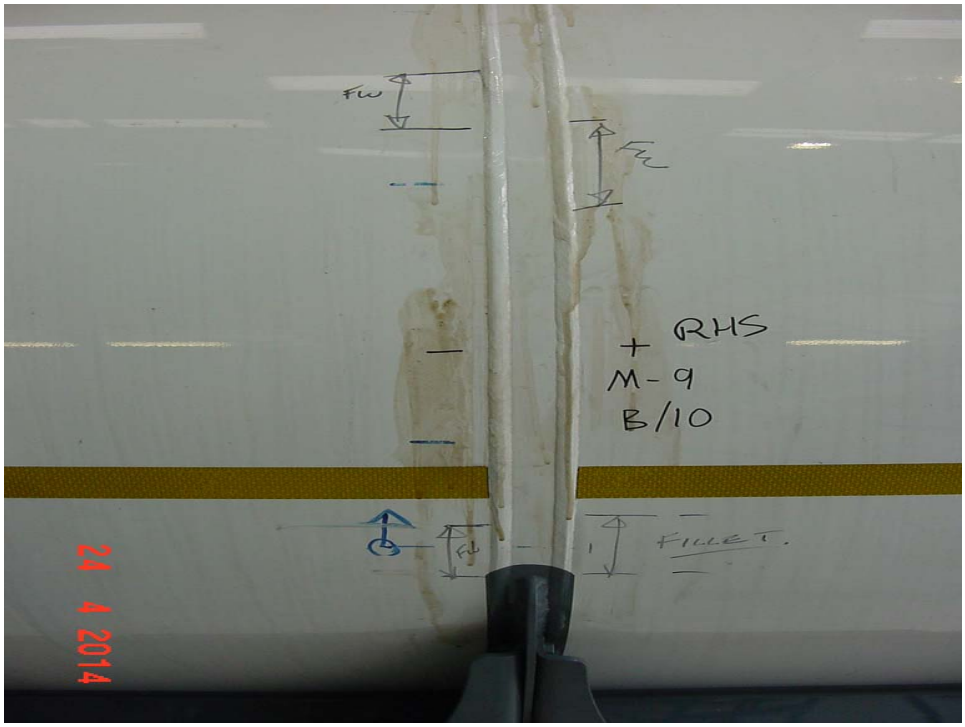

Figure A23 Offside (labelled right-hand side, RHS), Band B.

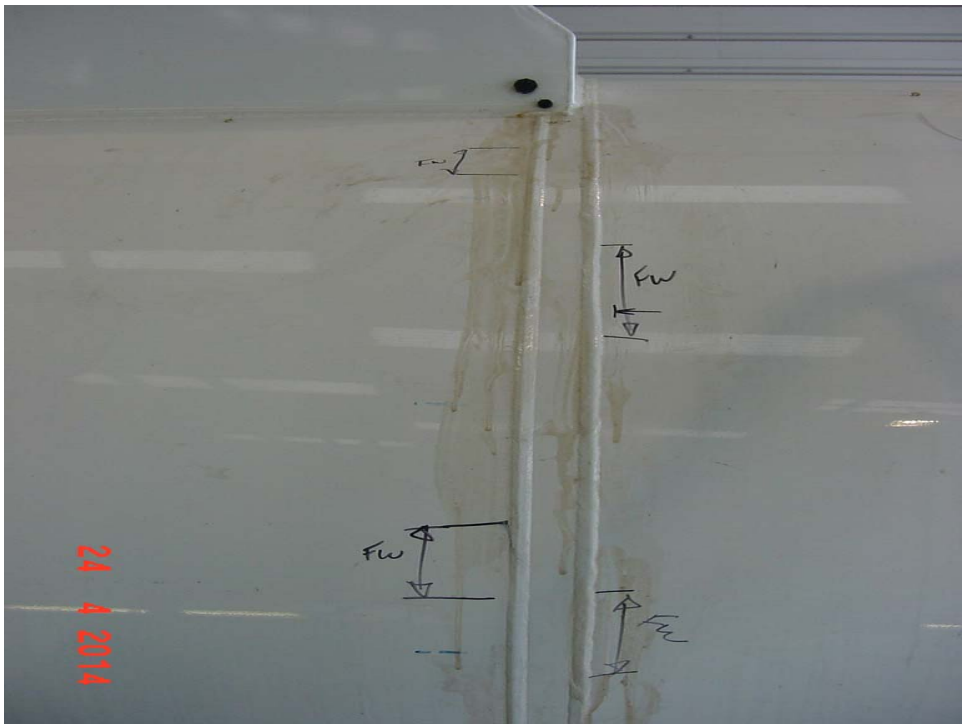

Figure A24 Offside (labelled right-hand side, RHS), Band B.

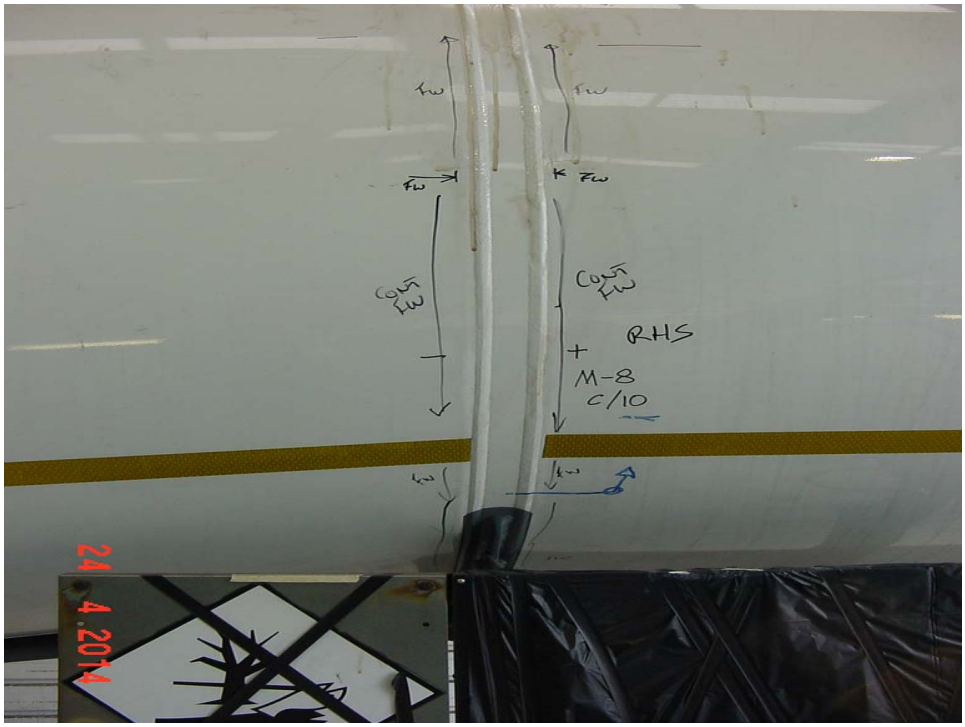

Figure A25 Offside (labelled right-hand side, RHS), Band C.

Figure A26 Offside (labelled right-hand side, RHS), Band C.

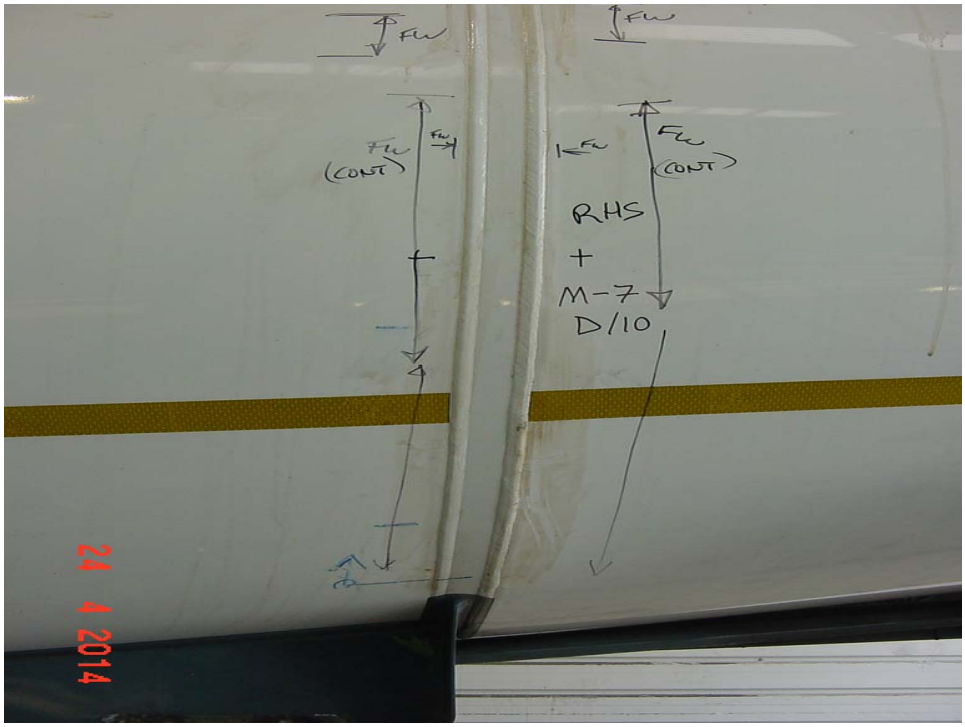

Figure A27 Offside (labelled right-hand side, RHS), Band D.

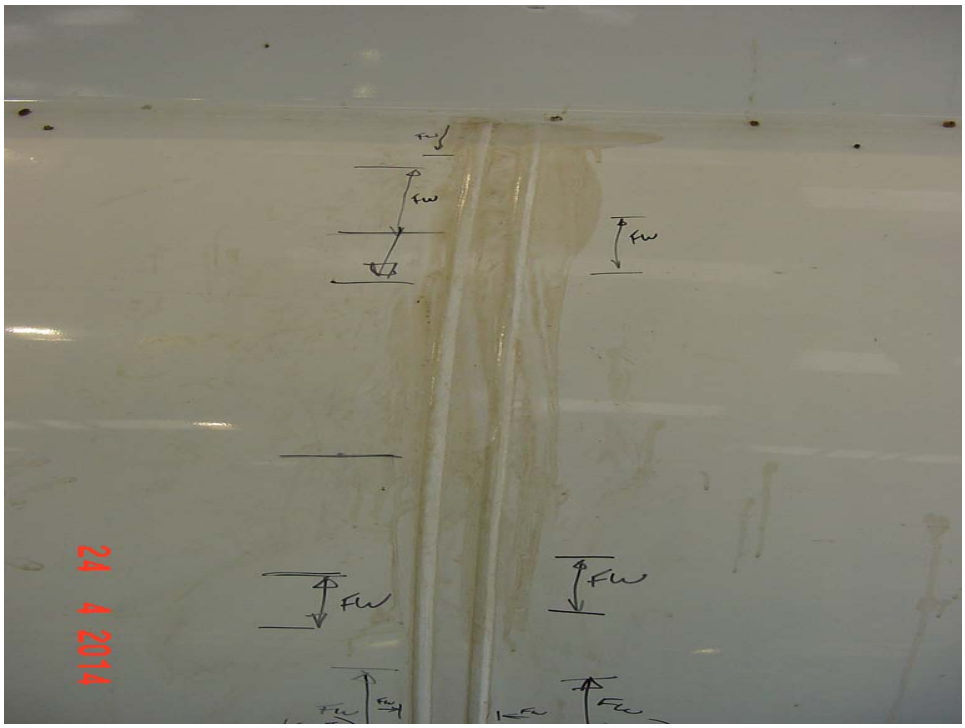

Figure A28 Offside (labelled right-hand side, RHS), Band D.

Figure A29 Offside (labelled right-hand side, RHS), Band E.

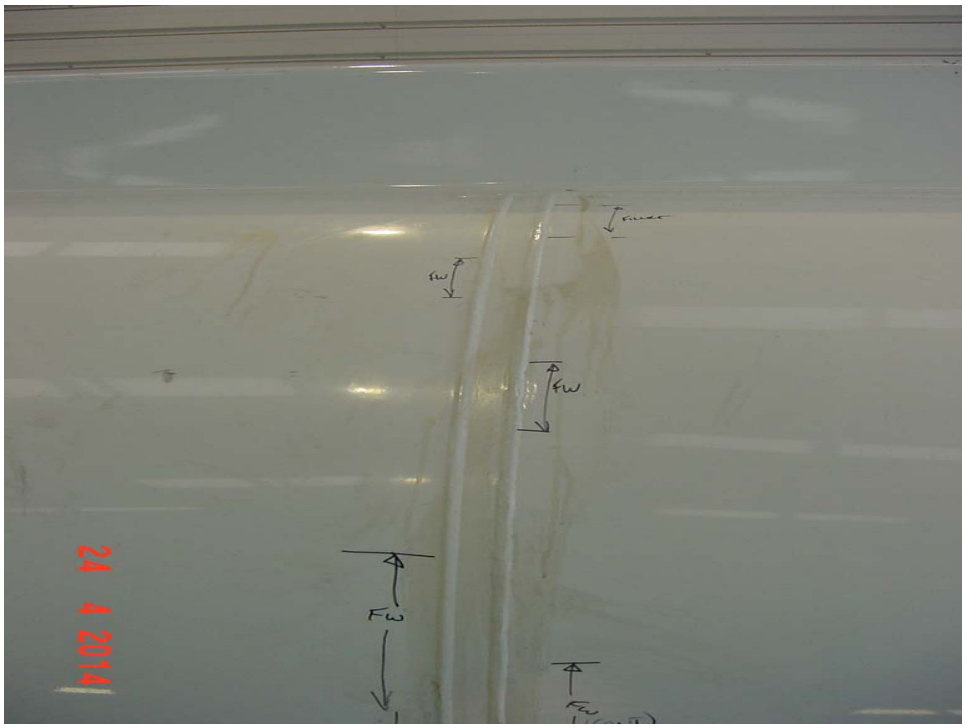

Figure A30 Offside (labelled right-hand side, RHS), Band E.

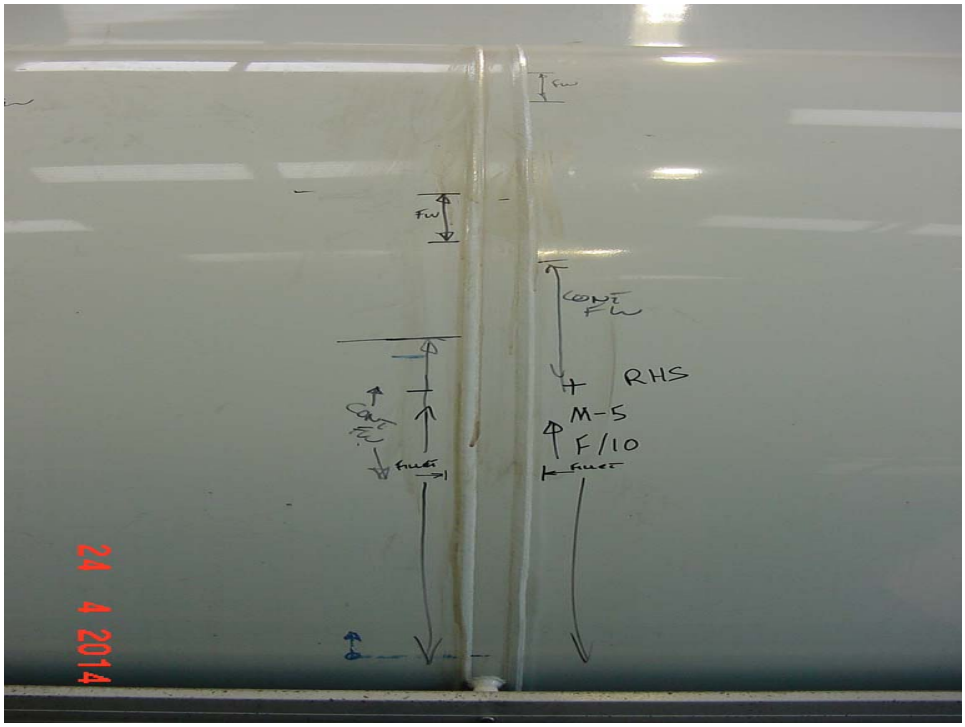

Figure A31 Offside (labelled right-hand side, RHS), Band F.

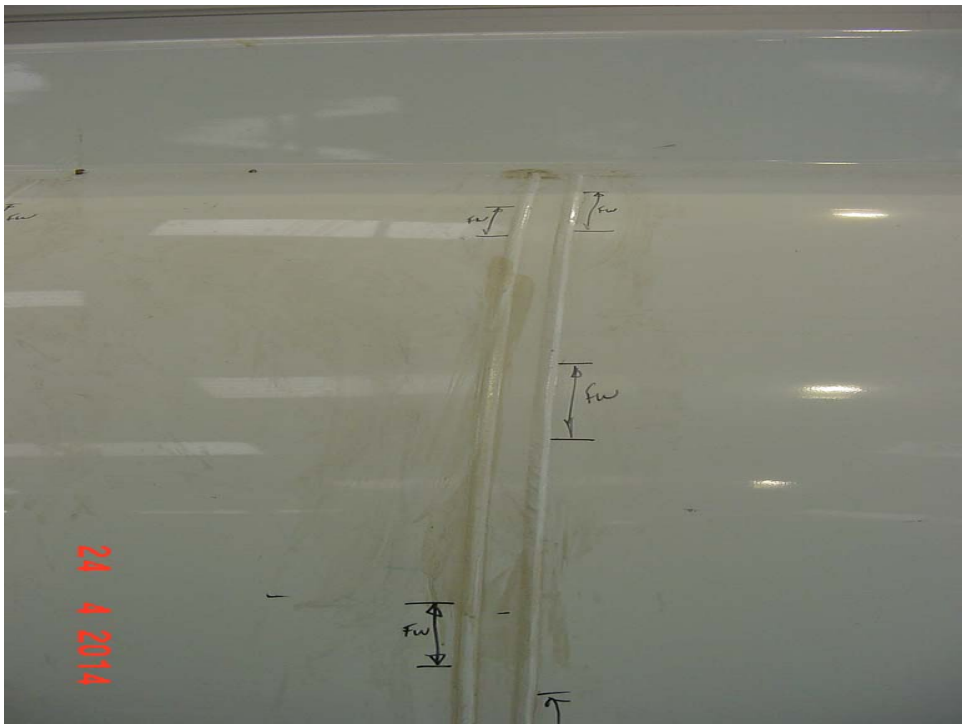

Figure A32 Offside (labelled right-hand side, RHS), Band F.

Figure A33 Offside (labelled right-hand side, RHS), Band G.

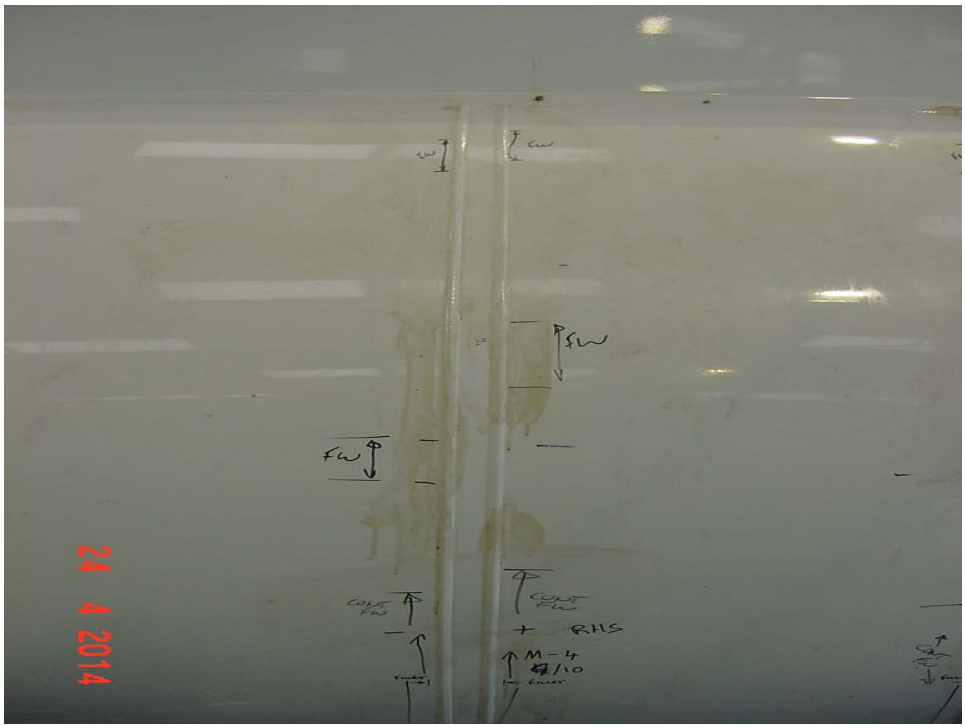

Figure A34 Offside (labelled right-hand side, RHS), Band G.

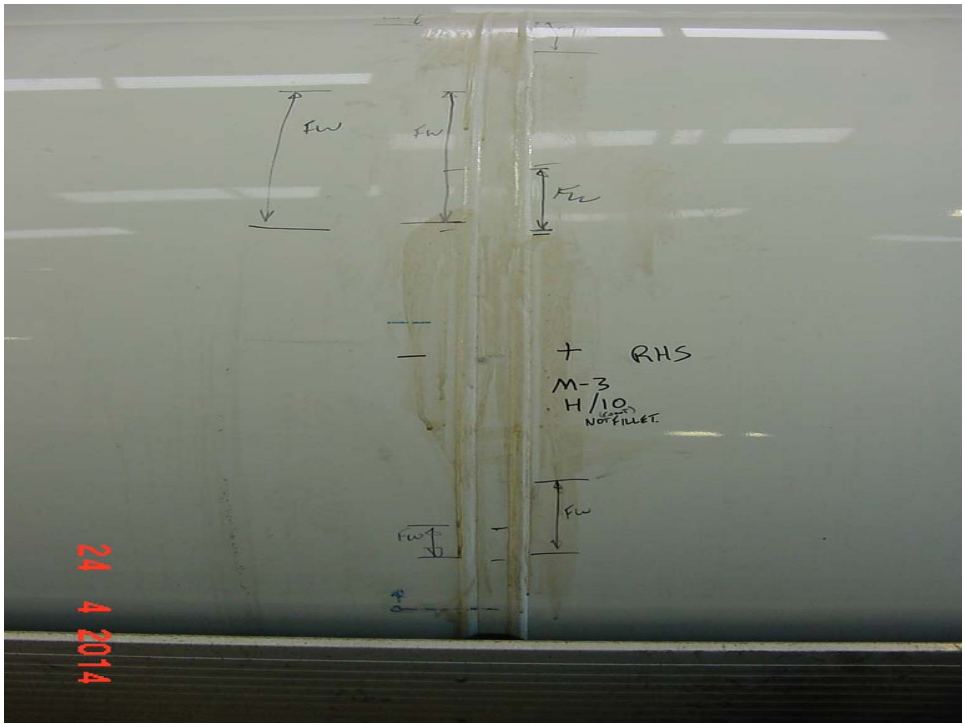

Figure A35 Offside (labelled right-hand side, RHS), Band H.

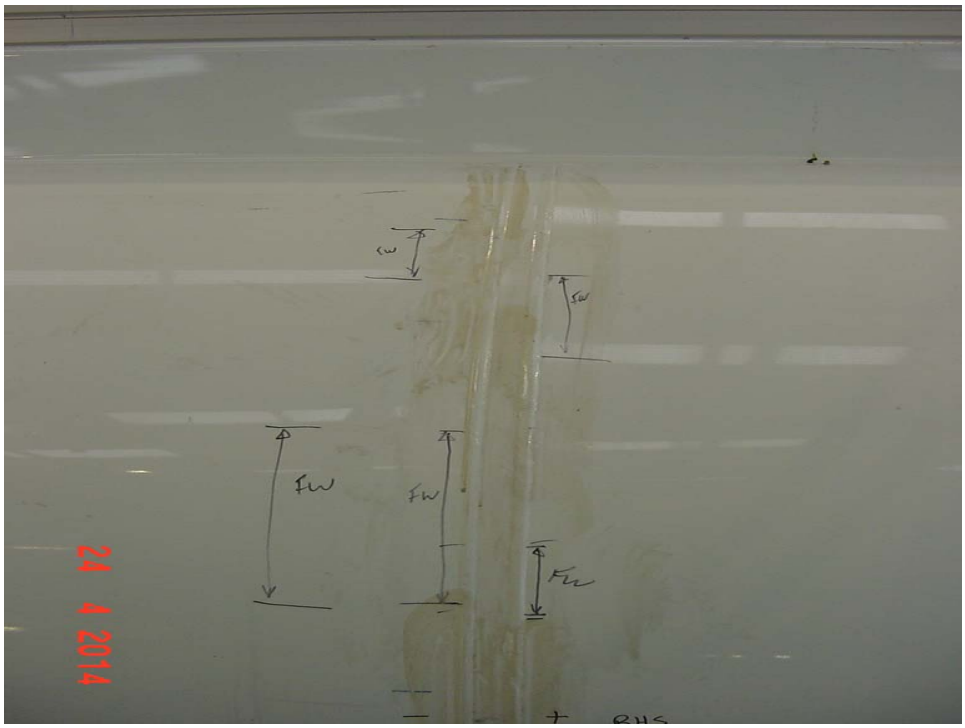

Figure A36 Offside (labelled right-hand side, RHS), Band H.

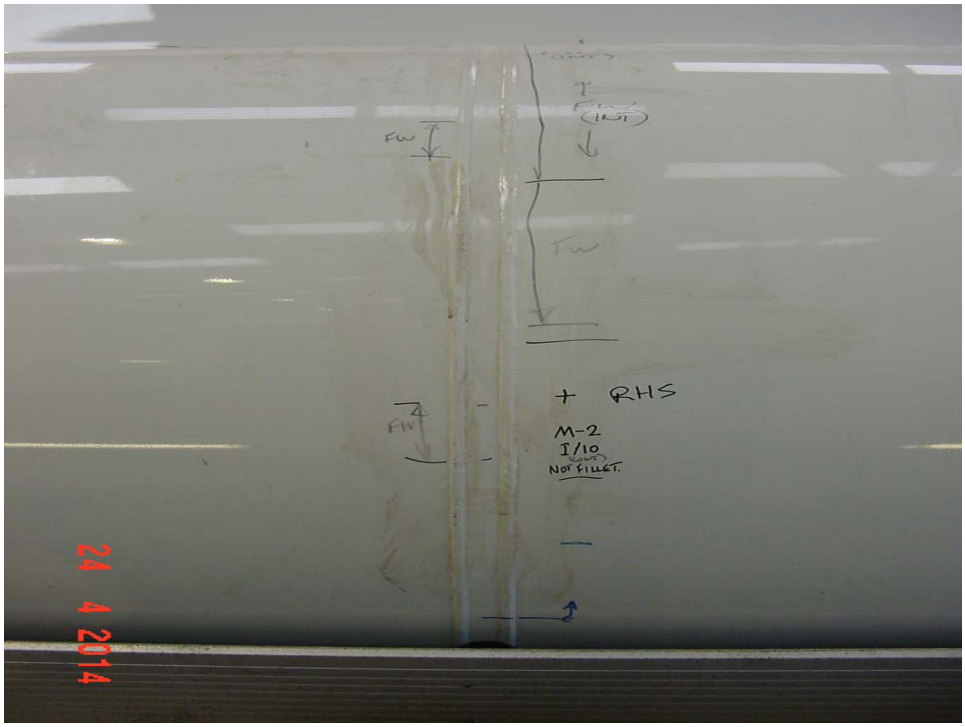

Figure A37 Offside (labelled right-hand side, RHS), Band I.

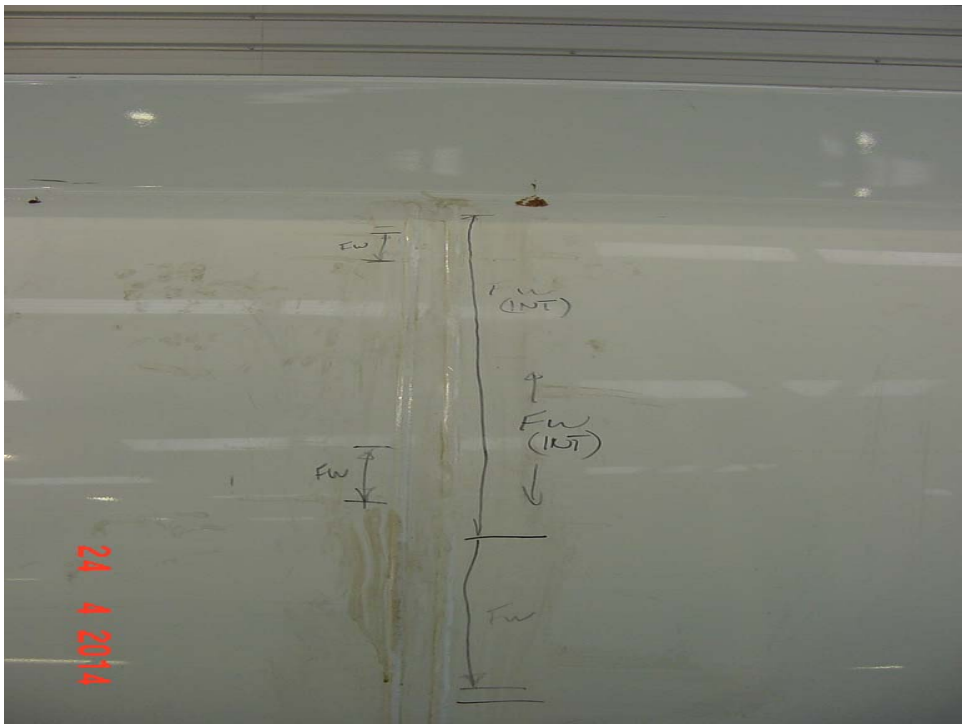

Figure A38 Offside (labelled right-hand side, RHS), Band I.

Figure A39 Offside (labelled right-hand side, RHS), Band J.

Figure A40 Offside (labelled right-hand side, RHS), Band J.

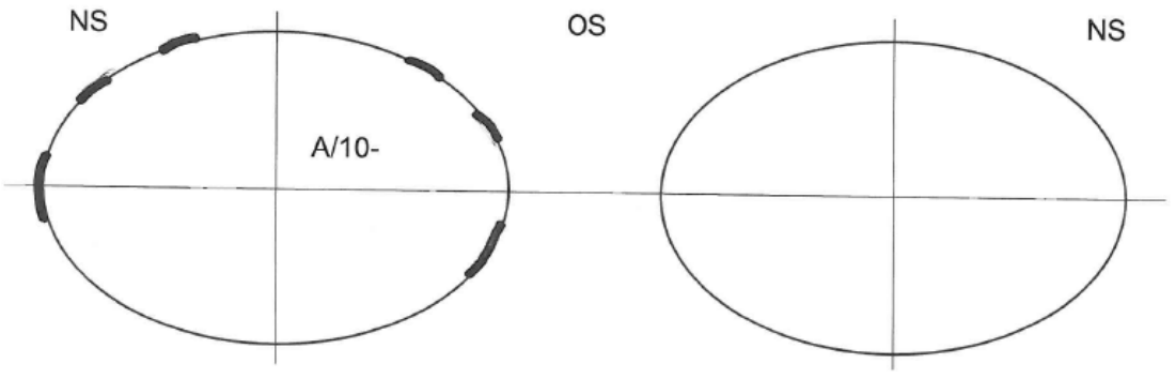

Figure A41 Fillet weld map diagram for band A/10.

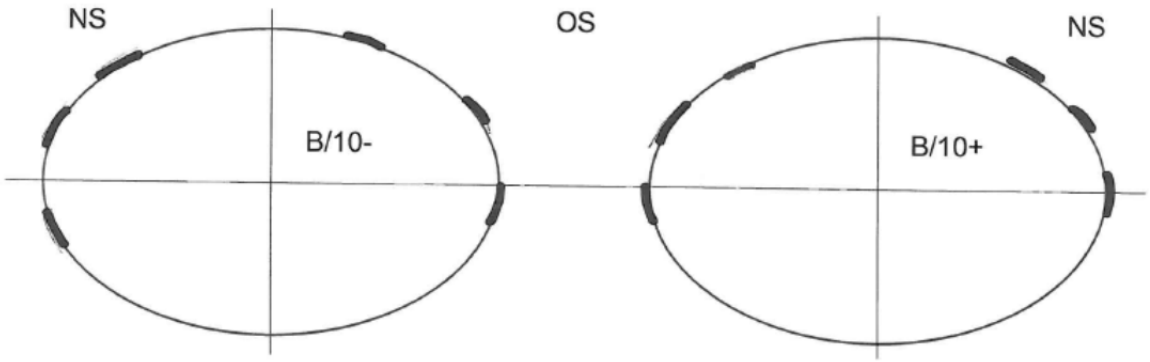

Figure A42 Fillet weld map diagram for band B/10.

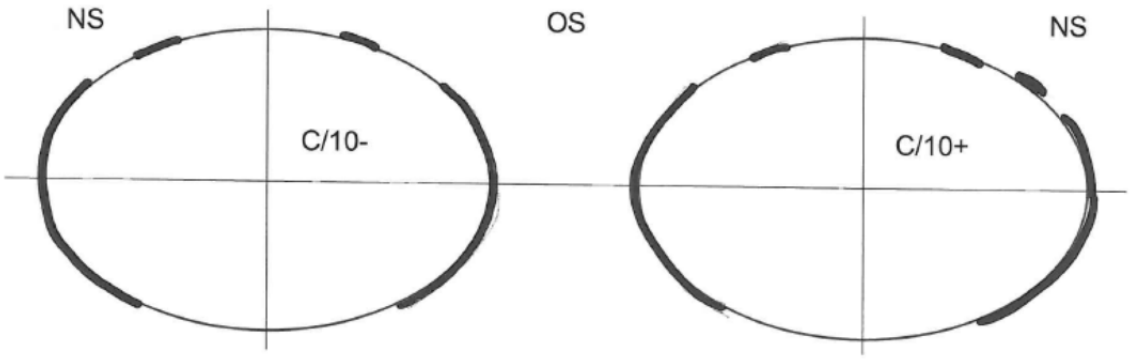

Figure A43 Fillet weld map diagram for band C/10.

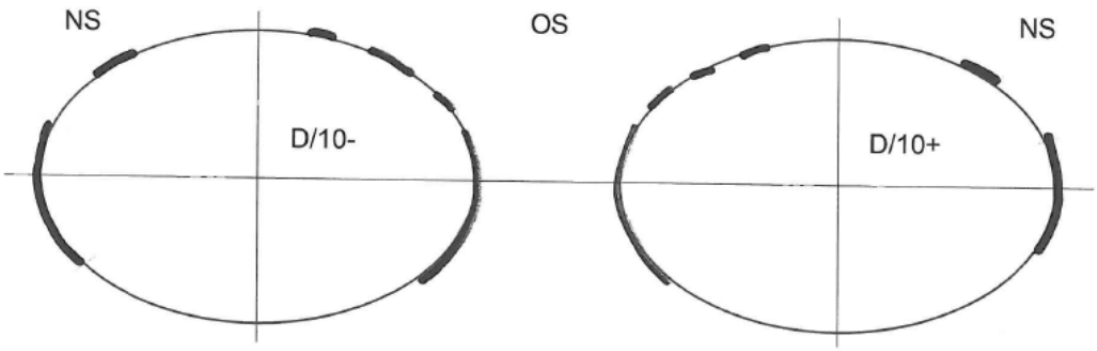

Figure A44 Fillet weld map diagram for band D/10.

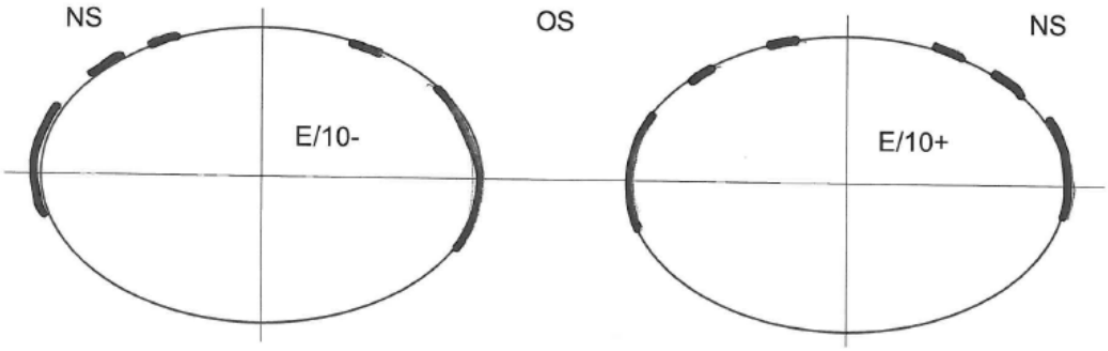

Figure A45 Fillet weld map diagram for band E/10.

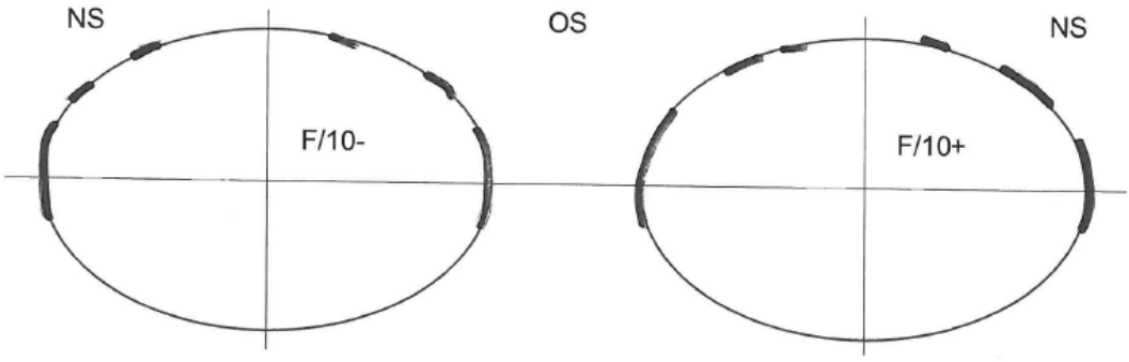

Figure A46 Fillet weld map diagram for band F/10.

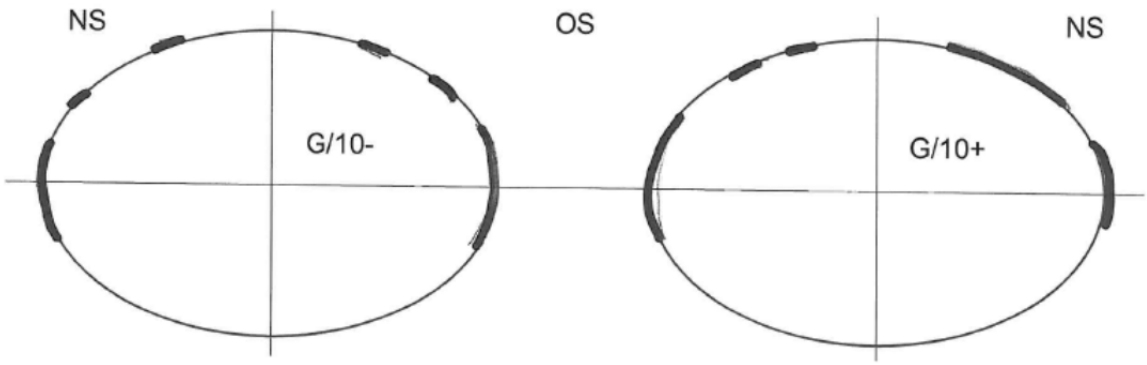

Figure A47 Fillet weld map diagram for band G/10.

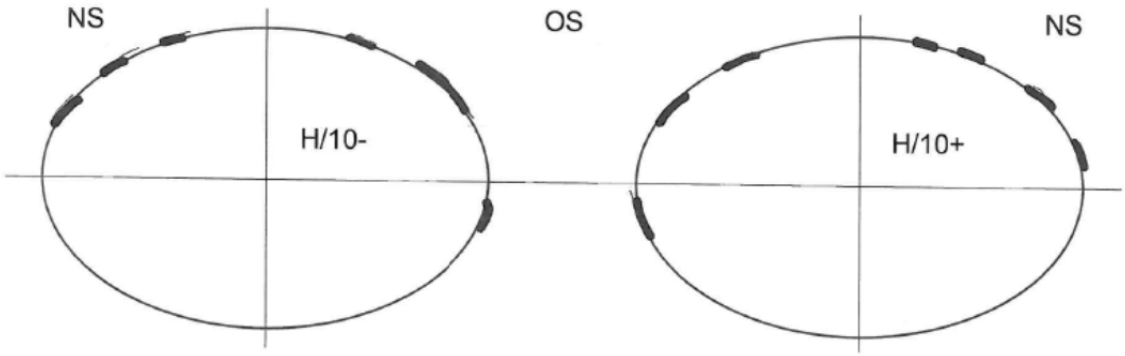

Figure A48 Fillet weld map diagram for band H/10.

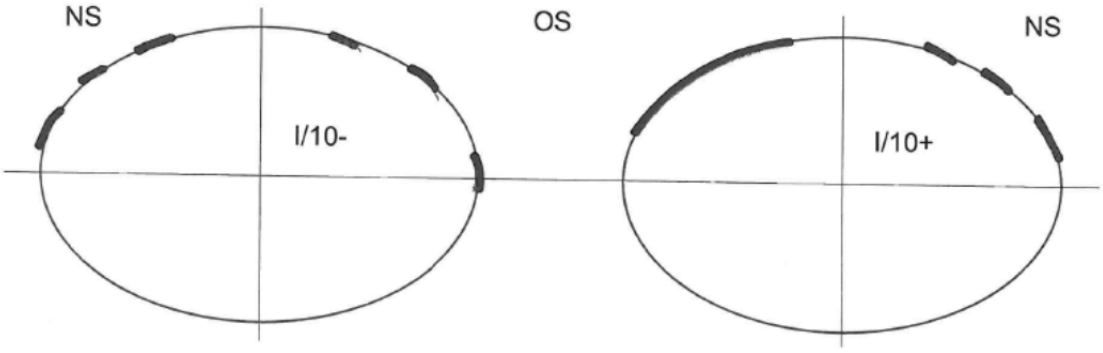

Figure A49 Fillet weld map diagram for band I/10.

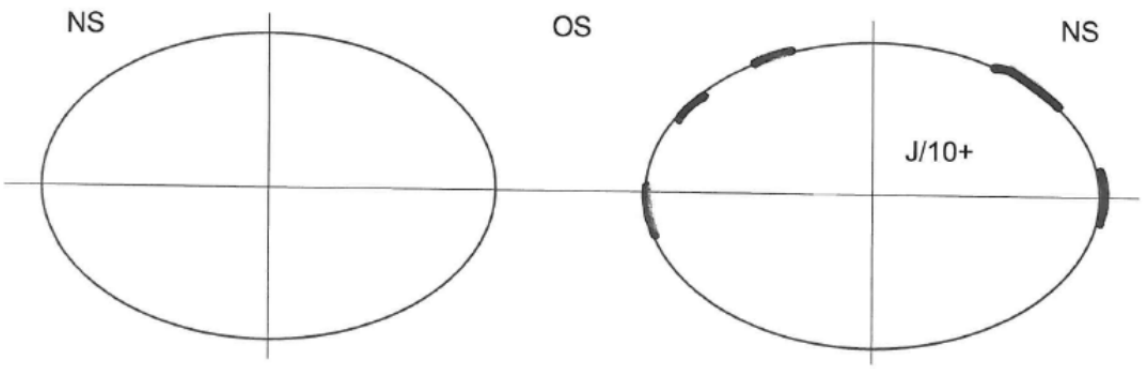

Figure A50 Fillet weld map diagram for band J/10.

Appendix B

Tanker Strain Gauge Plan

Appendix B: Strain Gauge Plan

1 Overview

The strain gauge plan for the data collection exercise involving tanker J3857 was briefly described in the main report. The strain gauge plan was developed based upon an assessment of GRW's analysis of a static model of the tanker. In this finite element model, three different loading conditions were considered: a 1g forward acceleration, 1g lateral acceleration and a 1g vertical acceleration. In each load case, the body accelerations were resisted by the king pin and/or suspension. From the results of these simulations, TWI identified regions where large stresses acted normal to the circumferential seam welds. These regions in turn represent positions on the tanker where it is likely that fatigue damage may be most severe. Based on this review of the simulation results, the following strategy was employed for the strain gauge positions:

- Tanker bands B and G were the most densely instrumented. Along these bands, both circumferentially- and axially-oriented strain gauges were placed at multiple positions along the circumference. In particular, the regions near the cradle featured a cluster of four axial gauges and one circumferential (hoop) gauge so that a local biaxial stress could be calculated and linearly extrapolated back to the hypothetical crack plane.
- Tanker bands C and D were the next most densely instrumented. For these two bands, circumferentially-oriented gauges were not employed, but axial gauges at the same circumferential position having different longitudinal offsets from the welds were used to enable linear stress extrapolation back to the hypothetical crack plane.
- For the remaining circumferential seam welds, a single axial gauge was placed on the offside of the tanker where the cradle attached to the tanker. This allowed for strain data to be collected from the same position from each circumferential seam weld of the tanker.
- Two 'remote' axial gauges were placed on the tanker away from the circumferential seam welds and other local stress raisers. One was placed half-way between bands E and F and one was placed half-way between bands I and J. In both cases, the gauges were located on the offside, mid-height. The purpose of these two gauges was to provide additional model validation/calibration in regions where high strain gradients were not expected.

2 Details of Strain Gauge Placement

Figure B1 provides a legend for the coloured blocks that refer to strain gauge placements around the circumference of the tanker. In the top left of this figure, a black rectangle indicates a single, axially-oriented gauge positioned 5mm from the toe of the extrusion profile. The dimension of 5mm was chosen as this is the nominal tanker shell wall thickness. When or if an additional internal fillet weld was found to be present at a location, the 5mm offset was taken to be from the fillet weld toe. A solid red block indicates two, axially-oriented strain gauges, one 5mm from the toe of the extrusion profile and one 20mm offset from the first gauge (equivalently, 25mm offset from the toe of the extrusion profile). A black and red hatched rectangle indicates the placement of three strain gauges: two axially oriented, spaced similarly to the red block, and one circumferentially oriented. Finally, a yellow and black hatched rectangle indicates a single uniaxial gauge and a single circumferential gauge, both 5mm offset from the toe of the extrusion profile with 20mm between the gauges.

Based on this strain gauge legend, Figures B2-B11 provide illustrations of the strain gauge positions around the circumference for each circumferential seam weld. For both the offside and nearside, three main locations were considered around the circumference of the tanker: one at the bottom of the tanker, adjacent to the cradle supports (stiffeners, plate cradle and gusset cradle); one mid-height, primarily only used for the ‘remote’ gauges, and one at the top, near the valence welds. For the cradle and valence strain gauges, the gauges were always positioned 5mm off the attachment. Note that in Figures B2-B11, the cross-section shown is from the finite element model and is kept constant for each band for convenience and orientation; the various parts of the cradle and suspension shown in the figures may not look identical to that directly below any given weld. In Figures B2-B11, images of the instrumentation on the near side have been provided for reference. A detail of the precise positioning of the strain gauges on the offside cradle position for band B/10 is shown in Figure B12.

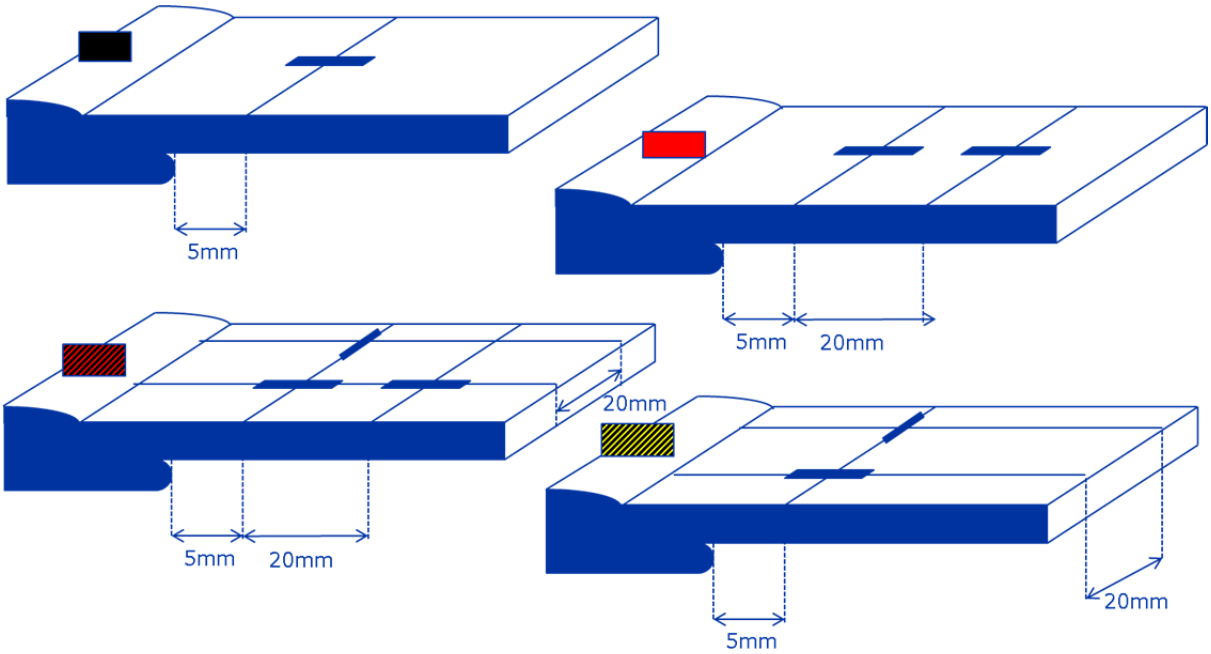

Figure B1 Strain gauge legend for the positions shown in Figures A2-A11.

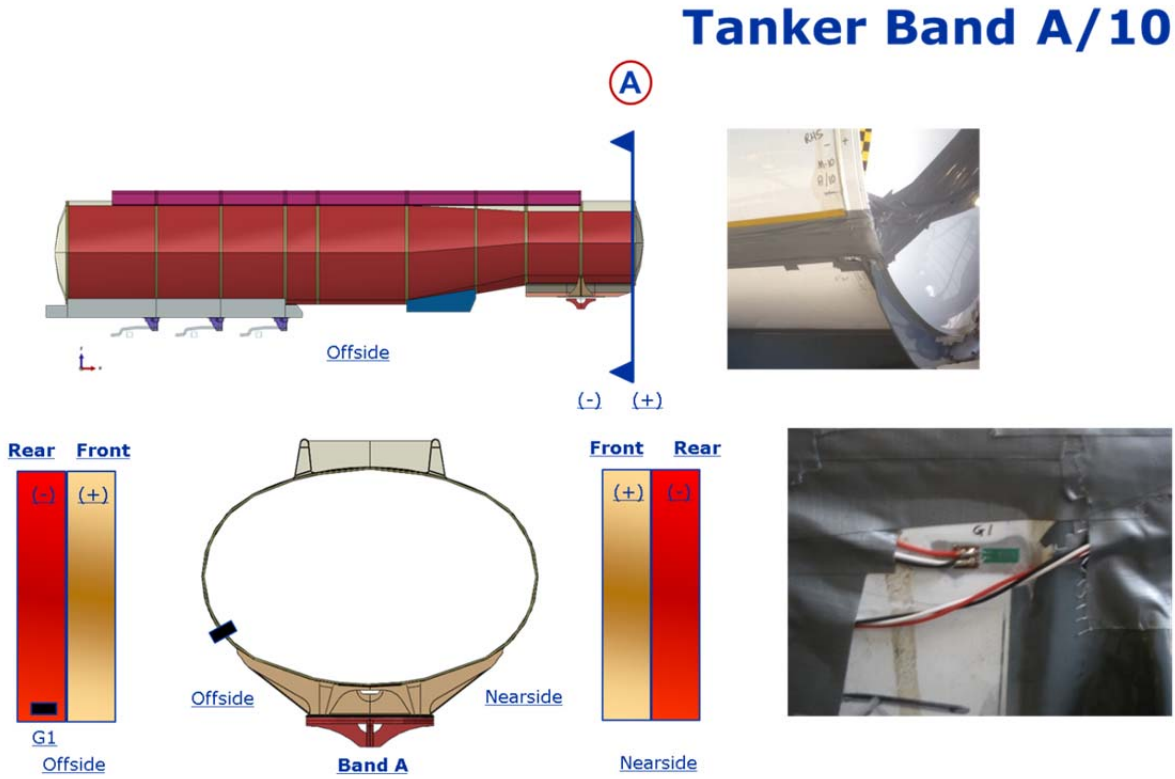

Figure B2 Illustration of the position of the single, axially-oriented strain gauge, G1, on band A/10 (-) on the near side.

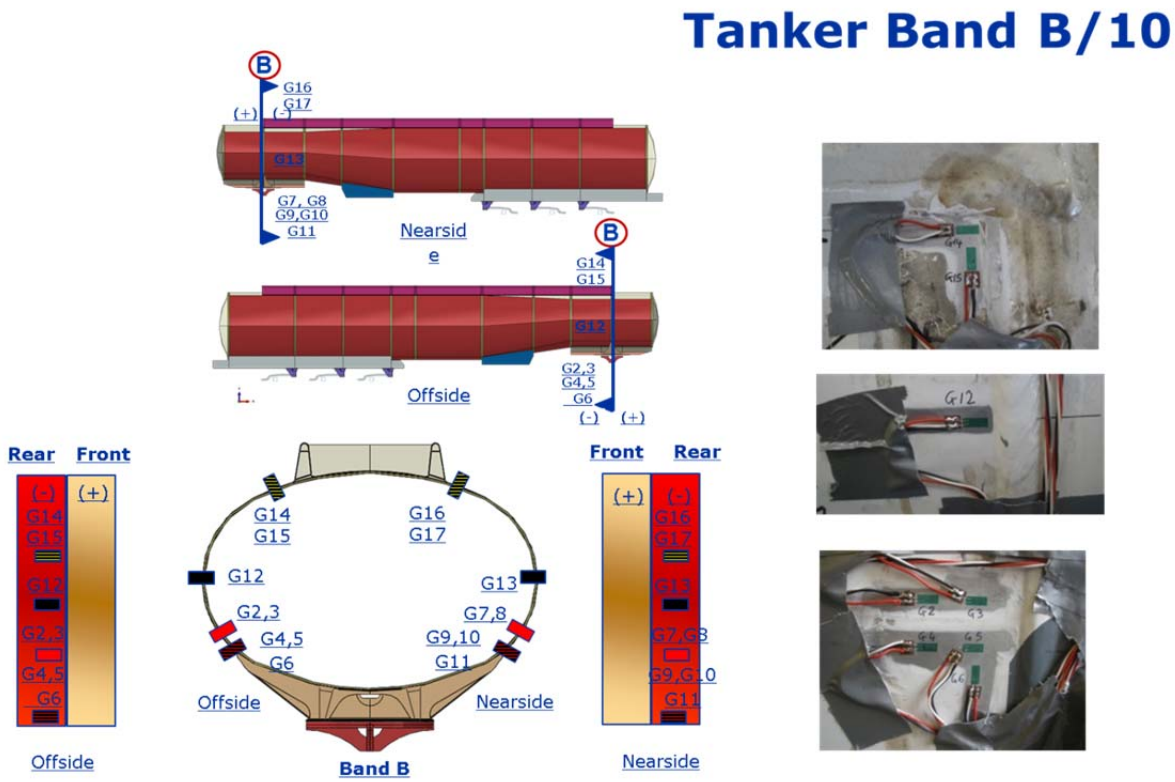

Figure B3 Illustration of the positions of strain gauges G2-17 on band B/10 (-).

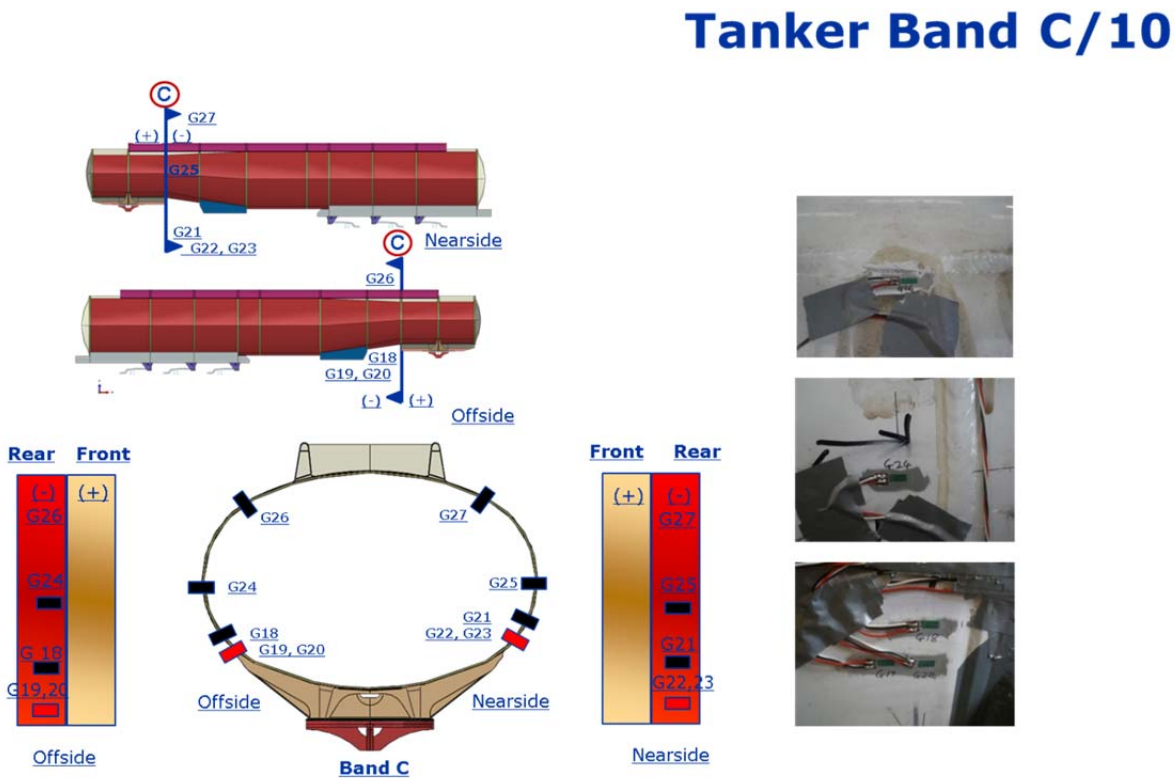

Figure B4 Illustration of the positions of strain gauges G18-27 for band C/10(-).

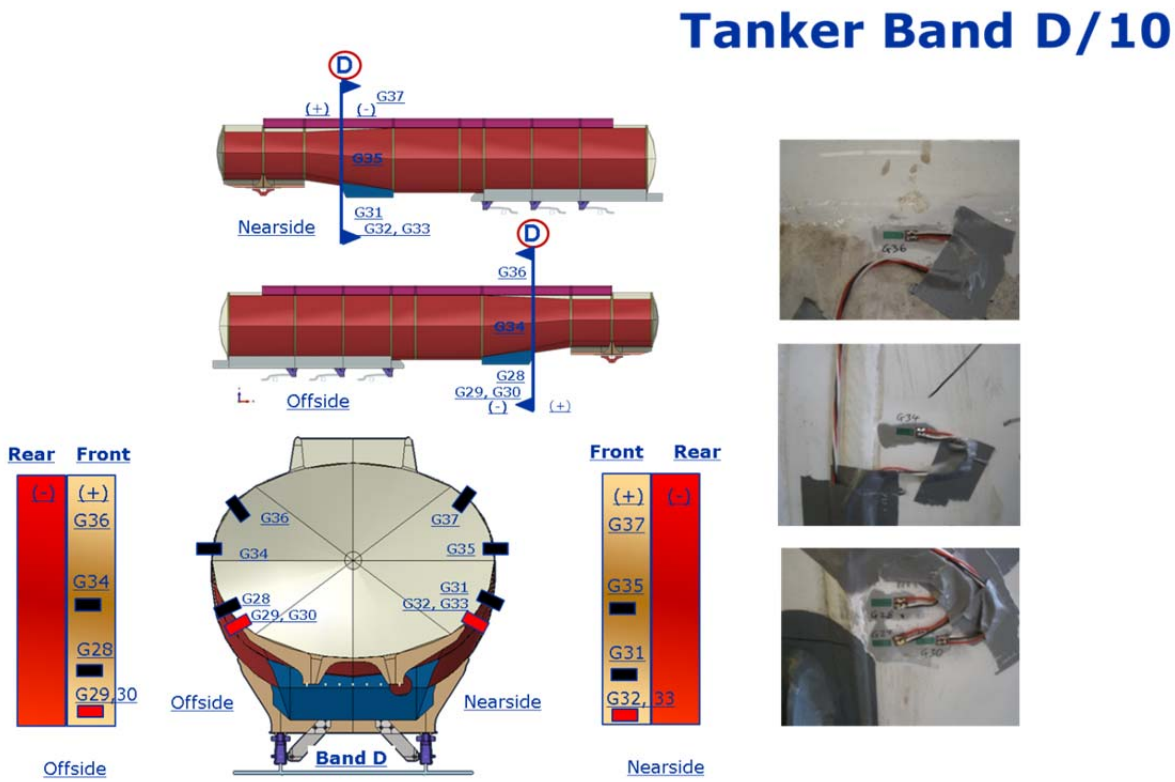

Figure B5 Illustration of the positions of strain gauges G28-37 for band D/10(+).

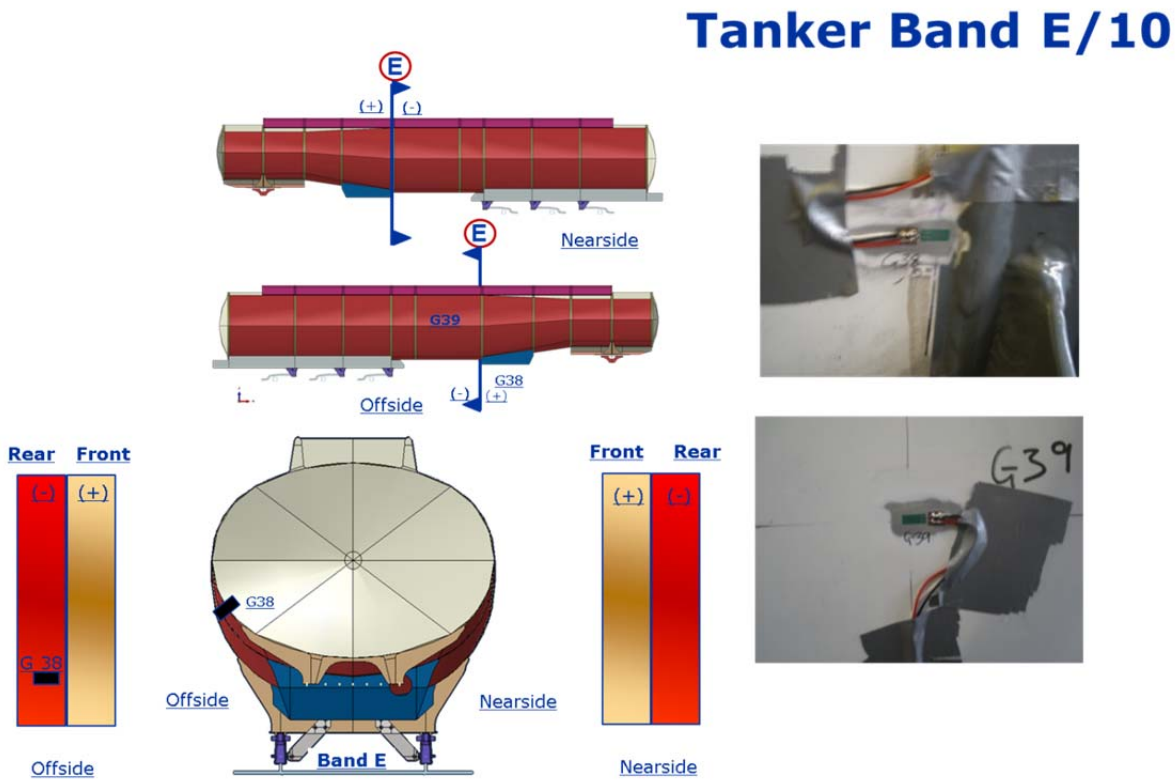

Figure B6 Illustration of the position of strain gauge G38 on band E/10(-) and the remote gauge G39, located midway between bands E and F.

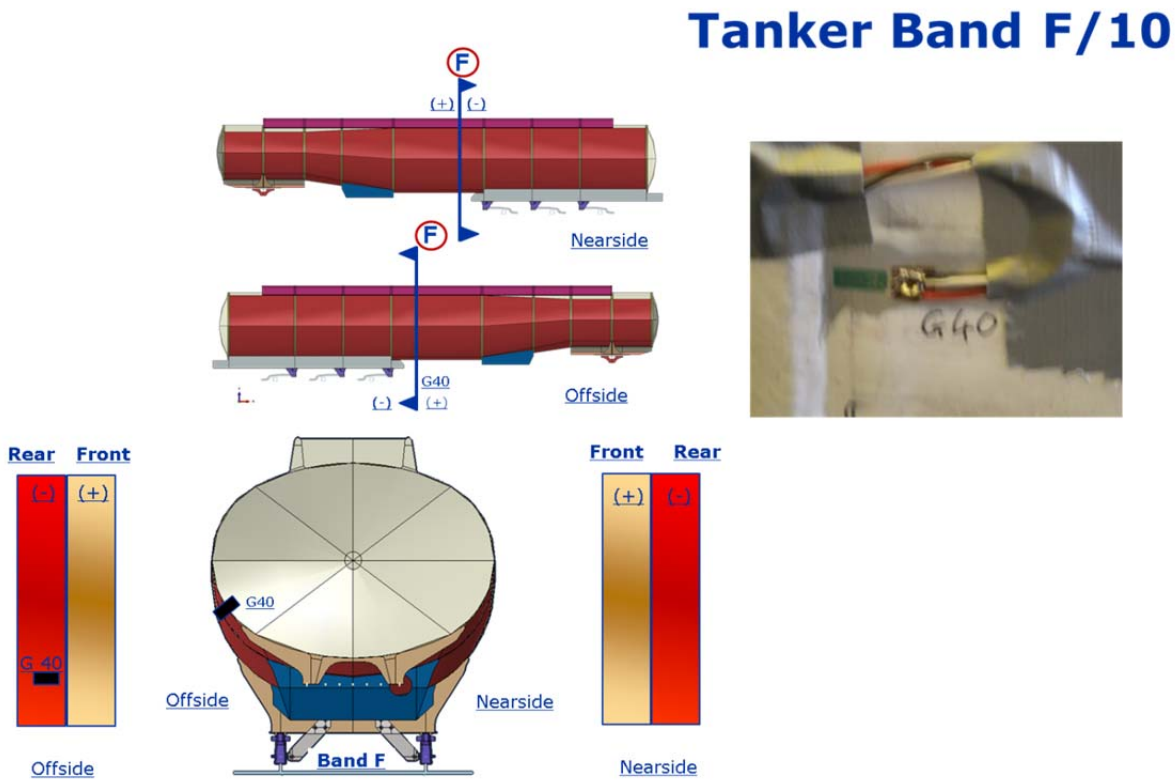

Figure B7 Illustration of the focussed gauge plan for band F/10(-).

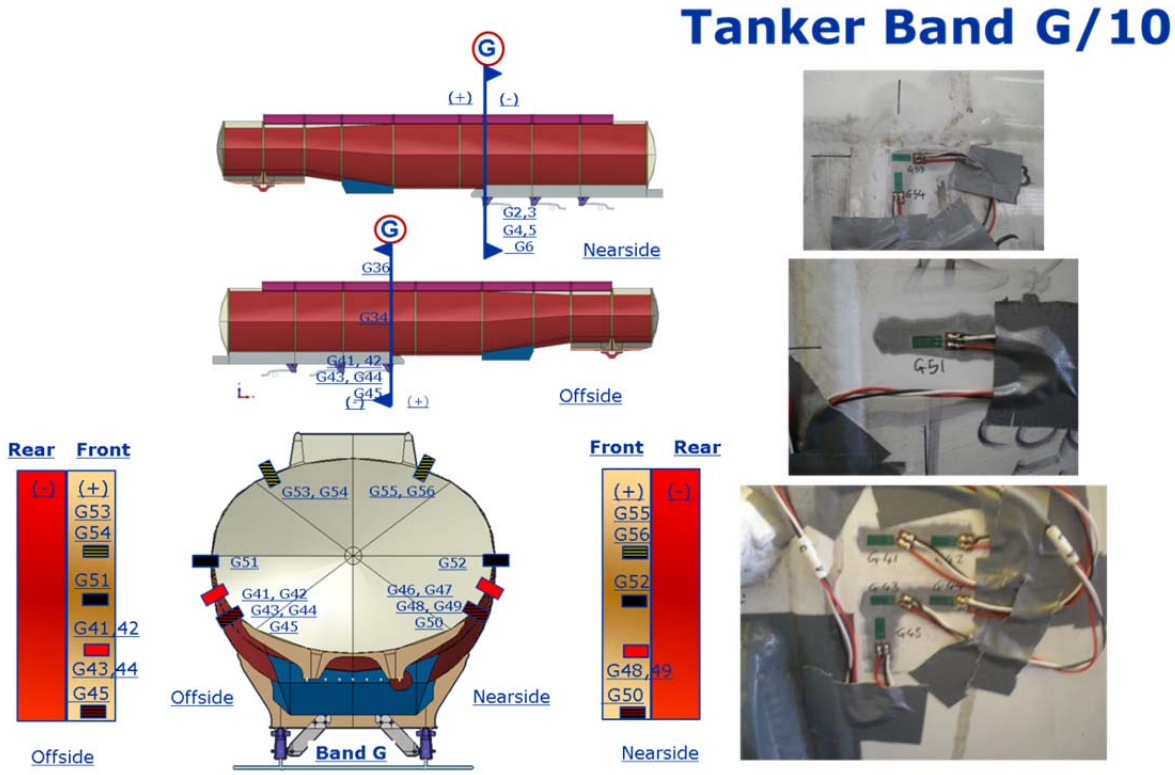

Figure B8 Illustration of the positions of strain gauges G41-56 on tanker band G/10(+).

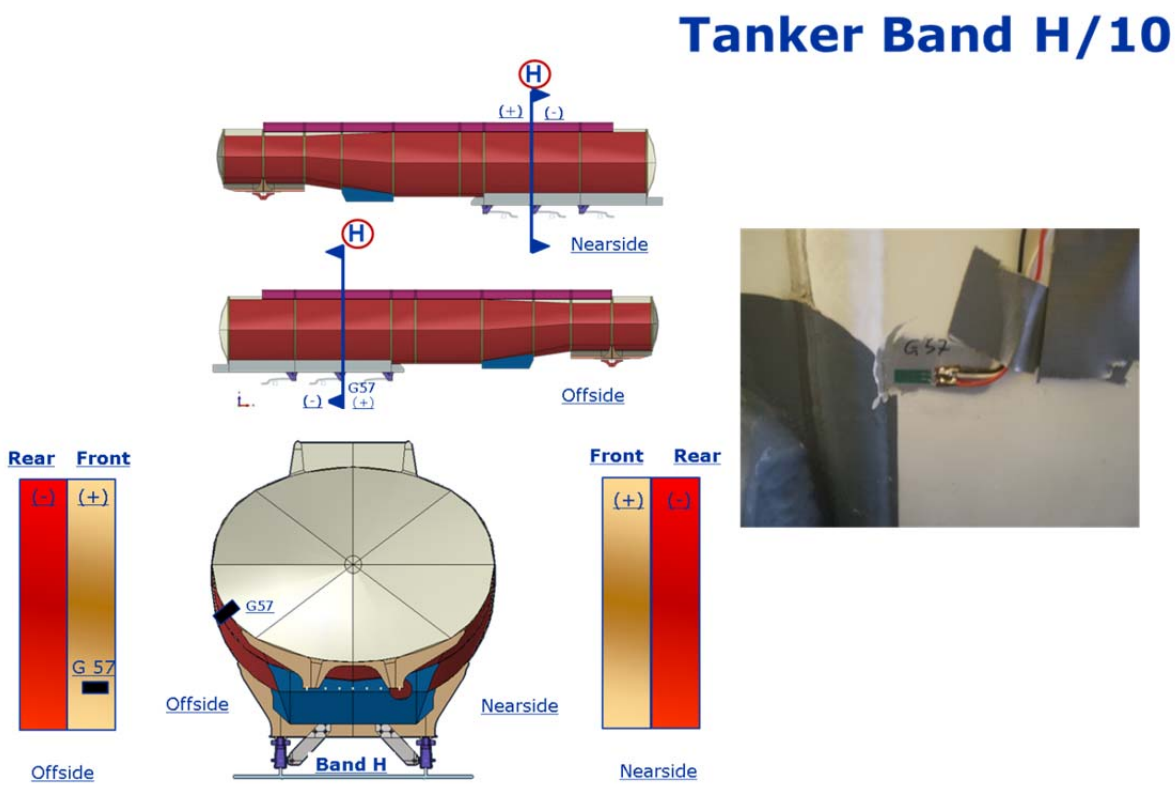

Figure B9 Illustration of the position of strain gauge G57 for band H/10(+).

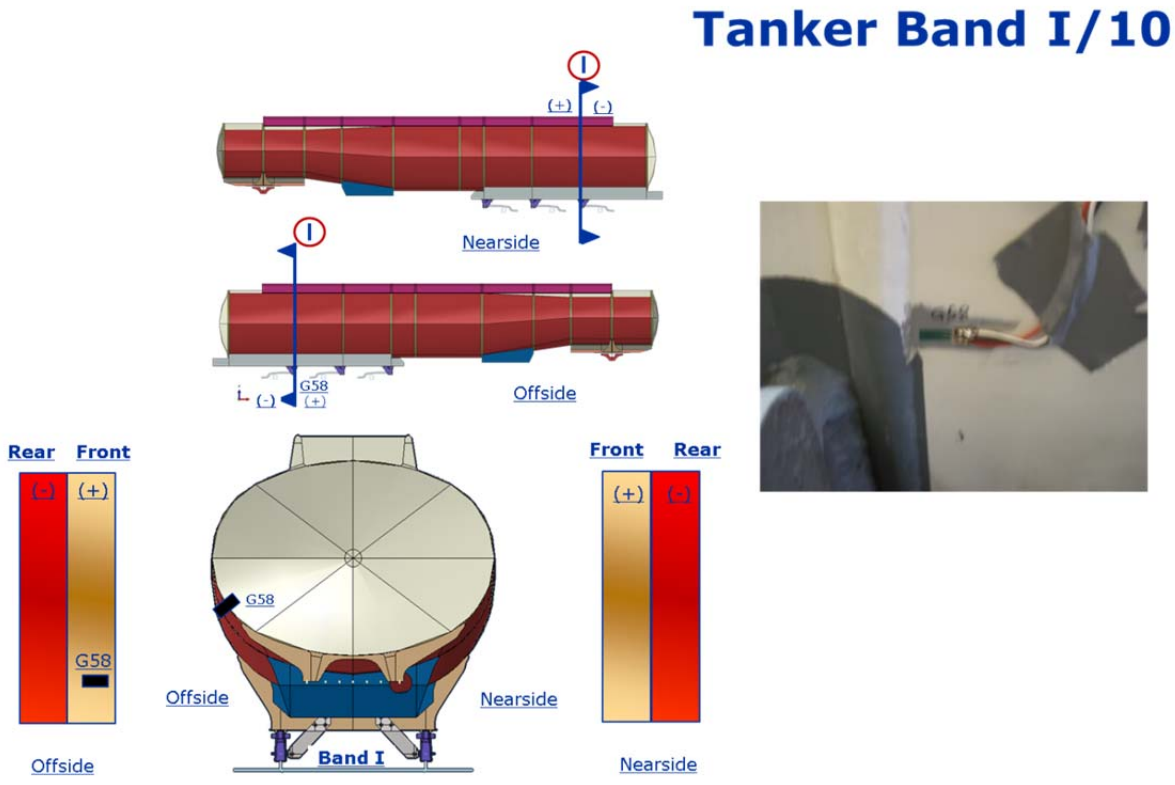

Figure B10 Illustration of the position of G58 for band I/10(+).

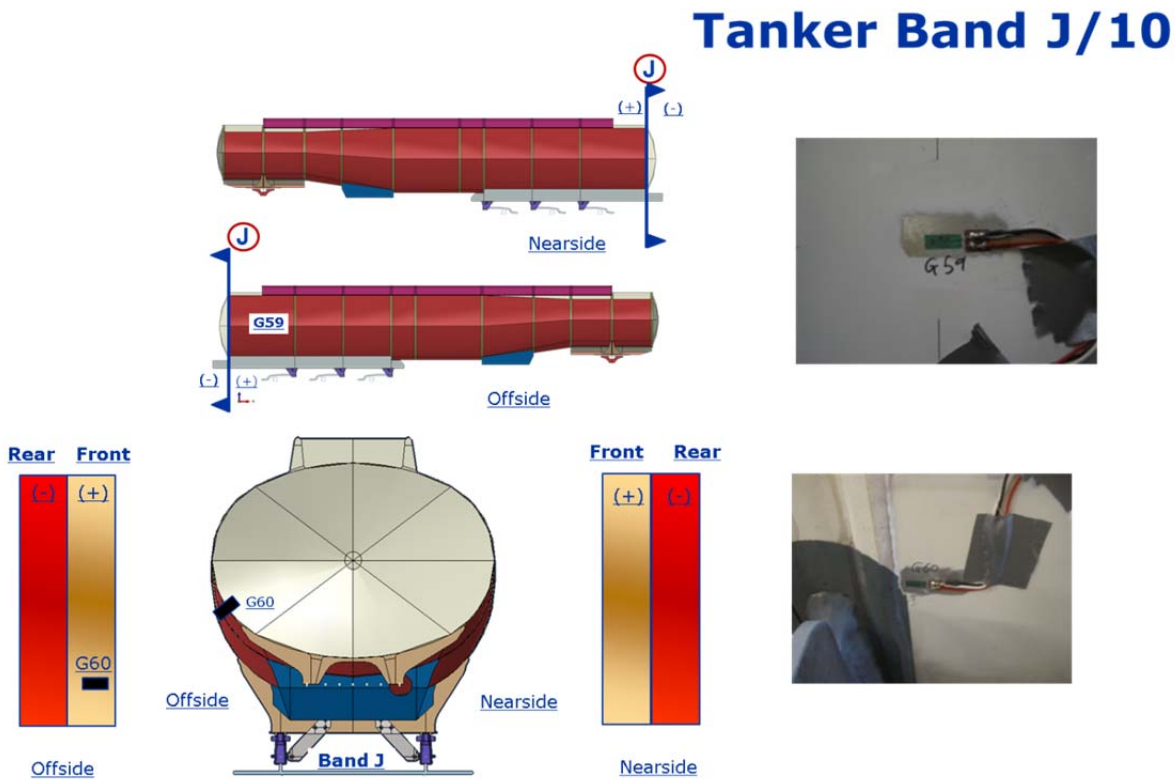

Figure B11 Illustration of the position of strain gauge G60 for band J/10(+) and the remote gauge G59 located between bands I and J.

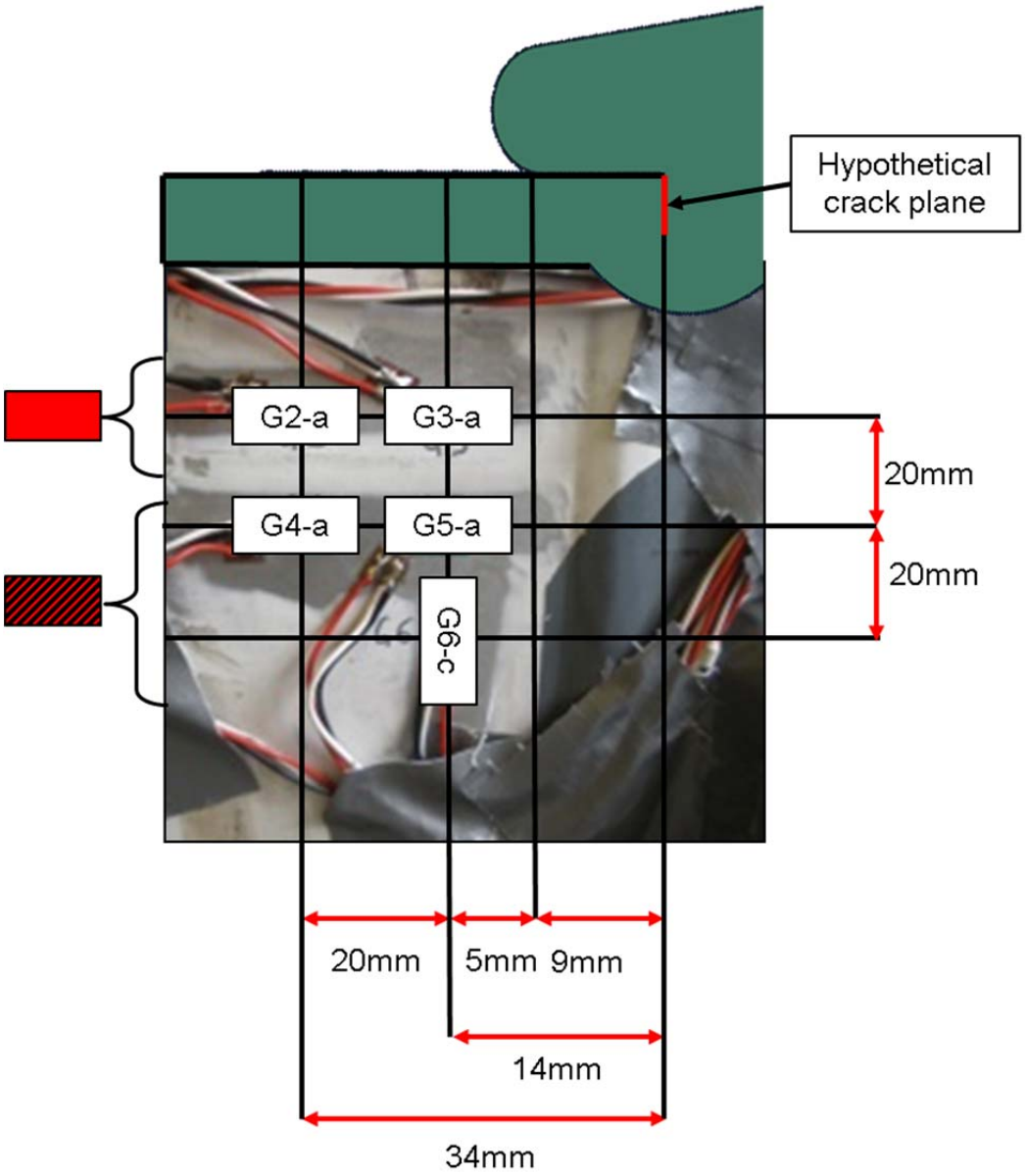

Figure B12 Illustration of the five-gauge assembly for local calculation and extrapolation of the stress taking into account biaxiality. The assembly shown is for the offside of band B adjacent to the cradle. The 9mm spacing is approximate and can vary from about 7.5mm to 9.0mm.

Appendix C

Event Log for Unladen Fatigue Data Collection and Filling Tanker

Appendix C: Event Log for Unladen Fatigue Data Collection and Filling Tanker

1 Overview

The unladen data collection exercise was carried out on Tuesday, 13 May and Wednesday 14 May 2014. In total, the unladen data collection exercise comprised 11 separate tests. In order to prevent strain gauge drift, before each test began, the strain gauges and accelerometers were zeroed. In this appendix, detailed descriptions of events and incidents that occurred during the test are recorded.

A summary of the key events are as follows:

- Number of recorded speed humps: 20
- Number of recorded pot hole events: 6
- Number of roundabout encounters: 92

Tables C1-C11 present the event logs for each of the eleven unladen tests. When applicable, each event is associated with a time from zero (start) time in both minutes and seconds as well as the clock time. The duration from start time can be used to analyse the strain and accelerometer data to identify the response of the tanker to the particular event.

Following the unladen data collection exercise, the tanker was filled with water at PCL on 12 June 2014. The compartments were filled sequentially from compartment (pot) 1 to compartment (pot) 6, with compartment 1 at the rear of the tanker and compartment 6 at the front of the tanker. The instrumentation on the tanker logged the strains associated with filling the tanker, and the times for each compartment are shown in Table C12.

Table C1 Event log for Test 1 – Verification of instrumentation activity

Date	13 May 2014		
Start time	-		
Event/Incident	Duration from zero time (min)	Duration from zero time (s)	Clock time
Technician generating signals by vibrating tanker	-	-	-

Table C2 Event log for Test 2 – Figure-of-eight manoeuvre

Date	13 May 2014		
Start time	4:38:00 PM		
Event/Incident	Duration from zero time (min)	Duration from zero time (s)	Clock time
Figure of 8	00:00:00	-	04:38:00 PM
Reverse into Bay	-	-	-
Finish	00:07:00	-	04:45:00 PM

Table C3 Event log for Test 3: Driving from Wincanton Yard to Coryton

Date	14 May 2014		
Start time	10:22:00 AM		
Event/Incident	Duration from zero time (min)	Duration from zero time (s)	Clock time
Leave yard	00:00:00	0.00	10:22:00 AM
Turn right	00:01:40	100.00	10:23:40 AM
Speed hump	00:02:30	150.00	10:24:30 AM
Turn left	00:03:00	180.00	10:25:00 AM
Speed hump	00:03:40	220.00	10:25:40 AM
Speed hump	00:04:00	240.00	10:26:00 AM
Turn right	00:04:40	280.00	10:26:40 AM
Pot holes	00:05:10	310.00	10:27:10 AM
Turn right	00:07:00	420.00	10:29:00 AM
Roundabout, 2nd exit	00:07:50	470.00	10:29:50 AM
Roundabout, 3rd exit	00:09:20	560.00	10:31:20 AM
Join A13 Tilbury, Roundabout, 3rd exit	00:11:03	663.00	10:33:03 AM
S R Left (?)	00:20:40	1240.00	10:42:40 AM
Roundabout, 3rd exit	00:21:10	1270.00	10:43:10 AM
Speed hump	00:23:30	1410.00	10:45:30 AM
Diversion	00:24:40	1480.00	10:46:40 AM
Roundabout, 4th exit	00:26:20	1580.00	10:48:20 AM
Speed hump	00:29:00	1740.00	10:51:00 AM
Turn left	00:29:30	1770.00	10:51:30 AM
Speed hump	00:32:10	1930.00	10:54:10 AM
Roundabout, 4th exit	00:33:20	2000.00	10:55:20 AM
Speed hump	00:33:40	2020.00	10:55:40 AM
Stop at Coryton	00:35:11	2111.00	10:57:11 AM

Table C4 Event log for Test 4: Figure-of-eight manoeuvre

Date	14 May 2014		
Start time	11:11:00 AM		
Event/Incident	Duration from zero time (min)	Duration from zero time (s)	Clock time
Start test	00:00:00	0.00	11:11:00 AM
End test	00:02:33	153.00	11:13:33 AM

Table C5 Event log for Test 5: Emergency Stop Test

Date	14 May 2014		
Start time	11:22:00 AM		
Event/Incident	Duration from zero time (min)	Duration from zero time (s)	Clock time
Start test	00:00:00	0.00	11:22:00 AM
Turn left	00:01:40	100.00	11:23:40 AM
Speed hump	00:01:50	110.00	11:23:50 AM
Emergency Stop	00:03:10	190.00	11:25:10 AM
Emergency Stop	00:05:00	300.00	11:27:00 AM
Speed hump	00:07:10	430.00	11:29:10 AM
Stop Test	00:08:08	488.00	11:30:08 AM

Table C6 Event log for Test 6: Coryton to A130 exit

Date	14 May 2014		
Start time	11:41:00 AM		
Event/Incident	Duration from zero time (min)	Duration from zero time (s)	Clock time
Start test in Coryton	00:00:00	0.00	11:41:00 AM
Turn left	00:01:15	75.00	11:42:15 AM
Speed hump	00:01:26	86.00	11:42:26 AM
Turn left	00:01:30	90.00	11:42:30 AM
Turn left	00:06:30	390.00	11:47:30 AM
Roundabout, 4th exit	00:06:50	410.00	11:47:50 AM
Roundabout, 3rd exit (A1014)	00:08:55	535.00	11:49:55 AM
Join A13, Turn left	00:12:27	747.00	11:53:27 AM
Roundabout, 1st exit (Basildon); Roundabout 3rd exit (A176)	00:16:12	972.00	11:57:12 AM
Speed hump / Traffic lights	00:14:50	890.00	11:55:50 AM
Roundabout, 2nd exit	00:15:58	958.00	11:56:58 AM
Roundabout, 3rd exit	00:16:28	988.00	11:57:28 AM
Traffic lights	00:17:35	1055.00	11:58:35 AM
Roundabout, 2nd exit	00:19:43	1183.00	12:00:43 PM
Roundabout, 1st exit	00:20:30	1230.00	12:01:30 PM
Roundabout, 2nd exit	00:21:47	1307.00	12:02:47 PM
Roundabout, 2nd exit	00:22:45	1365.00	12:03:45 PM
Roundabout, 3rd exit	00:23:24	1404.00	12:04:24 PM
Roundabout, 2nd exit	00:24:16	1456.00	12:05:16 PM
Roundabout, 2nd exit	00:26:30	1590.00	12:07:30 PM
Roundabout, 2nd exit	00:27:56	1676.00	12:08:56 PM
Roundabout, 3rd exit	00:28:42	1722.00	12:09:42 PM
Left turn (A130)	00:32:15	1935.00	12:13:15 PM
Stop test	00:34:47	2087.00	12:15:47 PM

Table C7 Event log for Test 7: A130 to A120 exit

Date	14 May 2014		
Start time	12:20:00 PM		
Event/Incident	Duration from zero time (min)	Duration from zero time (s)	Clock time
Start test (A130)	00:00:00	0.00	12:20:00 PM
Roundabout, 2nd exit	00:05:00	300.00	12:25:00 PM
Roundabout 3rd exit (join A12 North)	00:06:20	380.00	12:26:20 PM
Leave A12, Roundabout, 1st exit	00:11:36	696.00	12:31:36 PM
Roundabout, 2nd exit	00:12:43	763.00	12:32:43 PM
A130, roundabout 2nd exit	00:13:35	815.00	12:33:35 PM
Roundabout, 2nd exit	00:14:17	857.00	12:34:17 PM
Roundabout, 3rd exit	00:15:25	925.00	12:35:25 PM
Speed hump	00:16:00	960.00	12:36:00 PM
Roundabout, 2nd exit	00:16:50	1010.00	12:36:50 PM
Roundabout, 2nd exit	00:17:44	1064.00	12:37:44 PM
Roundabout, 2nd exit	00:18:40	1120.00	12:38:40 PM
Roundabout, 3rd exit	00:19:45	1185.00	12:39:45 PM
Pot hole	00:20:10	1210.00	12:40:10 PM
Roundabout, 2nd exit	00:22:40	1360.00	12:42:40 PM
Roundabout, 2nd exit	00:24:25	1465.00	12:44:25 PM
Roundabout, 1st exit	00:25:55	1555.00	12:45:55 PM
Roundabout, 1st exit	00:26:50	1610.00	12:46:50 PM
Roundabout, 2nd exit	00:27:55	1675.00	12:47:55 PM
Roundabout, 1st exit	00:28:20	1700.00	12:48:20 PM
Roundabout 3rd exit (Join A120)	00:29:17	1757.00	12:49:17 PM
Roundabout, 4th exit (A120)	00:32:00	1920.00	12:52:00 PM
Stop test	00:34:04	2044.00	12:54:04 PM

Table C8 Event log for Test 8: A120 to truck stop

Date	14 May 2014		
Start time	1:00:00 PM		
Event/Incident	Duration from zero time (min)	Duration from zero time (s)	Clock time
Start A120	00:00:00	0.00	01:00:00 PM
Roundabout, 2nd exit (A131)	00:02:27	147.00	01:02:27 PM
Speed hump	00:03:00	180.00	01:03:00 PM
Roundabout, 2nd exit	00:03:20	200.00	01:03:20 PM
Roundabout, 2nd exit	00:04:35	275.00	01:04:35 PM
Roundabout, 2nd exit	00:05:45	345.00	01:05:45 PM
Roundabout, 2nd exit	00:07:15	435.00	01:07:15 PM
Pot hole	00:07:20	440.00	01:07:20 PM
Roundabout, 2nd exit	00:09:10	550.00	01:09:10 PM
Roundabout, 1st exit	00:11:55	715.00	01:11:55 PM
Roundabout, 2nd exit	00:13:10	790.00	01:13:10 PM
Roundabout, 2nd exit	00:14:14	854.00	01:14:14 PM
Speed hump	00:14:30	870.00	01:14:30 PM
Roundabout, 2nd exit	00:15:10	910.00	01:15:10 PM
Roundabout, 1st exit	00:16:50	1010.00	01:16:50 PM
Roundabout, 2nd exit	00:18:00	1080.00	01:18:00 PM
Roundabout, 2nd exit	00:18:35	1115.00	01:18:35 PM
Roundabout, 1st exit	00:19:37	1177.00	01:19:37 PM
Roundabout, 2nd exit	00:20:50	1250.00	01:20:50 PM
Speed hump	00:20:58	1258.00	01:20:58 PM
Truck stop	00:22:18	1338.00	01:22:18 PM

Table C9 Event log for Test 9: Truck stop to Coryton

Date	14 May 2014		
Start time	2:16:00 PM		
Event/Incident	Duration from zero time (min)	Duration from zero time (s)	Clock time
Start truck stop	00:00:00	0.00	02:16:00 PM
Roundabout, 1st exit	00:02:00	120.00	02:18:00 PM
Roundabout, 3rd exit	00:02:50	170.00	02:18:50 PM
Roundabout, 3rd exit	00:03:19	199.00	02:19:19 PM
Roundabout, 3rd exit	00:09:15	555.00	02:25:15 PM
Speed hump	00:10:10	610.00	02:26:10 PM
Leave A130 onto A132	00:15:40	940.00	02:31:40 PM
Roundabout, 1st exit	00:16:10	970.00	02:32:10 PM
Roundabout, 1st exit	00:16:35	995.00	02:32:35 PM
Roundabout, 2nd exit	00:21:15	1275.00	02:37:15 PM
Roundabout, 2nd exit	00:22:18	1338.00	02:38:18 PM
Roundabout, 2nd exit	00:23:43	1423.00	02:39:43 PM
Roundabout, 2nd exit	00:26:26	1586.00	02:42:26 PM
Roundabout, 2nd exit	00:27:32	1652.00	02:43:32 PM
Roundabout, 2nd exit	00:28:30	1710.00	02:44:30 PM
Roundabout, 2nd exit	00:30:00	1800.00	02:46:00 PM
Roundabout, 2nd exit	00:31:25	1885.00	02:47:25 PM
Traffic lights	00:32:53	1973.00	02:48:53 PM
Roundabout, 1st exit	00:35:47	2147.00	02:51:47 PM
Roundabout, 2nd exit	00:36:09	2169.00	02:52:09 PM
Traffic lights	00:36:36	2196.00	02:52:36 PM
Traffic lights	00:38:07	2287.00	02:54:07 PM
Roundabout, 2nd exit	00:40:52	2452.00	02:56:52 PM
Roundabout, 3rd exit	00:41:10	2470.00	02:57:10 PM
Roundabout, 3rd exit	00:41:43	2503.00	02:57:43 PM
Onto A13 South	00:42:00	2520.00	02:58:00 PM
Onto A1014	00:44:52	2692.00	03:00:52 PM

Table C10 Event log for Test 9: Truck stop to Coryton continued

Traffic lights	00:45:15	2715.00	03:01:15 PM
Roundabout, 1st exit	00:45:40	2740.00	03:01:40 PM
Turn left	00:49:00	2940.00	03:05:00 PM
Speed hump	00:51:00	3060.00	03:07:00 PM
Roundabout, 3rd exit	00:52:06	3126.00	03:08:06 PM
Speed hump	00:52:30	3150.00	03:08:30 PM
Turn right	00:52:40	3160.00	03:08:40 PM
Stop at Coryton	00:53:53	3233.00	03:09:53 PM

Table C11 Event log for Test 10: Coryton to M25 and back to Coryton

Date	14 May 2014		
Start time	3:21:00 PM		
Event/Incident	Duration from zero time (min)	Duration from zero time (s)	Clock time
Start at Coryton	00:00:00	0.00	03:21:00 PM
Turn left and bump	00:01:00	60.00	03:22:00 PM
Roundabout 1st exit	00:01:38	98.00	03:22:38 PM
Pot hole	00:04:21	261.00	03:25:21 PM
Turn left	00:06:20	380.00	03:27:20 PM
Roundabout, 4th exit	00:07:20	440.00	03:28:20 PM
Roundabout 2nd exit (A13)	00:09:00	540.00	03:30:00 PM
Off A13 onto M25 anticlockwise	00:17:47	1067.00	03:38:47 PM
Roundabout 3rd exit	00:18:16	1096.00	03:39:16 PM
Traffic lights on roundabout (M25 J29)	00:18:47	1127.00	03:39:47 PM
Roundabout turn left?	00:26:40	1600.00	03:47:40 PM
Turn left	00:27:25	1645.00	03:48:25 PM
Back onto M25?	00:29:40	1780.00	03:50:40 PM
Off M25 at J28	00:33:06	1986.00	03:54:06 PM
Traffic lights	00:33:35	2015.00	03:54:35 PM
Traffic lights	00:33:42	2022.00	03:54:42 PM
Traffic lights	00:34:15	2055.00	03:55:15 PM
Re-join M25 clockwise (off J29 360° back onto M25)	00:34:56	2096.00	03:55:56 PM
Traffic lights	00:38:24	2304.00	03:59:24 PM
Traffic lights	00:40:18	2418.00	04:01:18 PM
Re-join (off M25 J30 onto A13)	00:40:55	2455.00	04:01:55 PM
Turn left	00:47:00	2820.00	04:08:00 PM
Off A13 roundabout 3rd exit (A1014)	00:56:40	3400.00	04:17:40 PM
Turn left	00:59:00	3540.00	04:20:00 PM
Roundabout third exit	01:03:46	-	04:24:46 PM
Speed hump and turn right	01:04:09	-	04:25:09 PM
Stop at Coryton	01:05:18	-	04:26:18 PM

Table C12 Event log for Test 11: Start at Coryton and return to Wincanton

Date	14 May 2014		
Start time	4:31:00 PM		
Event/Incident	Duration from zero time (min)	Duration from zero time (s)	Clock time
Start at Coryton	00:00:00	0.00	04:31:00 PM
Pot hole and turn left	00:01:30	90.00	04:32:30 PM
Roundabout 1st exit	00:01:50	110.00	04:32:50 PM
Turn left	00:05:42	342.00	04:36:42 PM
Roundabout 4th exit	00:07:20	440.00	04:38:20 PM
Roundabout 2nd exit (A13) roundabout 1st exit (off A13)	00:19:25	1165.00	04:50:25 PM
Roundabout 3rd exit	00:21:05	1265.00	04:52:05 PM
Roundabout 2rd exit	00:22:30	1350.00	04:53:30 PM
Roundabout 1st exit	00:23:30	1410.00	04:54:30 PM
Pot hole	00:24:50	1490.00	04:55:50 PM
Turn left	00:25:33	1533.00	04:56:33 PM
Roundabout 3rd exit	00:26:31	1591.00	04:57:31 PM
Speed hump	00:26:50	1610.00	04:57:50 PM
Arrive at yard, reverse into bay	00:31:20	1880.00	05:02:20 PM
Finish	00:31:50	1910.00	05:02:50 PM

Table C13 Event log for Test 12: Filling the tanker

Date	12 June 2014		
Start time	8:57:00 PM		
Event/Incident	Duration from zero time (min)	Duration from zero time (s)	Clock time
Start filling Pot 1	00:00:00	0.00	08:57:00 AM
Finish filling Pot 1	00:17:30	1050.00	09:14:30 AM
Start filling Pot 2	00:17:30	1050.00	09:14:30 AM
Finish filling Pot 2	00:35:45	2145.00	09:32:45 AM
Start filling Pot 3	00:35:45	2145.00	09:32:45 AM
Finish filling Pot 3	00:52:10	3130.00	09:49:10 AM
Start filling Pot 4	00:52:10	3130.00	09:49:10 AM
Finish filling Pot 4	01:10:10	-	10:07:10 AM
Start filling Pot 5	01:10:10	-	10:07:10 AM
Finish filling Pot 5	01:40:30	-	10:37:30 AM
Start filling Pot 6	01:40:30	-	10:37:30 AM
Finish filling Pot 6	01:57:05	-	10:54:05 AM

Appendix D

Event Log for Laden Fatigue Data Collection and Emptying Tanker

Appendix D: Event Log for Laden Fatigue Data Collection and Emptying Tanker

1 Overview

The laden data collection exercise was carried out on Friday, 13 June 2014. In total, the laden data collection exercise comprised 10 separate tests (starting at Test 13 as a continuation from the unladen test and filling test numbering). In order to prevent strain gauge drift, before each test began, the strain gauges and accelerometers were zeroed. In this appendix, detailed descriptions of events and incidents that occurred during the test are recorded.

A summary of the key events are as follows:

- Number of recorded speed humps: 6
- Number of recorded pot hole events: 5
- Number of roundabout encounters: 94

Tables E1-E10 present the event logs for each of the ten laden tests. When applicable, each event is associated with a time from zero (start) time in both minutes and seconds as well as the clock time. The duration from start time can be used to analyse the strain and accelerometer data to identify the response of the tanker to the particular event.

Following the laden data collection exercise, the tanker was emptied on 16 June 2014 at PCL (Test 23). The compartments were emptied sequentially from compartment (pot) 1 to compartment (pot) 6, with compartment 1 at the back of the tanker and compartment 6 at the front of the tanker. The instrumentation on the tanker logged the strains associated with the emptying test, and the times for each compartment are shown in Table E11.

Table D1 Event log for Test 13 – Pullman's yard to Coryton

Date	13 June 2014		
Start time	11:33:00 AM		
Event/Incident	Duration from zero time (min)	Duration from zero time (s)	Clock time
Start Pullman's Yard to Coryton	00:00:00	0.00	11:33:00 AM
Pot hole and turn left	00:02:58	178.00	11:35:58 AM
Speed hump	00:03:28	208.00	11:36:28 AM
Turn right	00:04:20	260.00	11:37:20 AM
Turn left	00:05:25	325.00	11:38:25 AM
Roundabout 3rd exit	00:07:00	420.00	11:40:00 AM
Roundabout 2nd exit	00:11:36	696.00	11:44:36 AM
Roundabout 3rd exit	00:13:35	815.00	11:46:35 AM
Onto A13	00:15:20	920.00	11:48:20 AM
Turn left	00:27:13	1633.00	12:00:13 PM
Speed hump	00:31:15	1875.00	12:04:15 PM
Roundabout 3rd exit	00:32:20	1940.00	12:05:20 PM
Speed hump	00:32:50	1970.00	12:05:50 PM
Turn right	00:33:07	1987.00	12:06:07 PM
Arrive at Coryton	00:34:00	2040.00	12:07:00 PM

Table D2 Event log for Test 14 –

Date	13 June 2014		
Start time	12:07:00 PM		
Event/Incident	Duration from zero time (min)	Duration from zero time (s)	Clock time
Zero Gauges	00:00:00	0.00	12:07:00 AM
Figure 8 Test	00:04:00	360.00	12:11:00 AM

Table D3 Event log for Test 15: Emergency stop tests

Date	13 June 2014		
Start time	12:12:00 PM		
Event/Incident	Duration from zero time (min)	Duration from zero time (s)	Clock time
Start	00:00:00	0.00	12:12:00 PM
Pot hole and turn left	00:01:30	90.00	12:13:30 PM
Emergency stop	00:03:14	194.00	12:15:14 PM
U-turn	00:04:30	270.00	12:16:30 PM
Emergency stop	00:05:55	355.00	12:17:55 PM
Roundabout 3rd exit	00:06:55	415.00	12:18:55 PM
Speed hump and turn left	00:07:30	450.00	12:19:30 PM
Stop at Coryton	00:08:00	460.00	12:20:00 PM

Table D4 Event log for Test 16: Coryton to A130 exit/lay by

Date	13 June 2014		
Start time	12:23:00 PM		
Event/Incident	Duration from zero time (min)	Duration from zero time (s)	Clock time
Start	00:00:00	0.00	12:23:00 PM
Pot hole and turn left	00:01:20	80.00	12:24:20 PM
Roundabout1st exit	00:01:40	100.00	12:24:40 PM
Roundabout 3rd exit	00:07:20	440.00	12:30:20 PM
Roundabout 3rd exit	00:09:40	580.00	12:32:40 PM
Onto A13 (Turn left free bells)	00:13:50	830.00	12:36:50 PM
Roundabout1st exit, onto A176	00:14:20	860.00	12:37:20 PM
Roundabout (?) exit	00:15:55	955.00	12:38:55 PM
Turn left	00:16:44	1004.00	12:39:44 PM
Roundabout 2nd exit	00:17:55	1075.00	12:40:55 PM
Roundabout 360	00:19:20	1160.00	12:42:20 PM
Roundabout 3rd exit	00:20:35	1235.00	12:43:35 PM
Turn left	00:21:12	1272.00	12:44:12 PM
Roundabout 2nd exit onto A152	00:22:50	1370.00	12:45:50 PM
Roundabout 2nd exit	00:23:55	1435.00	12:46:55 PM
Turn left	00:25:47	1547.00	12:48:47 PM
Roundabout1st exit	00:27:16	1636.00	12:50:16 PM
Roundabout 2nd exit	00:27:50	1670.00	12:50:50 PM
Roundabout 2nd exit	00:29:00	1740.00	12:52:00 PM
Queuing traffic	00:31:25	1885.00	12:54:25 PM
Roundabout 2nd exit	00:33:17	1997.00	12:56:17 PM
Roundabout 2nd exit	00:34:40	2080.00	12:57:40 PM
Roundabout 2nd exit	00:35:55	2155.00	12:58:55 PM
Turn left onto 130	00:39:40	2380.00	01:02:40 PM
Stop on A130 lay by	00:40:00	2400.00	01:03:00 PM

Table D5 Event log for Test 17: A130 to A120 exit

Date	13 June 2014		
Start time	1:07:00 PM		
Event/Incident	Duration from zero time (min)	Duration from zero time (s)	Clock time
Start on A130	00:00:00	0.00	01:07:00 PM
Roundabout 2nd exit	00:08:40	520.00	01:15:40 PM
Roundabout 3rd exit onto A12	00:09:25	565.00	01:16:25 PM
Turn left	00:12:50	770.00	01:19:50 PM
Roundabout 2nd exit	00:13:30	810.00	01:20:30 PM
Roundabout 3rd exit	00:15:35	935.00	01:22:35 PM
Roundabout 2nd exit	00:17:10	1030.00	01:24:10 PM
Roundabout 2nd exit	00:17:50	1070.00	01:24:50 PM
Roundabout 3rd exit	00:18:57	1137.00	01:25:57 PM
Roundabout 2nd exit	00:20:02	1202.00	01:27:02 PM
Roundabout 2nd exit	00:20:45	1245.00	01:27:45 PM
Roundabout 2nd exit	00:21:49	1309.00	01:28:49 PM
Roundabout 3rd exit	00:23:13	1393.00	01:30:13 PM
Roundabout 3rd exit onto A131	00:24:24	1464.00	01:31:24 PM
Roundabout 2nd exit	00:22:27	1347.00	01:29:27 PM
Roundabout 2nd exit	00:29:30	1770.00	01:36:30 PM
Roundabout 1st exit onto A131	00:31:08	1868.00	01:38:08 PM
Roundabout 2nd exit	00:32:30	1950.00	01:39:30 PM
Roundabout 2nd exit	00:33:45	2025.00	01:40:45 PM
Roundabout 2nd exit	00:34:40	2080.00	01:41:40 PM
Roundabout 3rd exit	00:35:35	2135.00	01:42:35 PM
Queuing traffic	00:38:38	2318.00	01:45:38 PM
Roundabout 360	00:41:56	2516.00	01:48:56 PM
Stop on A120 lay by	00:42:30	2550.00	01:49:30 PM

Table D6 Event log for Test 18: A120 lay by to truck stop

Date	13 June 2014		
Start time	1:58:00 AM		
Event/Incident	Duration from zero time (min)	Duration from zero time (s)	Clock time
Start on A120 lay by	00:00:00	0.00	01:58:00 PM
Roundabout 2nd exit	00:02:43	163.00	02:00:43 PM
Roundabout 1st exit onto A131	00:03:40	220.00	02:01:40 PM
Roundabout 2nd exit	00:04:20	260.00	02:02:20 PM
Roundabout 2nd exit	00:05:50	350.00	02:03:50 PM
Roundabout 2nd exit	00:07:14	434.00	02:05:14 PM
Roundabout 2nd exit	00:08:53	533.00	02:06:53 PM
Roundabout 2nd exit	00:10:55	655.00	02:08:55 PM
Roundabout 1st exit onto A130	00:13:50	830.00	02:11:50 PM
Roundabout 2nd exit	00:15:45	945.00	02:13:45 PM
Roundabout 2nd exit	00:16:50	1010.00	02:14:50 PM
Roundabout 2nd exit	00:17:55	1075.00	02:15:55 PM
Roundabout 2nd exit	00:19:00	1140.00	02:17:00 PM
Roundabout 1st exit	00:20:00	1200.00	02:18:00 PM
Roundabout 2nd exit	00:21:00	1260.00	02:19:00 PM
Roundabout 2nd exit	00:21:40	1300.00	02:19:40 PM
Roundabout 1st exit	00:22:38	1358.00	02:20:38 PM
Roundabout 1st exit	00:23:50	1430.00	02:21:50 PM
Stop at truck stop	00:25:00	1500.00	02:23:00 PM

Table D7 Event log for Test 19: Truck stop to Coryton

Date	13 June 2014		
Start time	2:57:00 PM		
Event/Incident	Duration from zero time (min)	Duration from zero time (s)	Clock time
Start at truck stop	00:00:00	0.00	02:57:00 PM
Roundabout 1st exit	00:01:20	80.00	02:58:20 PM
Roundabout 3rd exit onto A12	00:02:20	140.00	02:59:20 PM
Off A12 Roundabout 1st exit onto A130	00:08:10	490.00	03:05:10 PM
Off A130 Roundabout 1st exit onto A132	00:15:36	936.00	03:12:36 PM
Roundabout 1st exit	00:16:15	975.00	03:13:15 PM
Roundabout 1st exit	00:20:32	1232.00	03:17:32 PM
Queuing traffic	00:21:30	1290.00	03:18:30 PM
Roundabout 2nd exit	00:22:40	1360.00	03:19:40 PM
Roundabout 2nd exit	00:24:20	1460.00	03:21:20 PM
Roundabout 2nd exit	00:27:30	1650.00	03:24:30 PM
Roundabout 2nd exit	00:28:15	1695.00	03:25:15 PM
Roundabout 2nd exit	00:29:00	1740.00	03:26:00 PM
Roundabout 2nd exit	00:30:40	1840.00	03:27:40 PM
Roundabout 3rd exit	00:32:20	1940.00	03:29:20 PM
Roundabout 2nd exit	00:33:30	2010.00	03:30:30 PM
Roundabout 1st exit	00:37:00	2220.00	03:34:00 PM
Roundabout 2nd exit	00:37:20	2240.00	03:34:20 PM
Queuing traffic	00:38:10	2290.00	03:35:10 PM
Roundabout 2nd exit	00:41:15	2475.00	03:38:15 PM
Roundabout 2nd exit	00:43:00	2580.00	03:40:00 PM
Roundabout 3rd exit	00:43:45	2625.00	03:40:45 PM
Roundabout 3rd exit onto A13	00:44:05	2645.00	03:41:05 PM
Off A13	00:47:30	2850.00	03:44:30 PM
Roundabout 1st exit onto A1014	00:48:00	2880.00	03:45:00 PM

Table D8 Event log for Test 19: Truck stop to Coryton continued

Turn left	00:50:00	3000.00	03:47:00 PM
Roundabout 3rd exit	00:54:48	3288.00	03:51:48 PM
Speed hump and turn right	00:55:20	3320.00	03:52:20 PM
Stop at Coryton	00:56:00	3360.00	03:53:00 PM

Table D9 Event log for Test 20: Coryton to M25 excursion back to Coryton

Date	13 June 2014		
Start time	3:58:00 PM		
Event/Incident	Duration from zero time (min)	Duration from zero time (s)	Clock time
Start at Coryton	00:00:00	0.00	03:58:00 PM
Pot hole and turn left	00:01:20	80.00	03:59:20 PM
Roundabout 1st exit	00:01:40	100.00	03:59:40 PM
Turn left	00:06:25	385.00	04:04:25 PM
Roundabout 3rd exit	00:08:00	480.00	04:06:00 PM
Roundabout 1st exit onto A13	00:10:15	615.00	04:08:15 PM
Off A13	00:18:52	1132.00	04:16:52 PM
Roundabout 3rd exit onto M25	00:19:26	1166.00	04:17:26 PM
ACW J30 J29 360	00:27:40	1660.00	04:25:40 PM
Back onto M25 ACW J28 180	00:32:48	1968.00	04:30:48 PM
Back onto M25 CW J29 360	00:38:36	2316.00	04:36:36 PM
Back onto M25 CW J30 off M25 Roundabout 1st exit onto A13	00:52:47	3167.00	04:50:47 PM
Off A13 to Roundabout 3rd exit	01:02:02	-	05:00:02 PM
Turn left	01:05:00	-	05:03:00 PM
Onto A1014 Roundabout 2nd exit	01:09:00	-	05:07:00 PM
Speed hump and turn right	01:09:44	-	05:07:44 PM
Stop at Coryton	01:11:00	-	05:09:00 PM

Table D10 Event log for Test 21: __

Date	13 June 2014		
Start time	2:16:00 PM		
Event/Incident	Duration from zero time (min)	Duration from zero time (s)	Clock time
Test Cancelled			

Table D11 Event log for Test 22: Coryton back to Pullman's yard

Date	13 June 2014		
Start time	5:10:00 PM		
Event/Incident	Duration from zero time (min)	Duration from zero time (s)	Clock time
Start at Coryton	00:00:00	0.00	05:10:00 PM
Pot hole and turn left	00:01:50	110.00	05:11:50 PM
Roundabout 1st exit	00:02:11	131.00	05:12:11 PM
Turn left onto A1014	00:06:34	394.00	05:16:34 PM
Roundabout 3rd exit	00:07:30	450.00	05:17:30 PM
Roundabout 1st exit onto A13	00:09:40	580.00	05:19:40 PM
Off A13	00:18:38	1118.00	05:28:38 PM
Roundabout 1st exit onto A1306	00:19:11	1151.00	05:29:11 PM
Queuing traffic	00:20:30	1230.00	05:30:30 PM
Roundabout 3rd exit	00:22:20	1340.00	05:32:20 PM
Roundabout 2nd exit	00:23:25	1405.00	05:33:25 PM
Roundabout 1st exit	00:24:35	1475.00	05:34:35 PM
Turn left	00:25:30	1530.00	05:35:30 PM
Turn left	00:26:44	1604.00	05:36:44 PM
Turn right	00:27:30	1650.00	05:37:30 PM
Turn right	00:28:00	1680.00	05:38:00 PM
Finish	00:29:00	1740.00	05:39:00 PM

Table D12 Event log for Test 23: Emptying water at PCL

Date	16 June 2014		
Start time	11:52:00 PM		
Event/Incident	Duration from zero time (min)	Duration from zero time (s)	Clock time
Start empting pot 1	00:00:00	0.00	11:52:00 AM
Finish emptying pot 1	00:17:50	1070.00	12:09:50 PM
Start empting pot 2	00:17:50	1070.00	12:09:50 PM
Finish emptying pot 2	00:36:20	2180.00	12:28:20 PM
Start empting pot 3	00:36:20	2180.00	12:28:20 PM
Finish emptying pot 3	00:54:40	3280.00	12:46:40 PM
Start empting pot 4	00:54:40	3280.00	12:46:40 PM

Table D13 Event log for Test 23: Emptying water at PCL continued

Finish emptying pot 4	01:13:20	800.00	01:05:20 PM
Start empting pot 5	01:13:20	800.00	01:05:20 PM
Finish emptying pot 5	01:26:36	1596.00	01:18:36 PM
Start empting pot 6	01:26:36	1596.00	01:18:36 PM
Finish emptying pot 6	01:44:32	2672.00	01:36:32 PM

Appendix E

Preliminary Stress Range Histograms for Instrumented Locations

Appendix E: Stress Range Histograms for Instrumented Locations

1 Overview

As described in Section 3, strain gauge data were recorded during five hours of unladen testing, five hours of laden testing and during filling and emptying operations. The data were processed to obtain the stress acting transverse (normal) to the circumferential seam welds. The derived stress versus time series were then rain flow counted to obtain stress range histograms, ie the frequency of a given stress range acting at a particular location.

The figures presented in this appendix can be used as indicators of the severity of the fatigue stress spectra acting on each instrumented position of each of the ten circumferential seam welds. The following commentary is required to put the figures in the appropriate context:

- The curves indicated by the legend entry 'Empty' were obtained by concatenating the unladen data obtained from Test 2 through Test 11 (approximately five hours). Test 1 was omitted as this involved the technician generating vibrations of the tanker to ensure the instrumentation was active. Thus, the unladen concatenated data contains figure-of-eight manoeuvres, two emergency stops and various road conditions and events as detailed in Appendix C.
- The curves indicated by the legend entry 'Laden' were obtained by concatenating the laden data obtained from Test 13 through Test 22 (approximately five hours) *with the filling and emptying tests*. The latter was added for convenience as the events are short-term and constitute few cycles of the overall plots. The laden portion of the concatenated data contains figure-of-eight manoeuvres, two emergency stops and various road conditions and events as detailed in Appendix D. The representative duty cycle will split the contributions of the filling and emptying from the actual laden/unladen strain data.
- The curves indicated by the legend entry 'Axial' were obtained as described in Section 2.7.1.2 and 2.7.1.3 and indicate that circumferential (hoop) strains were not measured and hence were assumed to be zero.
- The curves indicated by the legend entry 'Biaxial' were obtained as described in Section 2.7.1.4 and Section 2.7.1.5 and indicate that the circumferential strains were measured at the location and therefore the derived stresses take into account biaxiality.
- Where useful, cross-sections of the tanker and the positions of the relevant gauges have been included in the plots. For more detailed information about the actual gauge identification and position, see Appendix B.

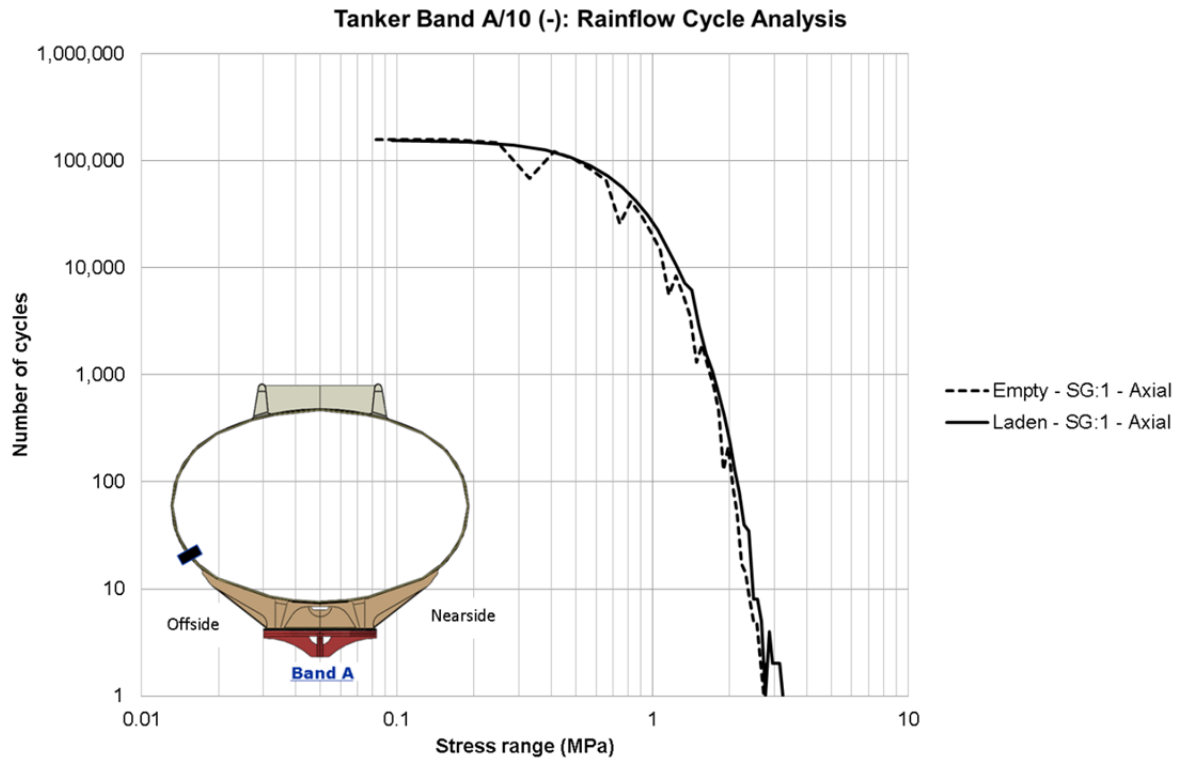

Figure E1 Stress range histogram for the one instrumented location on band A/10(-).

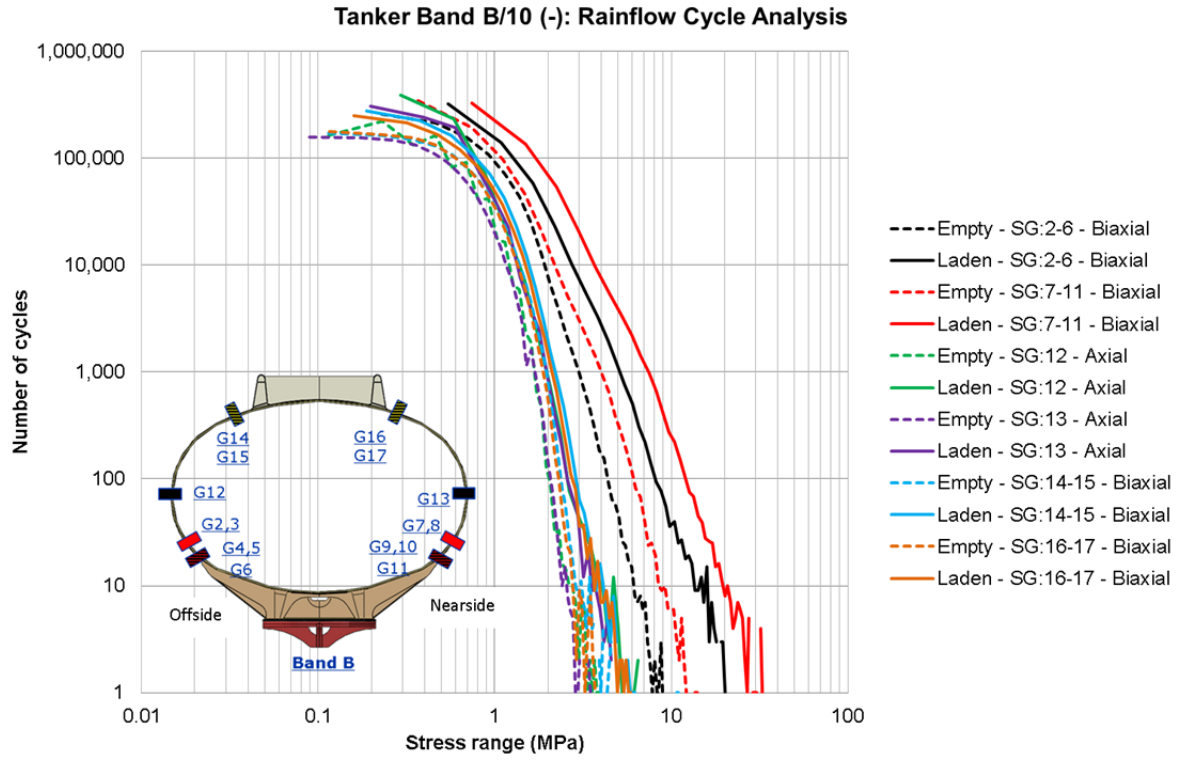

Figure E2 Stress range histograms for the six distinct instrumented locations on band B/10(-).

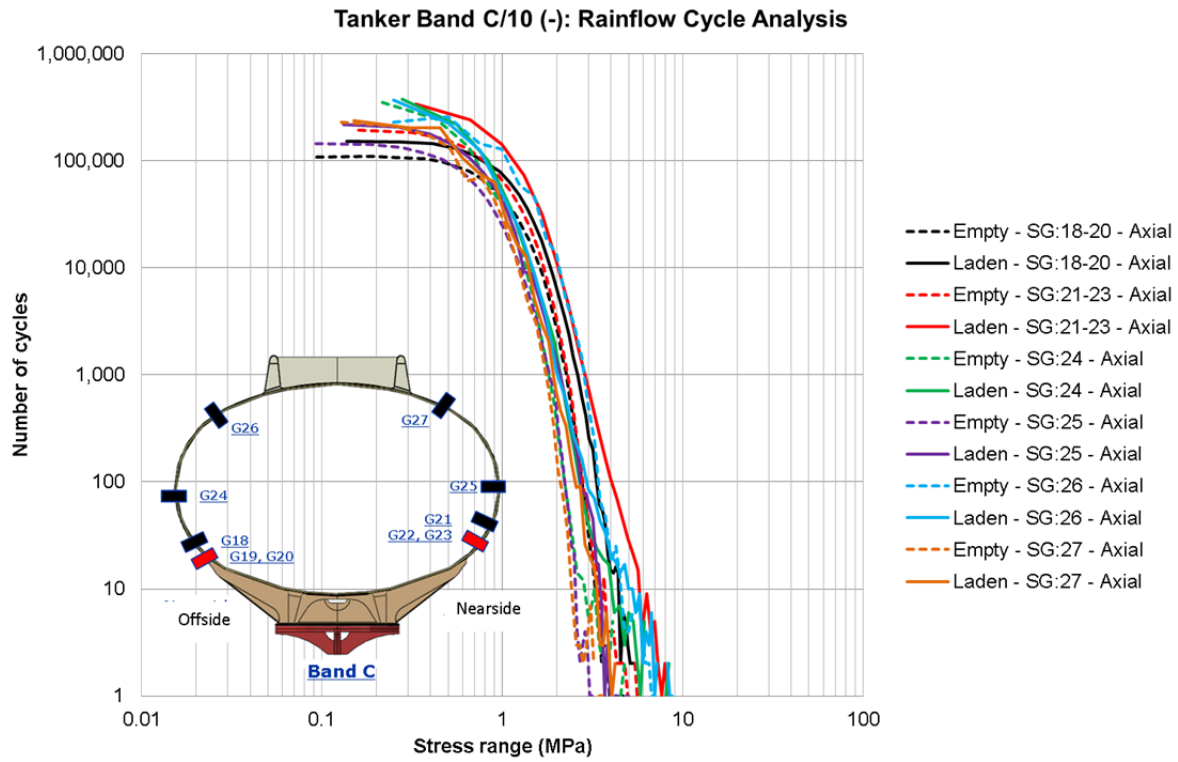

Figure E3 Stress range histograms for the six distinct instrumented locations on band C/10(-).

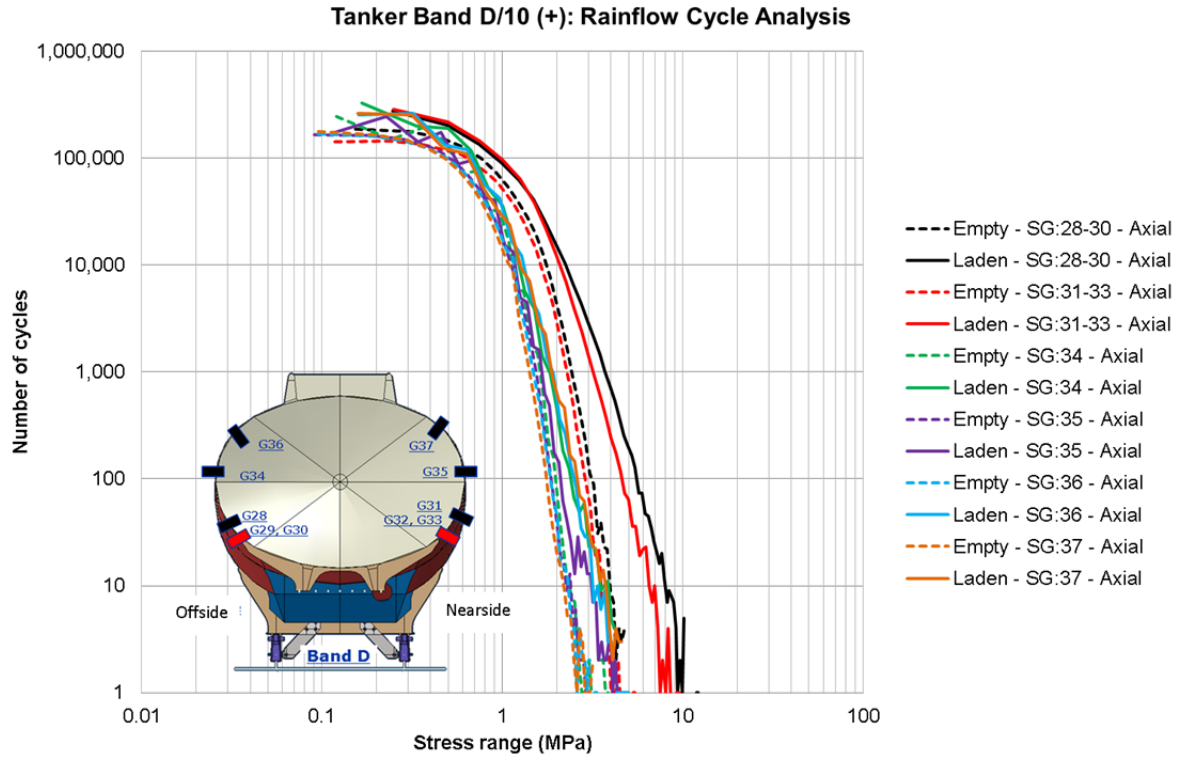

Figure E4 Stress range histograms for the six distinct instrumented locations on band D/10(+).

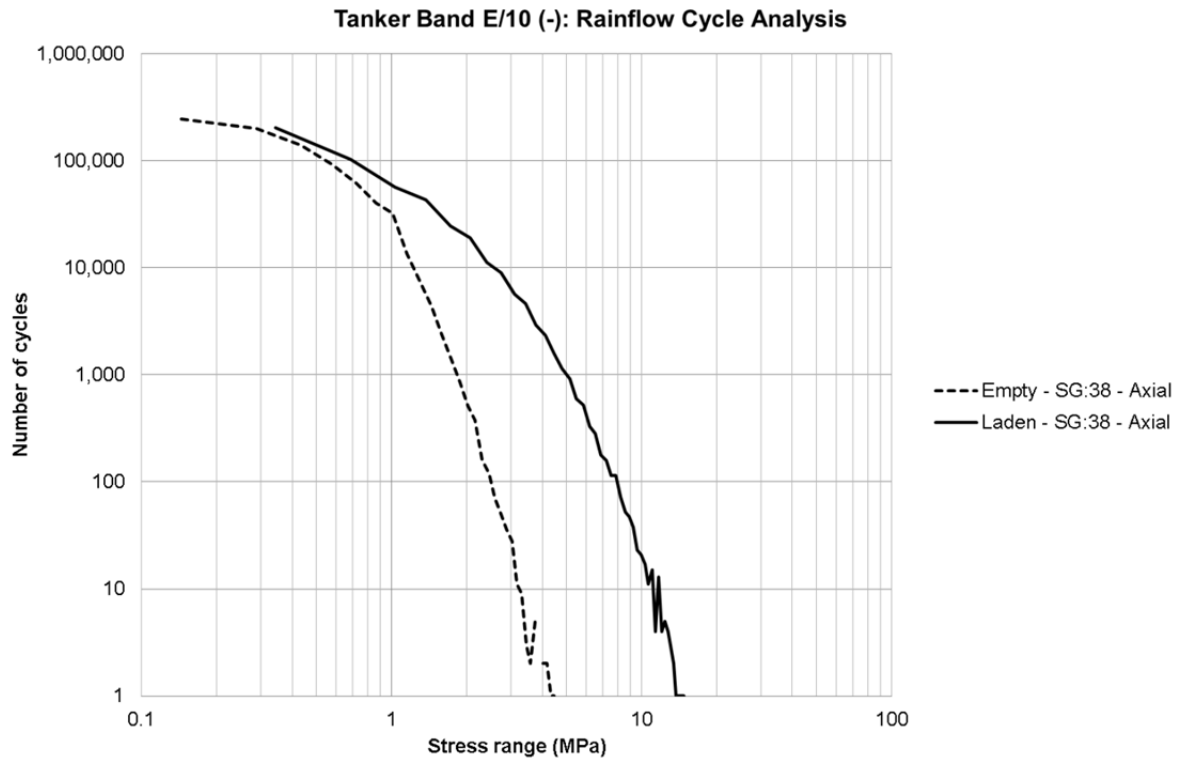

Figure E5 Stress range histogram for the one instrumented location on band E/10(-).

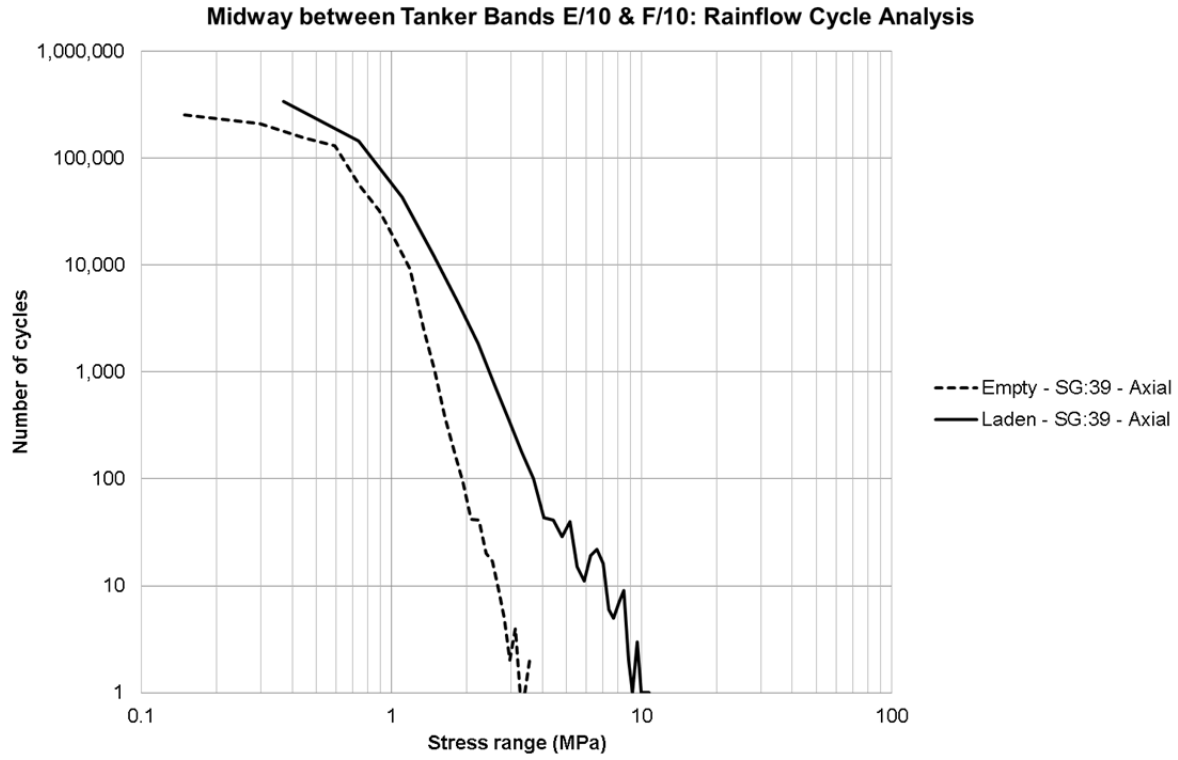

Figure E6 Stress range histogram for the 'remote' gauge located between bands E/10 and F/10.

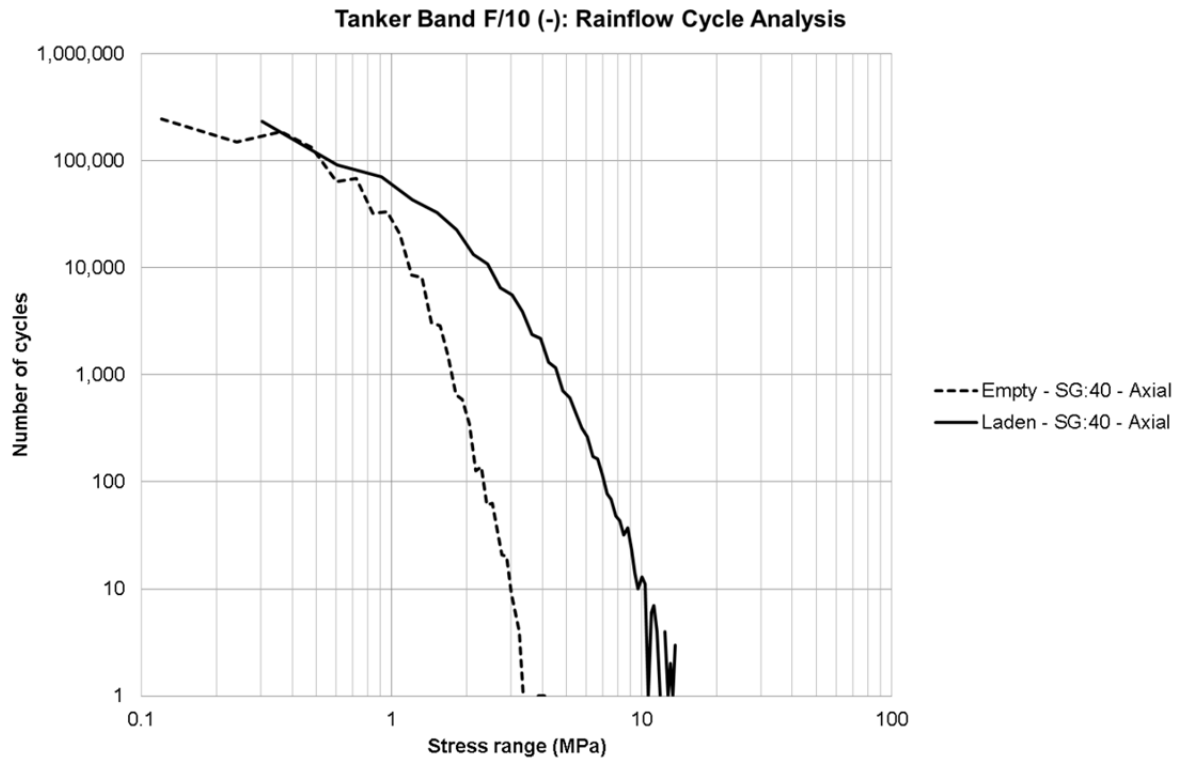

Figure E7 Stress range histogram for the one instrumented location on band F/10(-).

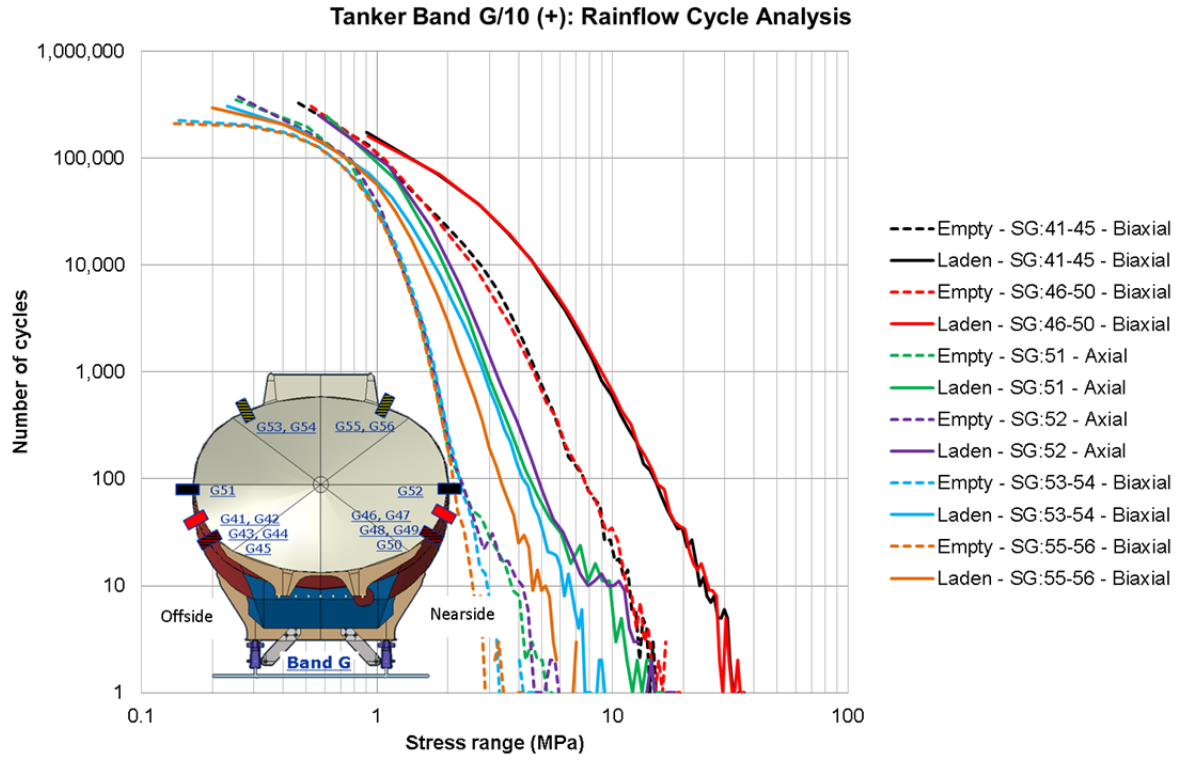

Figure E8 Stress range histograms for the six distinct instrumented locations on band G/10(+).

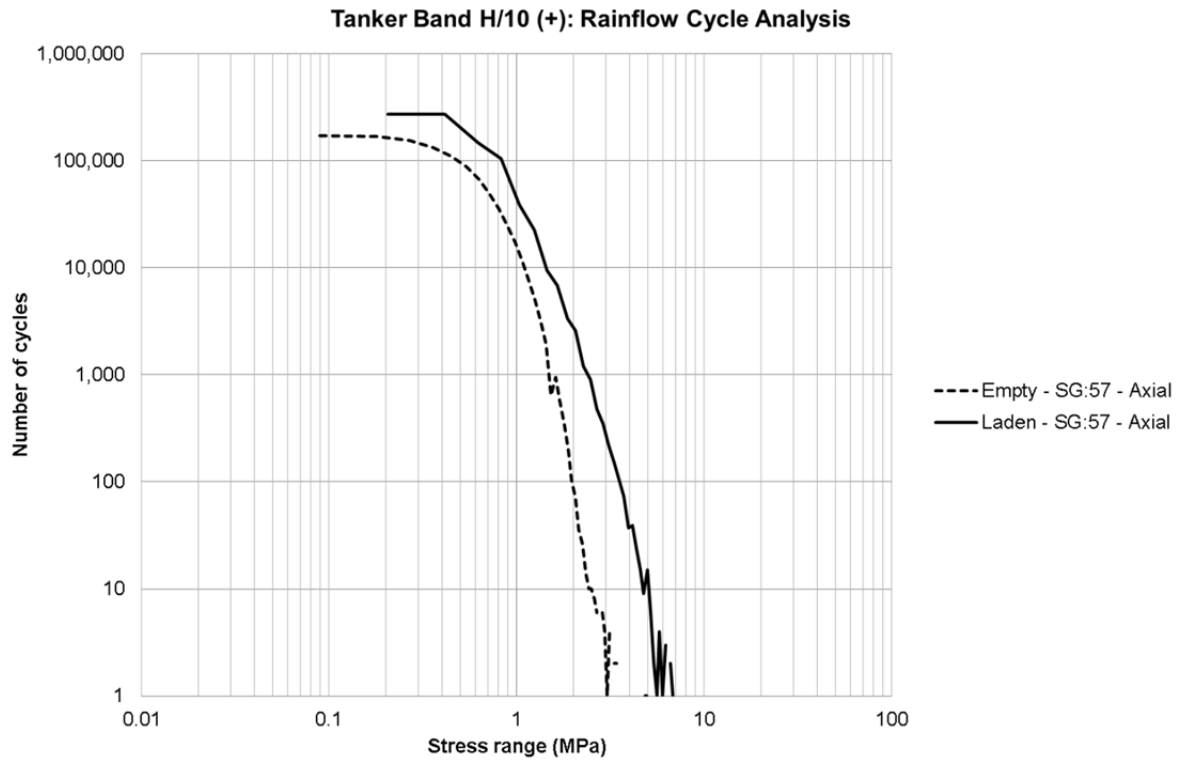

Figure E9 Stress range histogram for the one instrumented location on band H/10(+).

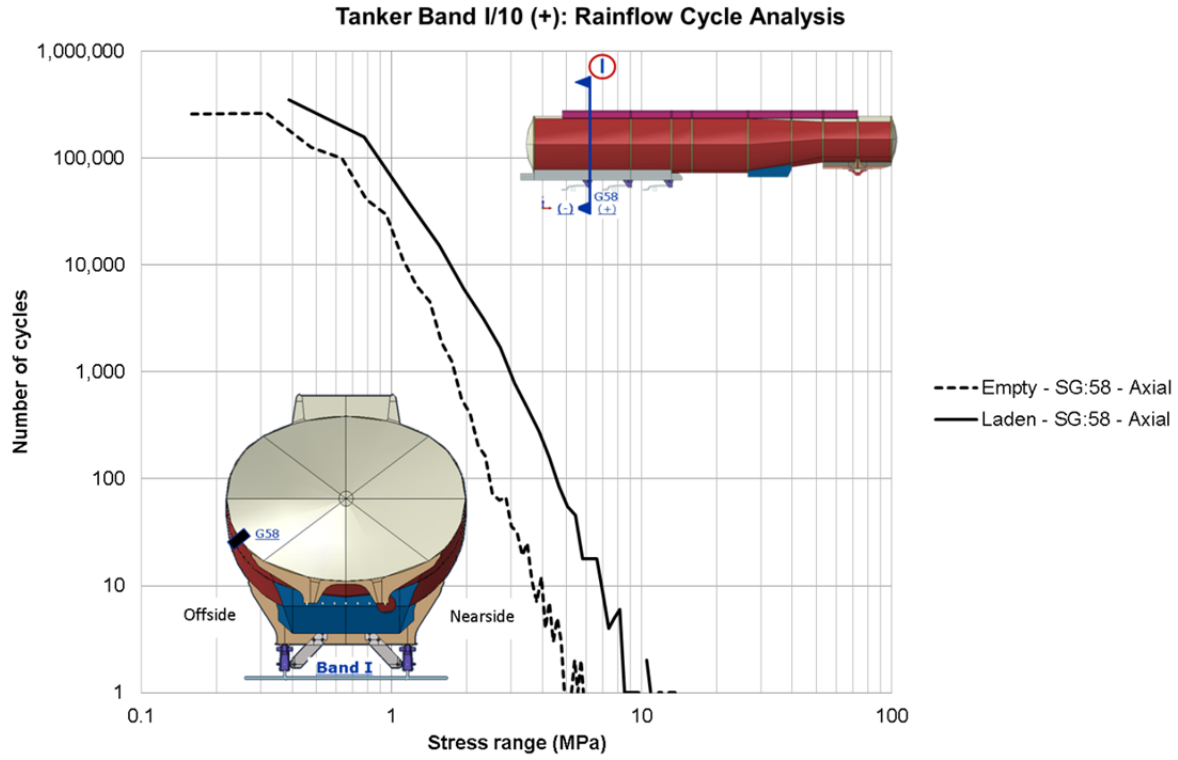

Figure E10 Stress range histogram for the one instrumented location on band I/10(+).

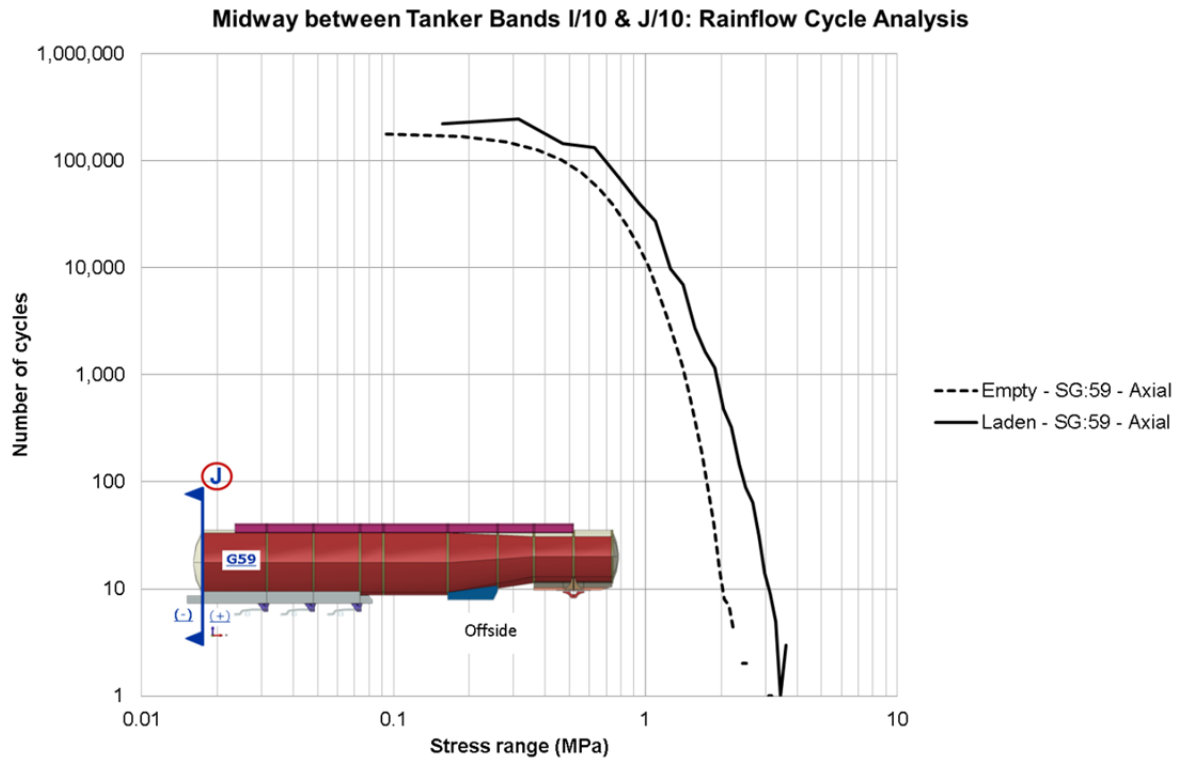

Figure E11 Stress range histogram for the 'remote' gauge located between bands I/10 and J/10.

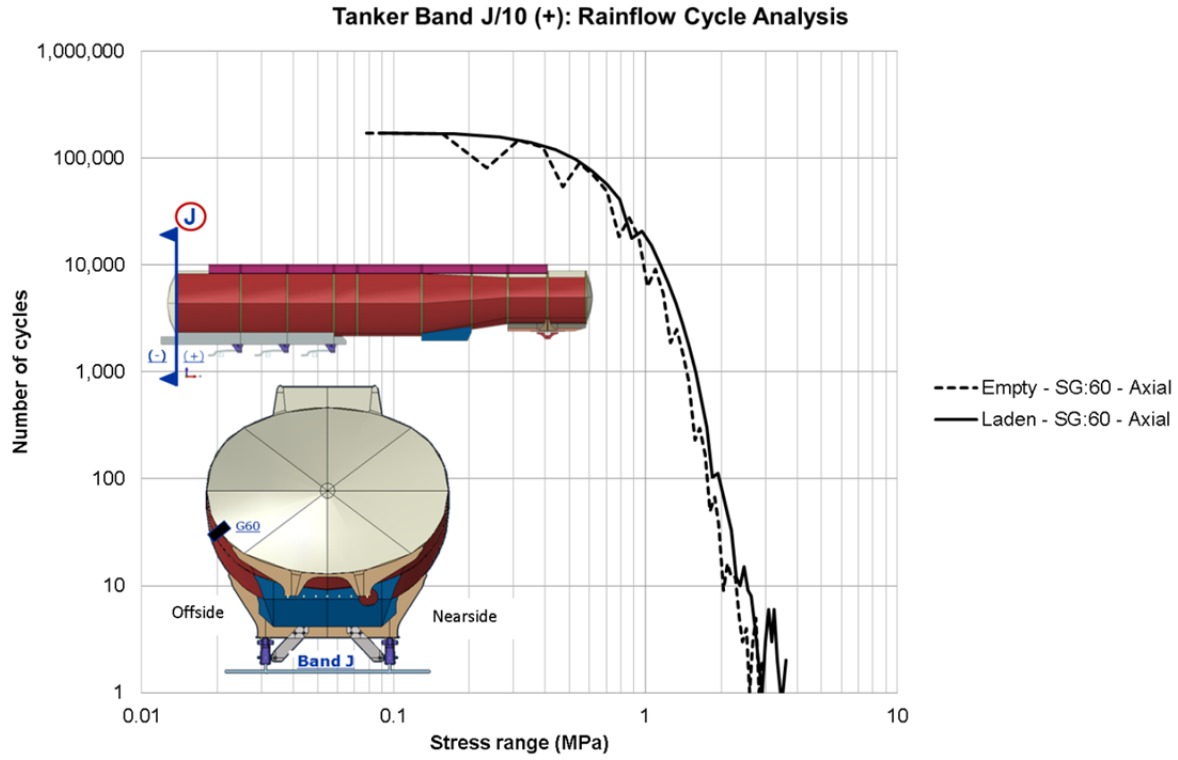

Figure E12 Stress range histogram for the one instrumented location on band J/10(+).

Appendix F

Modification of GRW Proprietary Tanker Finite Element Model

Appendix F: Modification of GRW Tanker Proprietary Finite Element model

1 Overview

TWI has conducted finite element analysis (FEA) of a fuel-tanker, J3857, in order to perform fracture and fatigue engineering critical assessment calculations using BS 7910. The FEA model was originally produced by GRW (2013). TWI has modified the geometry, meshing strategy and stress extraction method in order to more accurately predict the stresses in the tanker. Hot spot stresses were extracted from the model for each tanker band weld for three different load cases: vertical, lateral and longitudinal unit load accelerations. The stresses predicted from the FEA model were then scaled by real acceleration measurements in order to produce stress-time histories for use in a fatigue analysis.

2 Geometry

The J3857 tanker geometry was modelled in detail (see Figure 1), including the tanker shell, baffles and bulkheads, extrusion bands, valance, undercarriage and suspension system. The tanker was predominantly modelled with shells, which is appropriate for a thin-walled vessel. The suspension system was modelled using a combination of beams, linear springs, hinges, ball joints and bushings.

Cracks have been observed in the tankers between the extrusion bands and the tanker shell. Therefore, this is the most critical part of the geometry, where stresses would be extracted from the model. This means that any key features of the geometry around these locations that may affect the stresses should be included in the model. On inspection of the geometry of the GRW model compared to engineering drawings (GRW, 2008 (1) and (2)), it appears that some details were omitted from the model which may impact the stresses in those areas. In particular, a bulkhead (solid plate) in the model should in fact be a baffle (central hole in plate) (see Figure 2). Also, the modelling of the baffles did not include a small hole at the bottom of the baffle (Figure 3), which would act as a stress concentrating feature at this location. Stiffeners were also not included on the LL box, which may affect the stresses in the shell near this location. These features have all been included in the TWI model (see Figure 4), using tie constraints between the baffles and extrusion bands to simplify the meshing strategy.

The modelling methodology used for the extrusion band geometry was also changed from the original GRW model in order to make it more representative of the real tanker geometry. This is illustrated in Figure 5, where the tanker band extends from A to D, with welds positioned at B and C. The GRW model used a constant section thickness of 15mm for section A to C, and a constant section thickness of 5mm for section A to D. This underestimates the bending stiffness of the component, because the areas of the band from A to B and from C to D are not included in the model. TWI have modelled the tanker band with 15mm thickness from B to D, but this shell is only connected to the tanker shell at locations A and C (using Abaqus TIE constraints). This means the model is representing the bending stiffness of the bands more realistically, whilst keeping the weld toes in the correct position.

3 Mesh

The tanker was meshed with 1.8 million quadratic quadrilateral elements (type S8R in Abaqus), 672,000 linear quadrilateral elements (type S4R in Abaqus), 23,000 linear triangular elements (type S3 in Abaqus)

and 2,478 linear line elements (type B31 in Abaqus) for the suspension and bolts. The GRW was originally meshed entirely with linear elements, which may not predict stresses accurately enough in a static 1g analysis without significant mesh refinement. Hence, the TWI model used quadratic elements in the shell and tanker bands, where the stresses would be extracted from the model. The local mesh size at the intersection between the extrusion bands and the shell tanker was 5mm, which is equal to the tanker shell thickness. Elements of the order of the shell thickness are recommended for accurate stress prediction. A global mesh size of 25mm was used far away from the areas of interest, with a smooth transition in element size being used, as shown in Figure 6.

4 Boundary Conditions

The same boundary conditions were used as in the GRW model. The king pin was fixed in all directions and the wheels fixed in the vertical direction (z-axis) to simulate the grounded wheels. A single wheel was also fixed in the lateral direction (y-axis) to prevent rigid body motion. For the lateral acceleration (y-axis) load case, all wheels were fixed in the lateral direction (y-axis) to simulate the friction from the grounded wheels.

5 Loads

Unit acceleration loads were applied in the longitudinal direction (x-axis), lateral direction (y-axis) and vertical direction (z-axis) in three separate steps of the analysis.

6 Stress Extraction

A surface stress extrapolation technique was used as described in BS 7608 (2014) to accurately predict the hot spot stress at the tanker band welds. This involved extracting the stresses at distances of 0.4t and t from the weld toe, where t is the shell thickness. The structural stress at the weld toe was then be found by extrapolating the stresses from these two locations.

Four different linear combinations of the unit acceleration loads were considered. These load cases are called the ADR load cases as in the main report.

- Load Case 1: 2g forward acceleration
- Load Case 2: 1g vertical upwards acceleration
- Load Case 3: 2g vertical downwards acceleration
- Load Case 4: 1g lateral sideways acceleration

It was found that Load Case 4 did not result in the most significant stresses amongst the four ADR load cases. For the other three cases, the surface stress extrapolation results are presented as follows: for Load Case 1-3, and for each stress variable (membrane stress, through-wall bending stress and net section stress), the tanker band experiencing the largest tensile stress variable is identified. The stress variable is then plotted around the entire circumference of this band and shown in the figures below.

For Load Case 1 (2g forward acceleration), the results are shown in Figures 7, 8 and 9 for net section stress, membrane stress and through-wall bending stress, respectively. For Load Case 2 (1g vertical upwards acceleration), the results are shown in Figures 10, 11 and 12, and for Load Case 3 (2g vertical downwards acceleration), the results are shown in Figures 13, 14 and 15.

A summary of the key results is shown in Tables 1 and 2. There key findings are as follows:

- The load case resulting in the largest tensile net section stress is ADR Load Case 3 (2g vertical downward acceleration). Tanker band B/10(-) is the location of the largest tensile net section stress at the triple junction where the cradle gusset plate meets the chassis rails and are joined to the tanker shell. At this position (or at both symmetric positions, either side of the tanker axis), the net section stress is 69.46MPa, the through-wall bending stress is 57.93MPa and the membrane stress is 11.53MPa.
- The load case resulting in the largest tensile membrane stress is also ADR Load Case 3 (2g vertical downward acceleration). Tanker band E/10(+) is the location of the largest tensile membrane stress, also at the triple junction where the cradle gusset plate meets the chassis rails and are joined to the tanker shell. At this position (or at both symmetric positions, either side of the tanker axis), the net section stress is 67.45MPa, the through-wall bending stress is 40.53MPa and the membrane stress is 26.92MPa.

By taking into consideration that through-wall bending results in a smaller stress intensity factor than the equivalent magnitude membrane stress, it was decided that the second key finding above would be used to define the most severely stressed location for the ADR load case ECA. That is, even though the total net section stress is smaller (67.45MPa versus 69.46MPa), the degree of bending at the second position is less than the degree of bending at the first position and therefore the overall stress intensity factor will be higher.

7 Conclusions

TWI has produced a detailed finite element model of the J3857 fuel tanker based on the original model provided by GRW. The GRW model represented the global geometry very well. However, TWI made various changes to make the stress prediction more accurate:

1 Potential stress concentrating features were included near the extrusion band weld toes, such as baffle plate holes and undercarriage stiffeners. One bulkhead was corrected to a baffle, as shown in the engineering drawings.
2 The tanker band geometry was adjusted to more accurately represent the bending stiffness of the real band geometry.
3 A more refined mesh was used (2.5 million elements approximately), with quadratic elements in the tanker bands and tanker shell. Local refinement of 5mm elements were also employed around all tanker bands.
4 Hot spot stresses were calculated using the surface stress extrapolation method to more accurately predict stresses at the weld toes, as described in BS 7608 (2014).

The surface stress extrapolation method was used to identify ADR Load Case 3 as generating the most severe stresses.

8 References

BS 7608, 2014: ‘Guide to fatigue design and assessment of steel products’, British Standards Institute.

GRW, 2008 (1): ‘Tank assembly 500 manhole no sensor flanges’, Drawing number: 085-44-500-01, Tanker description: 44100 Lt 6 Comp Tridem.

GRW, 2008 (2): ‘Baffle 2530x1650mm’, Drawing number: A503-27-00, Tanker description: Portfolio drawing.

GRW, 2013: ‘Critical crack size & crack growth estimate – an extended study’, Product verification and validation report, PVVR20121101, revision no. 3, Danie du Plessis.

Table 1 Severely stressed bands based on net section stress

ADR Load Case	Location of highest net section stress	Net section stress (MPa)	Through-wall bending stress (MPa)	Membrane stress (MPa)
Load Case 1	G/10(-)	58.76	23.02	35.74
Load Case 2	H/10(+)	34.01	19.03	14.98
Load Case 3	B/10(-)	69.46	57.93	11.53

Table 2 Severely stressed bands based on membrane stress

ADR Load Case	Location of highest net section stress	Net section stress (MPa)	Through-wall bending stress (MPa)	Membrane stress (MPa)
Load Case 1	G/10(+)	-3.72	73.22	69.50
Load Case 2	I/10(+)	32.37	-0.99	33.36
Load Case 3	E/10(+)	67.45	40.53	26.92

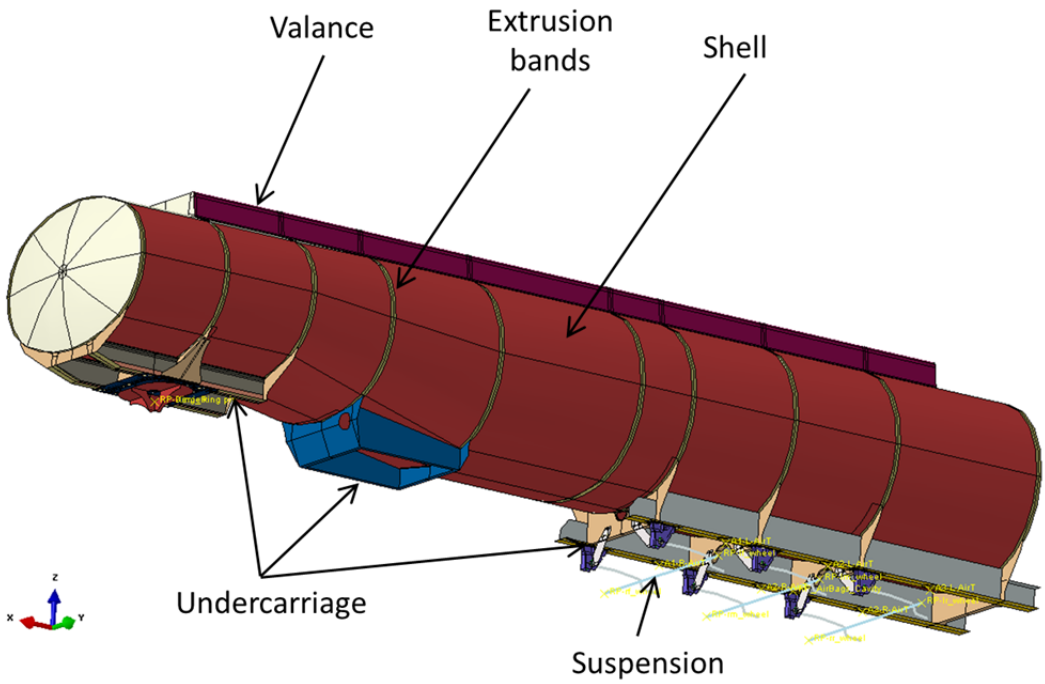

Figure 1 Key features of TWI model geometry.

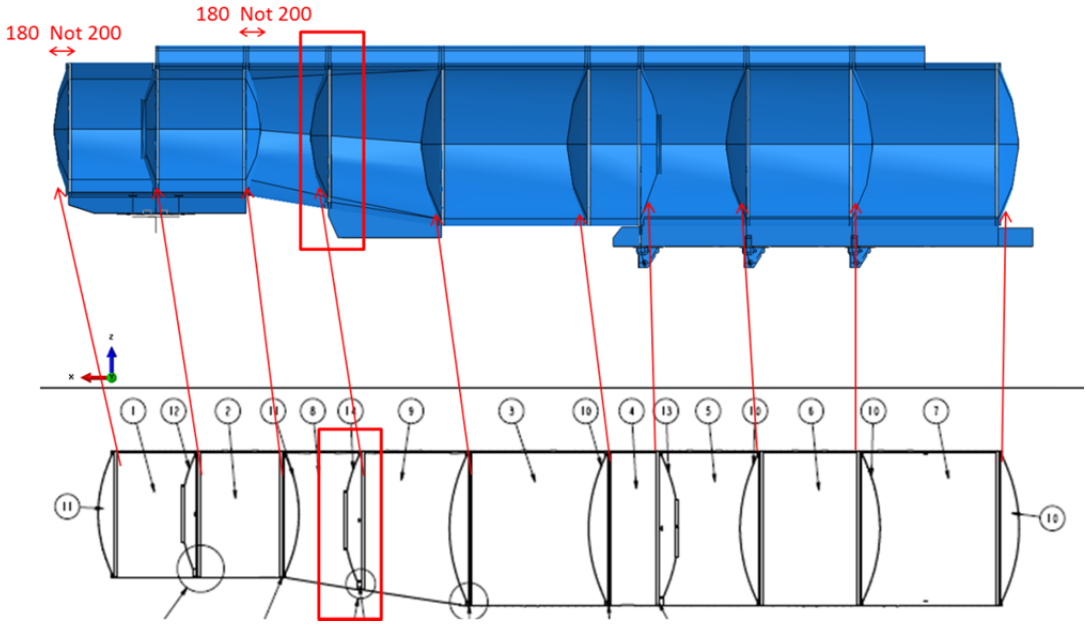

Figure 2 Bulkheads and baffles in GRW model (top) compared to engineering drawings (bottom) (GRW, 2008 (1)).

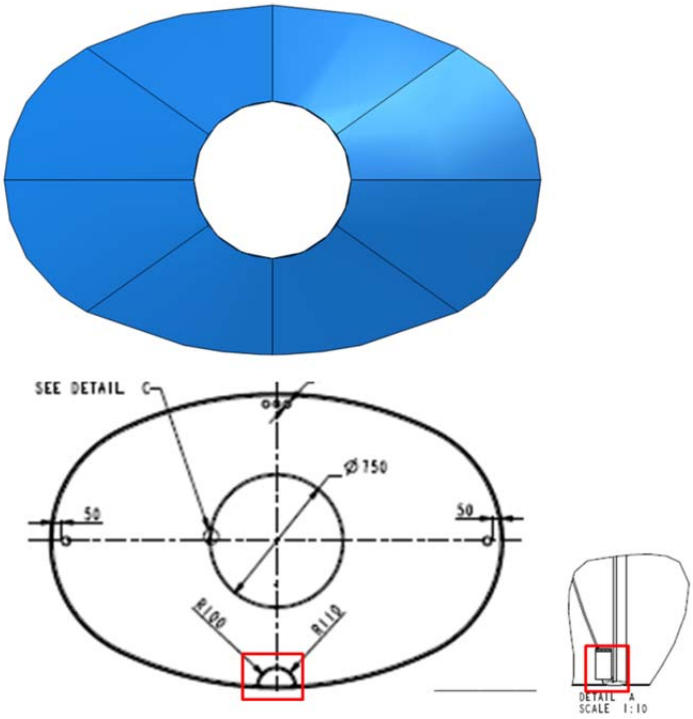

Figure 3 Baffle plate hole detail in model (top) and engineering drawing (bottom) (GRW, 2008 (1), GRW 2008 (2)).

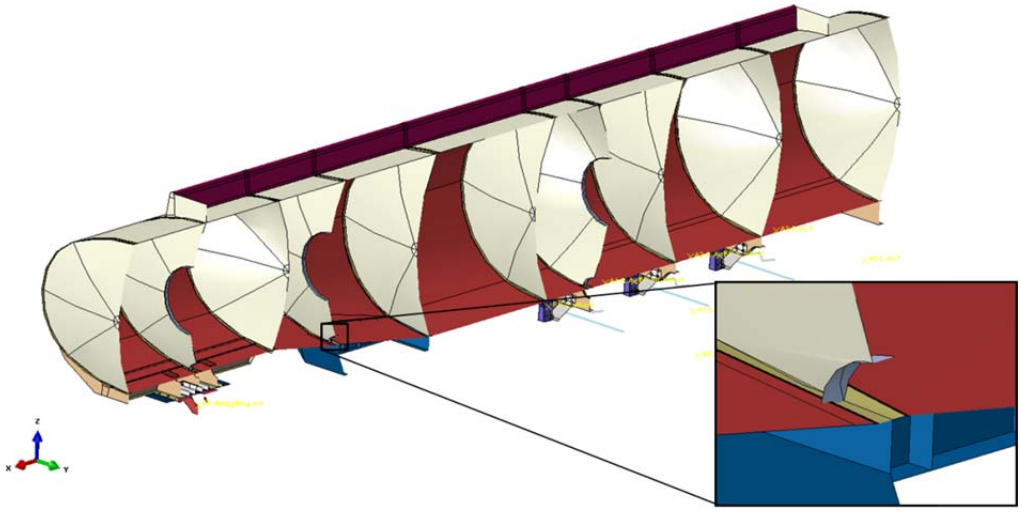

Figure 4 TWI model geometry (only half of model shown to allow view of internal features).

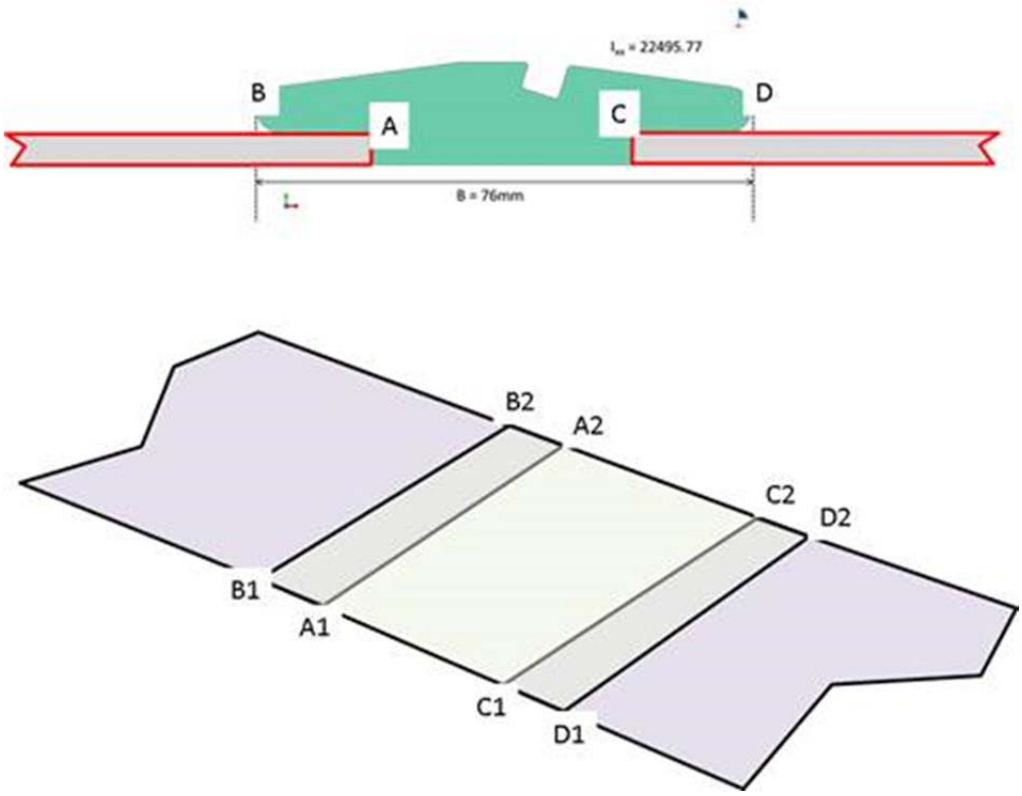

Figure 5 Illustration of model geometry used for tanker bands.

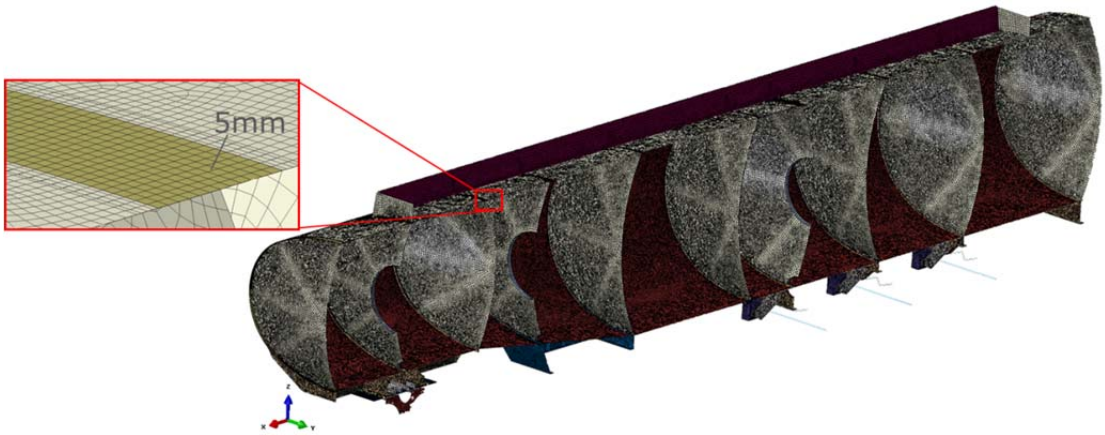

Figure 6 TWI model mesh, with local mesh refinement around all tanker band welds.

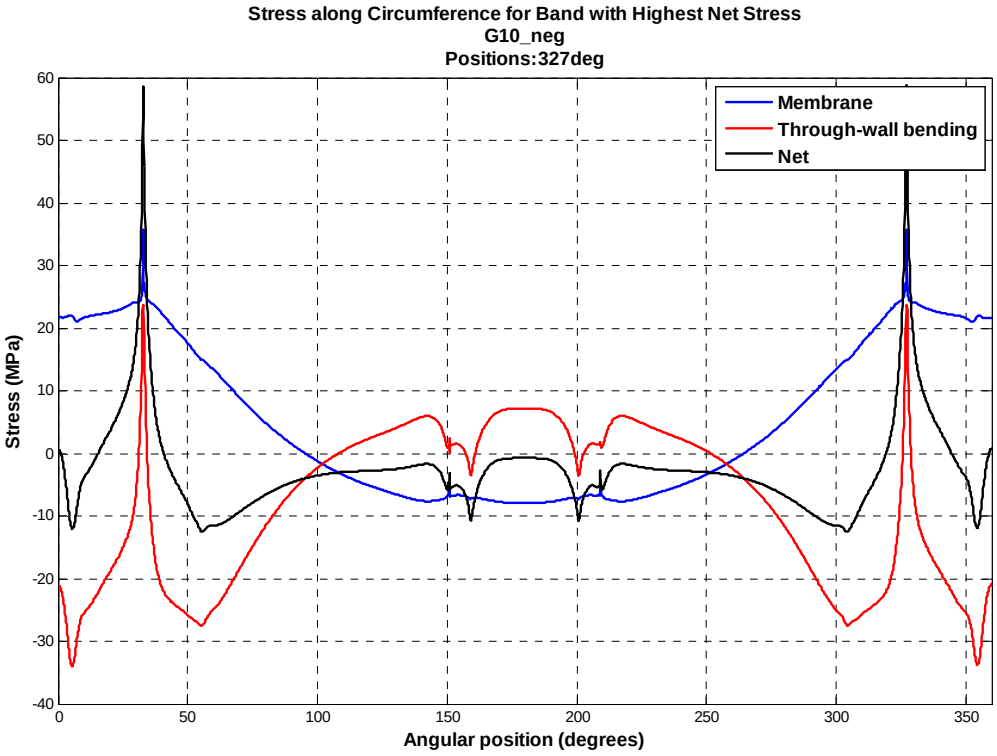

Figure 7 Surface stress extrapolation results for ADR Load Case 1 (2g forwards acceleration) around the circumference for the band where the largest net section stress was extracted.

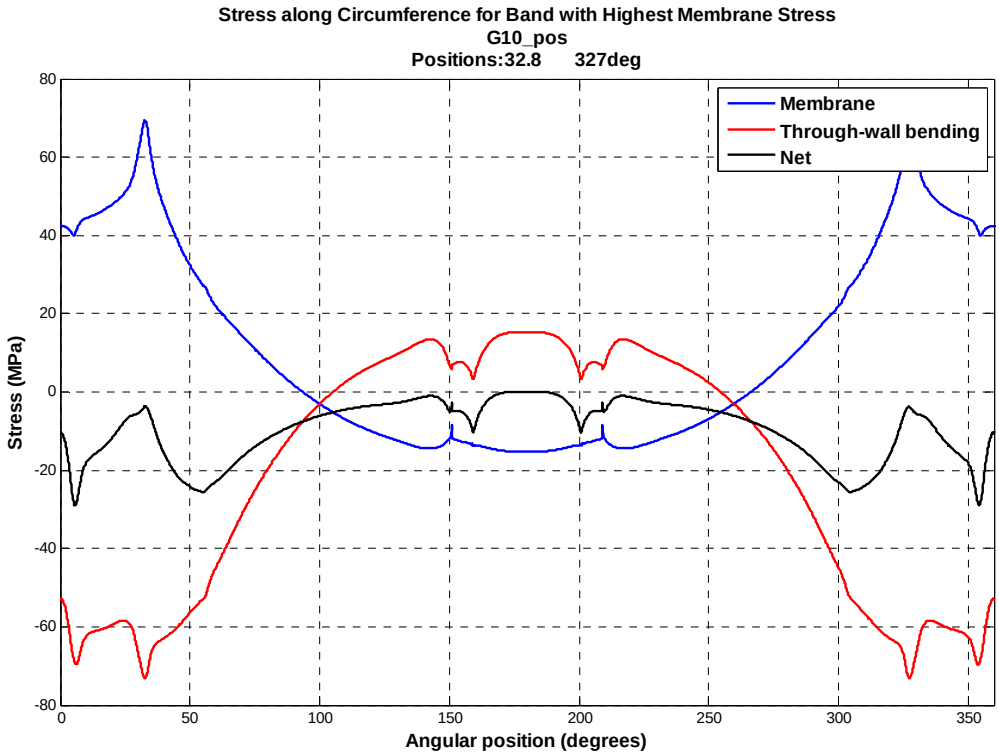

Figure 8 Surface stress extrapolation results for ADR Load Case 1 (2g forwards acceleration) around the circumference for the band where the largest membrane stress was extracted.

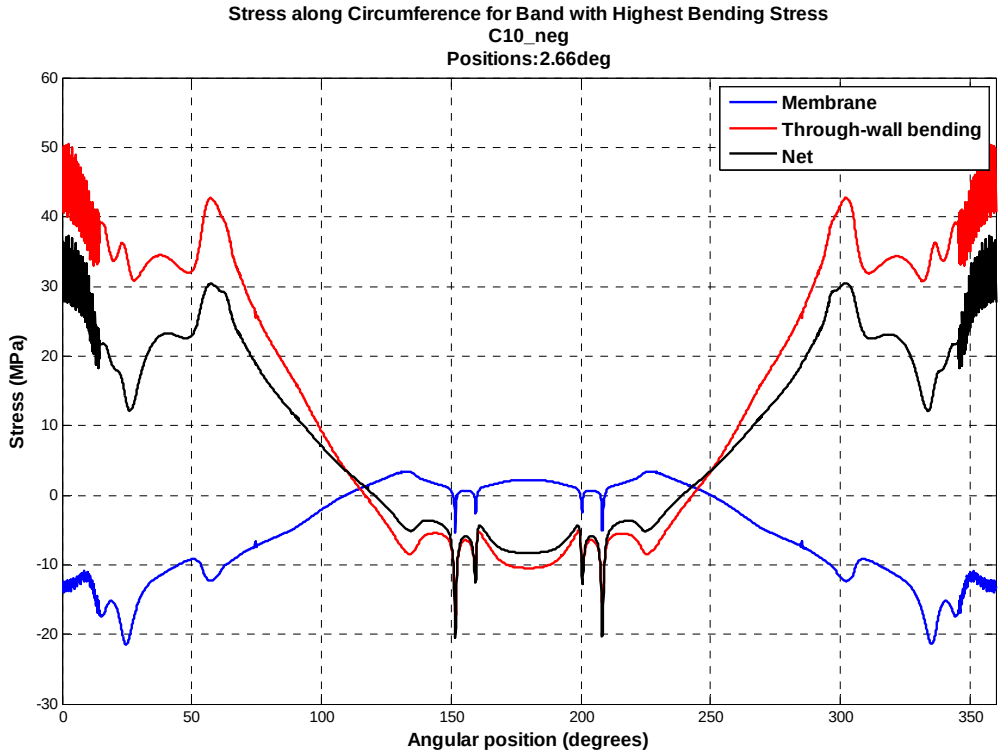

Figure 9 Surface stress extrapolation results for ADR Load Case 1 (2g forwards acceleration) around the circumference for the band where the largest bending stress was extracted.

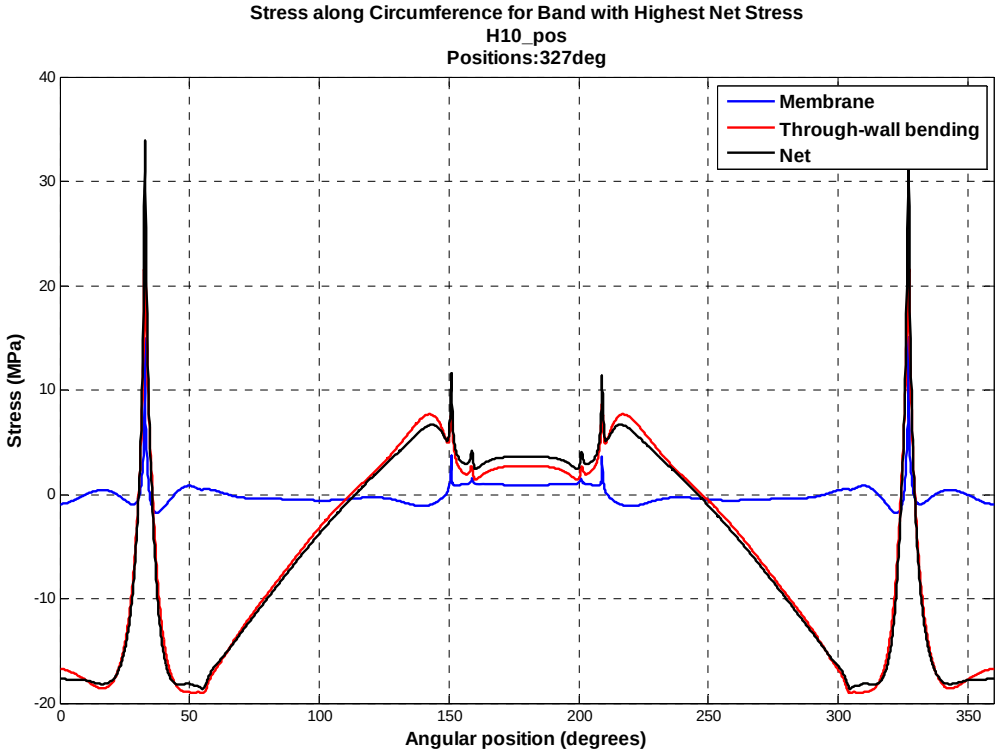

Figure 10 Surface stress extrapolation results for ADR Load Case 2 (1g vertical upwards acceleration) around the circumference for the band where the largest net section stress was extracted.

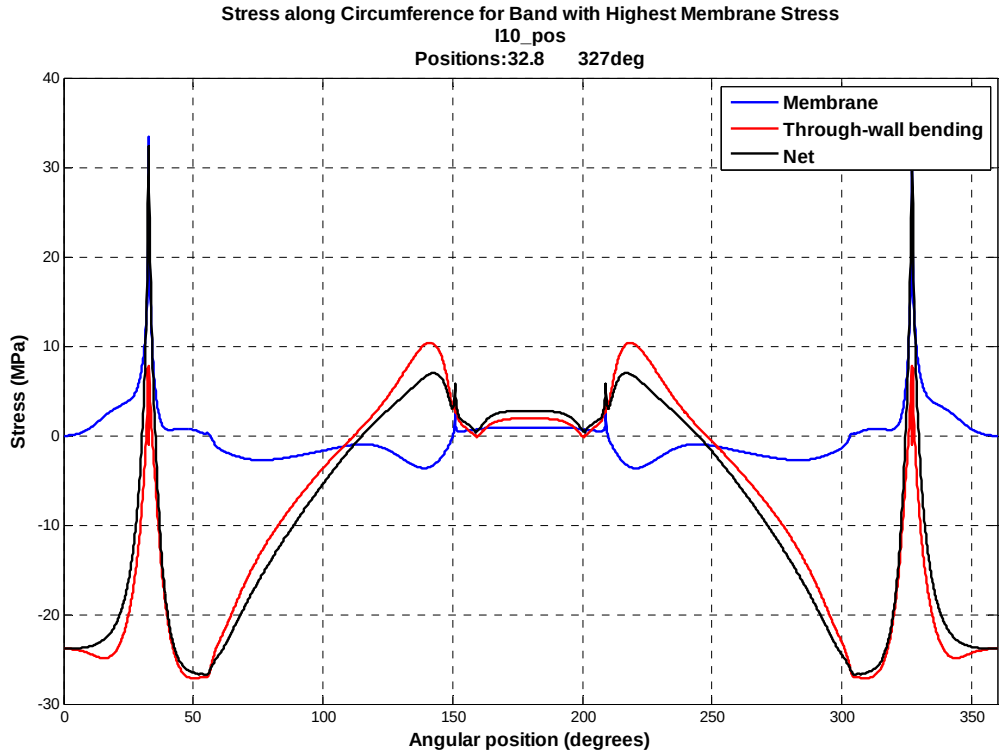

Figure 11 Surface stress extrapolation results for ADR Load Case 2 (1g vertical upwards acceleration) around the circumference for the band where the largest membrane stress was extracted.

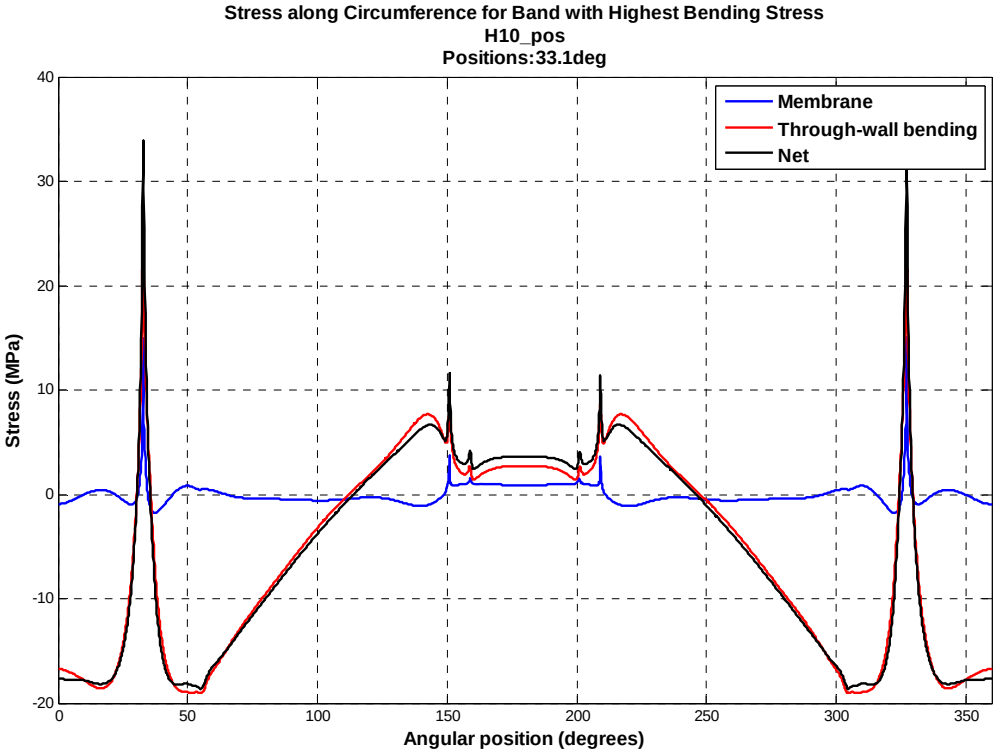

Figure 12 Surface stress extrapolation results for ADR Load Case 2 (1g vertical upwards acceleration) around the circumference for the band where the largest bending stress was extracted.

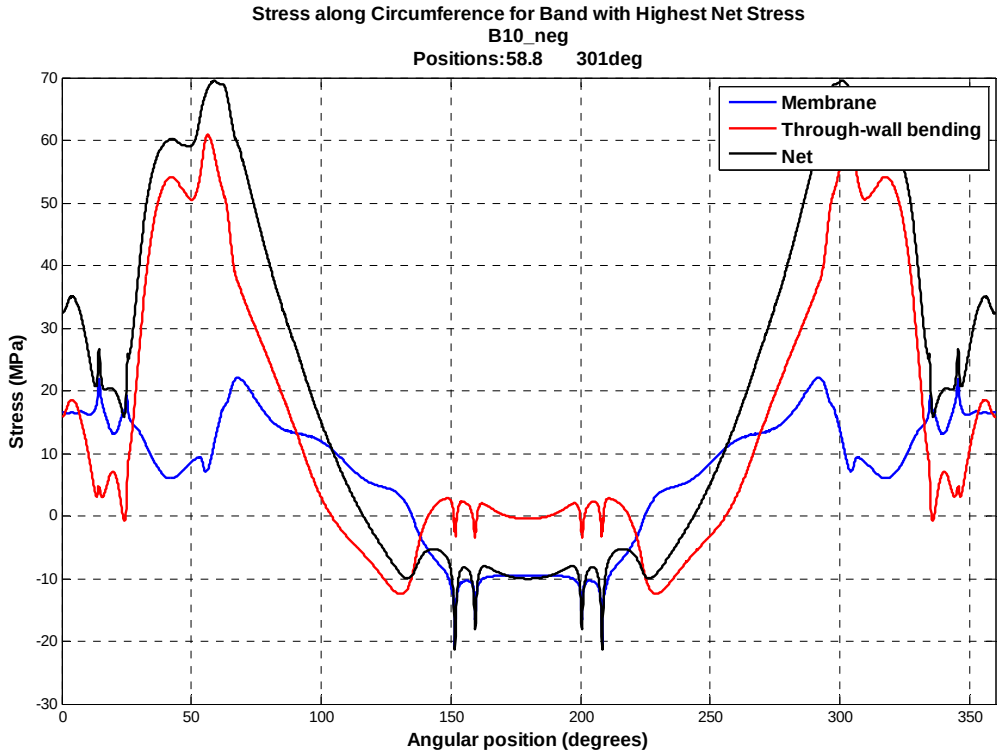

Figure 13 Surface stress extrapolation results for ADR Load Case 3 (2g vertical downwards acceleration) around the circumference for the band where the largest net section stress was extracted.

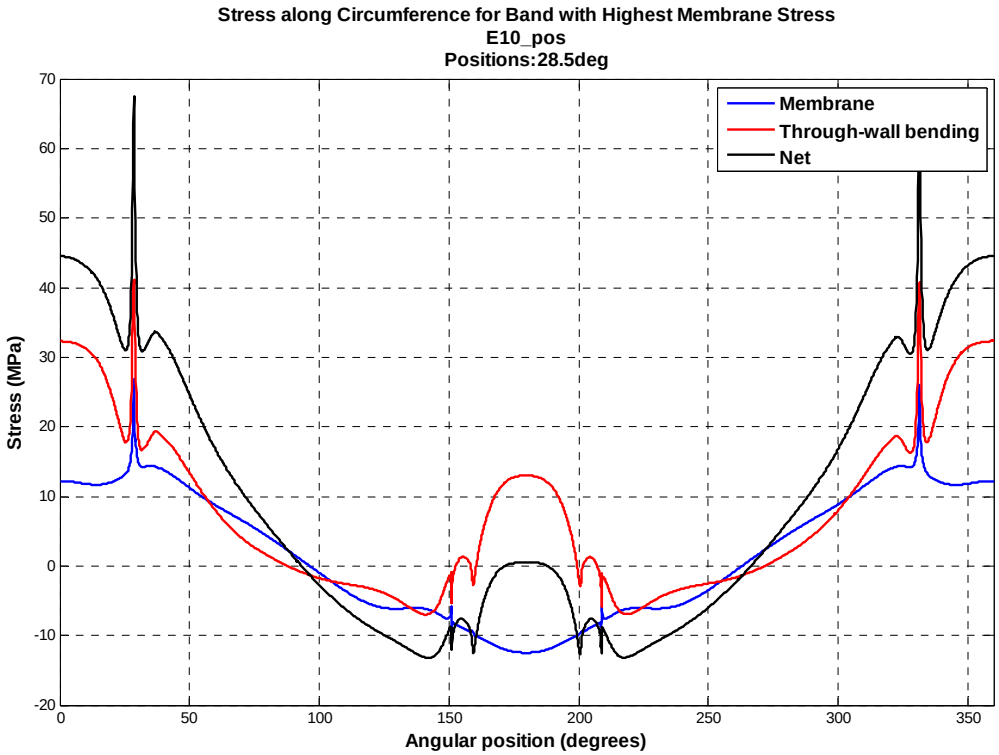

Figure 14 Surface stress extrapolation results for ADR Load Case 3 (2g vertical downwards acceleration) around the circumference for the band where the largest membrane stress was extracted.

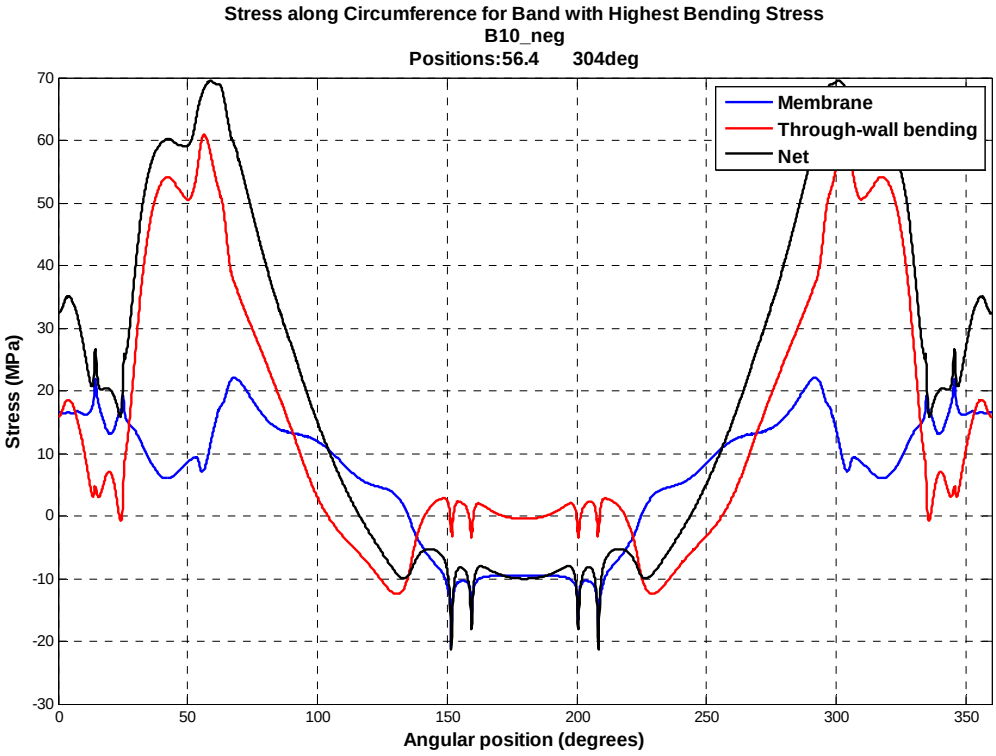

Figure 15 Surface stress extrapolation results for ADR Load Case 3 (2g vertical downwards acceleration) around the circumference for the band where the largest bending stress was extracted.

Appendix G

Finite Element Simulation of Welding Residual Stresses

Appendix G: Finite Element Simulation of Welding Residual Stresses

1 Overview

As described in Section 2, a potential source of over-conservatism in previous engineering critical assessments of the GRW circumferential seam welds was the assumption of yield-magnitude tensile residual stresses. Although a report, commissioned on behalf of GRW, provided X-ray diffraction measurements of the residual stresses in a GRW tanker band joint, the technical review of this report noted possible short-comings and sources of errors in these measurements. Specifically, the sample was extensively cold worked before measurements were made and the measurements were only sub-surface.

In order to provide additional insight into the potential residual stress state in the tanker band joints, TWI has performed a thermo-elastic-plastic finite element simulation of the welding procedure.

2 Objective

- To predict the transverse (axial) welding residual stresses in the GRW tanker band joint by simulating the welding procedure for this joint.

3 Approach

3.1 Geometry

An axisymmetric finite element model of a single band of the GRW tanker band joint was produced in Abaqus/CAE version 6.13-2. The details of the joint geometry are as described in the main report.

For the heat transfer analysis, the finite element mesh was comprised entirely of quadrilateral, linear, 4-node axisymmetric heat transfer elements (type DCAX4 in Abaqus). For the thermal stress analysis, bi-quadratic, axisymmetric, reduced-integration elements were employed. An image of the finite element mesh is shown in Figure G3.

3.2 Material properties

The parent and weld materials as described in a previous technical GRW report (2013) are 5182-H111 and 5183, respectively. Similar alloys also described in (GRW, 2013) are 5083-O and 5182 (or 5183) for the plate and filler wire, respectively. A brief literature review of (Abedrabbo et al, 2007), (AFROX, 2014), (Summers et al, 2014) as well as the online materials databases eFunda (2014) and MatWeb (2014) provided indicative tensile properties. Both materials exhibit relatively similar thermo-mechanical properties. Although room temperature tensile testing has been performed on both parent and weld material samples within the context of the present phase of work, elevated temperature testing was not completed. Therefore, for consistency, tensile properties obtained from literature were employed in the finite element model. The room temperature values used in the finite element simulation (and obtained from literature) are not very different from results obtained from room temperature tensile testing.

The material properties used in the welding simulation are shown in Table G1.

3.3 Loads and boundary conditions

The welding simulation was performed by using a sequential thermal-mechanical analysis. To do so, first a transient heat transfer analysis

was performed in order to obtain the time-dependent temperature distribution. After the heat transfer analysis was completed, the transient temperature field was used to define thermal boundary conditions for a thermal-stress (mechanical) analysis.

For the transient heat transfer analysis, the heat input per weld pass was obtained from calculations based on information contained in the GRW welding procedure document (GRW, 2010). The following assumptions were made:

- The weld pool length, L, is equal to four times the weld pool width (see the shaded region in Figure G3). Specifically, the weld pool width is 9.6mm and the weld pool length is therefore 38.4mm.
- Heating occurs for a time period, τ, equal to the time taken for the weld pool to pass through the model, ie $\tau = L/v$ where v is the travel speed. For the simulations undertaken, v = 73cm/min (or equivalently, v = 12.2mm/sec).
- The heat input provided by the weld is assumed to be ηIV where IV is the welding power (amps multiplied by voltage), and η is the welding process efficiency, assumed to be 0.7.
- During the heating period, the volumetric heating flux should therefore be $Q = \eta IV/AL$, where A is the cross-sectional area of the heated region, approximately 50mm^2.

Based on these assumptions (and the values specified in Table G2), the volumetric heat flux is Q = 2.6 W/mm^3.

Kinematic strain hardening and standard heat loss to the environment were assumed. Convection and radiation thermal boundary conditions were applied to surfaces of the model. The parameters shown in Table G3 were additional used in the finite element model, with the emissivity and convective heat transfer coefficient being based upon TWI's experience of modelling welding processes.

For the thermal-stress analysis, mechanical boundary conditions restraining axial displacements were specified at one end of the finite element model on the tanker shell as shown in Figure G2. The reason for specifying axial restraints at only one end was to simulate the effect of constructing the tanker from end-to-end. For this reason, the transverse residual stress field is very low on the free end (low restraint implies low residual stress) and higher on the restrained end.

4 Results

Von Mises and axial (transverse) stress contour plots are shown in Figure G4. The stress contour plots shown are after cooling. In the bottom frame of this figure, two black arrows indicate the paths along which the transverse residual stress was output. The radial path starts at the root of the weld, at the base of the positioning lip of the extrusion band, and ends at the weld cap. From this figure, it can be seen that the restrained end (the right hand side) exhibits through-wall bending stress, as indicated by the large tensile axial stress on the inner surface of the shell and the compressive axial stress on the outer surface of the tanker shell.

The resulting transverse residual stress profiles are shown in Figure G5. In this figure, the solid curves indicate the actual transverse residual stress as measured from the finite element model. The dashed lines indicate the linearised membrane stress, Qm. This has been calculated as follows: at the root of the weld, define σ_0 =121.15MPa, which is the transverse residual stress

at the root. For a radial position, a, with a = 0 corresponding to the root and a = 5 corresponding to the outer surface of the shell (sub-surface in this case, since a weld cap is present), define σ(a) to be the transverse residual stress at the radial position a. Then the linearised residual membrane stress, Qm(a) is defined by:

$$Q_m(a) = \frac{1}{2}(\sigma_0 + \sigma(a))$$

That is, Qm is the average of the stress at the root and the stress at the radial position a.

Two sets of curves (actual transverse stress and Qm) have been plotted; one for the restrained in and one for the unrestrained end. As expected, the restrained end exhibits higher residual stress than the free end.

5 Conclusions

For a sensitivity study, and to remove the potential over-conservatism of assuming yield-magnitude, tensile residual stresses, it is recommended that the residual stress field specified in this report is employed. Note that at the weld root, the linearised membrane residual stress is equal to 121.15MPa, almost equivalent to the yield stress of the material under consideration. Thus, for shallow defects, the use of Qm is almost equivalent to the assumption of full yield magnitude residual stresses. However, as the defect height increases (and therefore the radial position gets closer to the outer surface of the joint), Qm decreases to be less than 50MPa, or less than half of the yield stress.

Note that the material properties assumed for the welding residual stress simulation will have an effect on the resulting residual stress profile; however, the Qm profile described in this appendix can be used as an indicative profile of potential welding residual stresses in the joint. In particular, as described in the report, the finite element analysis of the welding residual stresses appear to agree will with the experimental measurements over a significant proportion of the joint through-wall thickness.

6 References

Abedrabbo N, Pourboghrat F and Carsley J (2007): 'Forming of AA5182-) and AA5754-O at elevated temperatures using coupled thermo-mechanical finite element models', International Journal of Plasticity, Vol 23, pp 841-875.

AFROX (2014): 'Product Data Sheet: Afrox Filmax 5183 and Afrox TIG 5183', **www.afrox.com**.

efunda (2014): 'Propreties of Aluminium Alloy AA5083', retrieved from **www.efunda.com/Materials/alloys/aluminum/show_aluminum.cfm?ID=AA_5083&show_prop=all&Page_Title=AA%205083.**

GRW (2010): 'Welding Procedure Specification (WPS)', GRW Engineering, 08/02/2010.

GRW (2013): 'Critical crack size & Crack growth estimate – an extended study', GRW Report No. PVVR20121101, Revision 3. Report Date 30 September 2013. Received from DfT via memory stick on Friday, 25/04/2014.

MatWeb (2014): 'ASM Material Data Sheet – Aluminium 5083-H116; 5083-H321', retrieved from http://asm.matweb.com/search/SpecificMaterial.asp?bassnum=MA5083H116,

Summers PT, Case SW and Lattimer BY (2014): 'Residual mechanical properties of aluminium alloys AA5083-H116 and AA6061-T651 after fire', 'Engineering Structures', Vol 76, pp 49-61.

Table G1 Material properties used for the welding simulation

Material Properties	Source	Unit	Temp, °C	Parent metal	Weld metal*
Thermal expansion	(efunda, 2014)	10^{-6}/°C	-	23.4	23.4
Thermal conductivity	(efunda, 2014)	W/mm.K	-	0.120	0.120
Density	(efunda, 2014)	kg/mm^3	-	2.66E-06	2.66E-06
Elastic modulus	(efunda, 2014)	MPa	20	70,000	70,000
			600	7,000**	7,000**
Yield strength	(efunda, 2014) and (Afrox, 2014)	MPa	20	195	125
			600	19.5**	12.5**
Tensile strength	(efunda, 2014)	MPa	20	305, 10% strain	275, 10% strain
			600	19.5	12.5
Specific heat capacity	(Matweb, 2014)	J/kg.°C	-	900	900
Melting point	(Matweb, 2014)	°C	-	591-638	591-638

*Assumed material properties unless stated otherwise
**Assumed 10% of room temperature values

Table G2 Values used to derive the volumetric heat flux

Weld pass	Area (mm^2)	Heat input (J/mm)	Heating period (s)	Heat flux (W/mm^3)
1A	49.22	49.15	3.15	2.6
1B	49.52	49.15	3.15	2.6

Table G3 Additional thermal properties included in the finite element model.

Absolute zero	-273°C
Stefan-Boltzmann constant	5.67·10E-14 W/mm^{2}K^4
Emissivity	0.3
Convective heat transfer coefficient	10^{-5}W/mm^{2}K

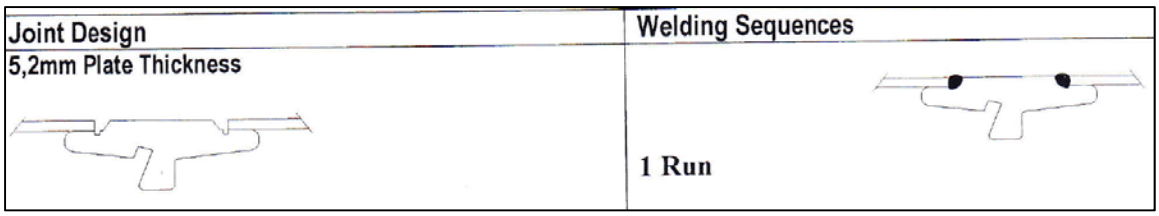

Figure G1 Schematic of the joint under consideration (GRW, 2010).

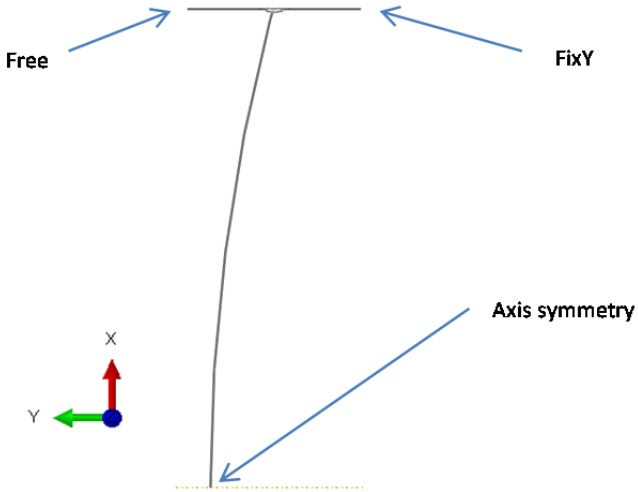

Figure G2 Axi-symmetric cross-sectoin of the welded area.

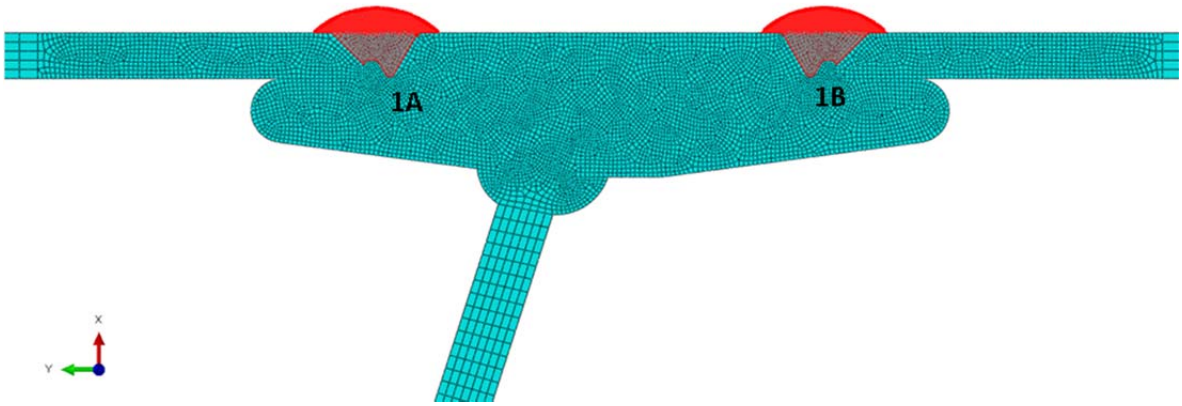

Figure G3 Weld passes. Note that a 'seam' was used to model the unfused surfaces between the tanker band extrusion profile and the tanker shell.

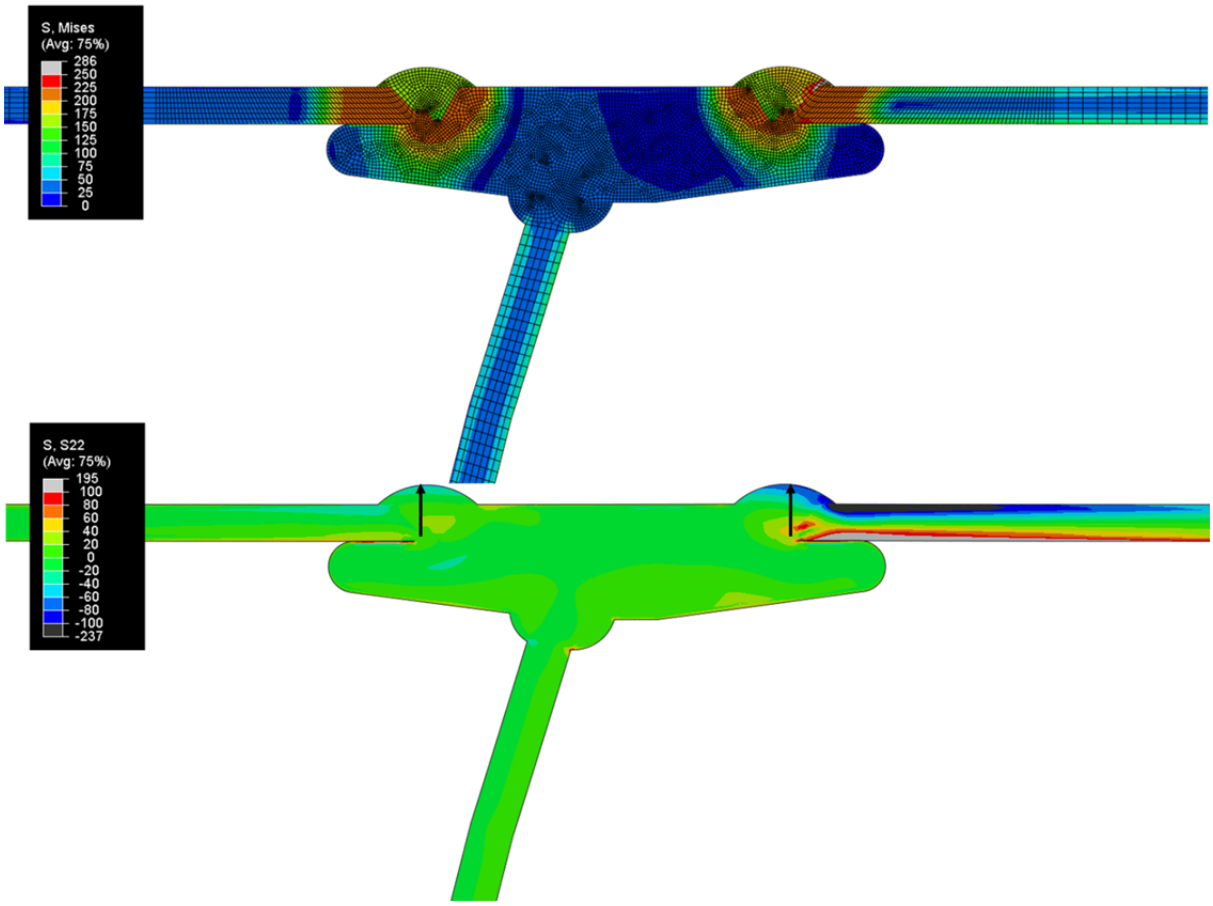

Figure G4 Von Mises stress contour (top) and axial (transverse) stress contour (bottom) for the joint after cooling. The arrows indicate the lines for residual stress measurement.

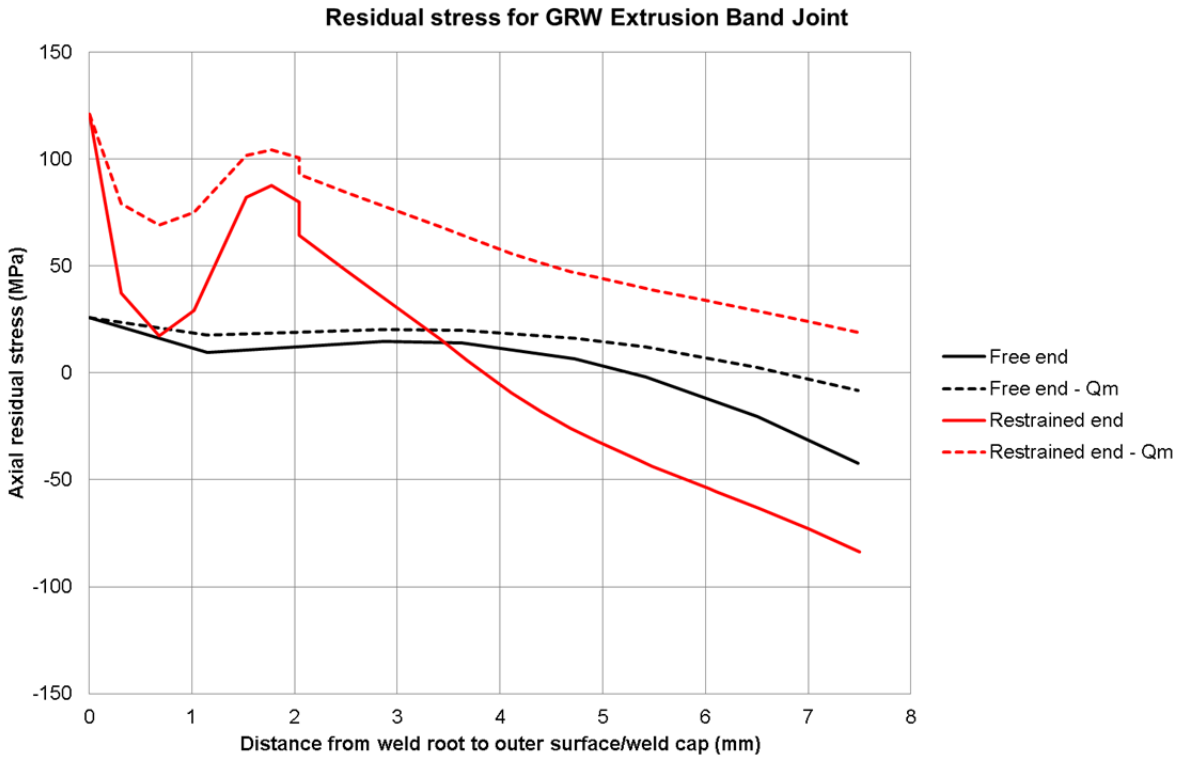

Figure G5 Transverse residual stress profile and resultant linearised membrane stress (Qm).

Appendix H

Mechanical Testing

Appendix H: Mechanical Testing

1 Overview

Mechanical testing has been performed for two reasons: firstly, the aim to establish mechanical properties (tensile behaviour and fracture toughness) for the engineering critical assessment. The second objective is to compare the mechanical properties from two different tankers.

In the previous TWI project on the integrity of GRW circumferential seam welds, mechanical testing was undertaken on samples extracted from GRW tanker J3025. A series of tensile tests and fracture toughness tests were undertaken to obtain stress-strain curves for the tanker shell material and weld metal and to generate a tearing-resistance, J-R curve for the weld metal. A similar series of mechanical tests was undertaken in the present research project in order to obtain information about the scatter of tensile properties and fracture toughness. For the present work, the samples were obtained from a section removed from GRW tanker J3164.

2 Material Tested

TWI performed fracture toughness testing on single edge notched bend (SENB) specimens, extracted from a section taken from GRW tanker J3164. Testing was performed at the minimum design temperature stated in the ADR code: -20°C. Testing was performed to BS 7448:1997 Part 4, using the multi-specimen approach. Six specimens were notched through-thickness at the weld metal centre line to determine stable tearing resistance J R-curves.

In order to provide tensile properties for the fracture toughness testing and resulting four M4 round tensile specimens were machined. Two of these specimens were taken from the parent material (M01-01, M01-02) and two were taken from the welds (W01-07, W01-08). These specimens were tested at the minimum design temperature of -20°C in accordance with the latest version of BS EN ISO 6892-1. The test traces show ‘serrated yielding’ (the appearance of saw tooth-like features on the stress-strain trace) which is a relatively common occurrence in this grade of aluminium. The lower bound values were used for the fracture toughness testing and resulting.

3 Specimen Geometry

Six single edge notched bend (SENB) specimens (W01-01 to 06) were extracted from the circumferential seam weld, with a Bx3B cross section, in which B is as close to the shell plate thickness (5.2mm) as was practically achievable. Standard SENB specimens have a typical cross section of BxB or Bx2B. BS 7448:1997 part 4 allows up to Bx4B. The choice for Bx3B was made to increase the ligament in the specimen, allowing for more (stable) tearing to occur, but still limiting the risk of buckling instability which is likely in a Bx4B geometry.

The SENB specimen geometry gives high crack tip constraint, and can give over-conservative toughness results for material that is predominantly loaded in tension. However, given that present engineering critical assessment concerns load cases that involve significant through-wall bending stresses, the SENB specimen is appropriate. Additionally, a constraint-based analysis has been performed by analysing the T-stress to check the constraint in the test specimen is higher than in the structural component under consideration.

It should be noted that due to the small size of the specimen, the amount of stable tearing that could occur was very limited, which means that the J R-curve is truncated and does not show the material behaviour at greater levels of tearing. This again may lead to a conservative assessment.

4 Notch Location

The specimens were notched through-thickness at the weld metal centre line.

The SENB specimens were tested at the minimum design temperature of -20°C in accordance with Part 4 of BS 7448:1997, using the multi specimen approach.

5 Fracture Toughness Test Results

Tensile test results and fracture toughness test results are presented in Tables H1 and H2. The results do not strictly qualify to BS 7448:1997 Part 4. For this reason, the results should be viewed as indicative. The main causes for the non-compliances are the small specimen size and the low material strength. The tearing resistance J R-curve calculated from the test results is given in Figure H1. All specimens taken past maximum load failed in a ductile manner.

Table H1 Tensile test results

	Specimen ID	0.2% yield strength (MPa)	0.5% yield strength (MPa)	UTS (MPa)
Shell Plate	M01-01	150.9	167.1	304.5
	M01-02	154.5	170.3	308.0
Weld Metal	W01-07	166.6	184.6	284.3
	W01-08	185.2	202.3	283.7

Table H2 SENB toughness test summary. The specimens were loaded to different levels and their results used to determine the material tearing resistance curve (Figure 1)

Specimen	Specimen dimensions, mm			Load	Δa	J_{corr}	δ_{corr}	Qualified
number	W	B	ao	kN	mm	kJ/m²	mm	to standard
W01-01	14.910	5.000	7.759	0.99	0.84	53.825	0.228	No
W01-02	14.900	5.080	7.679	1.03	0.14	17.655	0.074	No
W01-03	14.940	4.970	7.669	0.98	0.34	27.338	0.122	No
W01-04	14.920	5.040	7.698	1.03	0.44	40.565	0.173	No
W01-05	14.920	5.000	7.896	0.90	0.54	40.425	0.181	No
W01-06	15.020	5.010	7.791	0.94	0.74	44.509	0.213	No

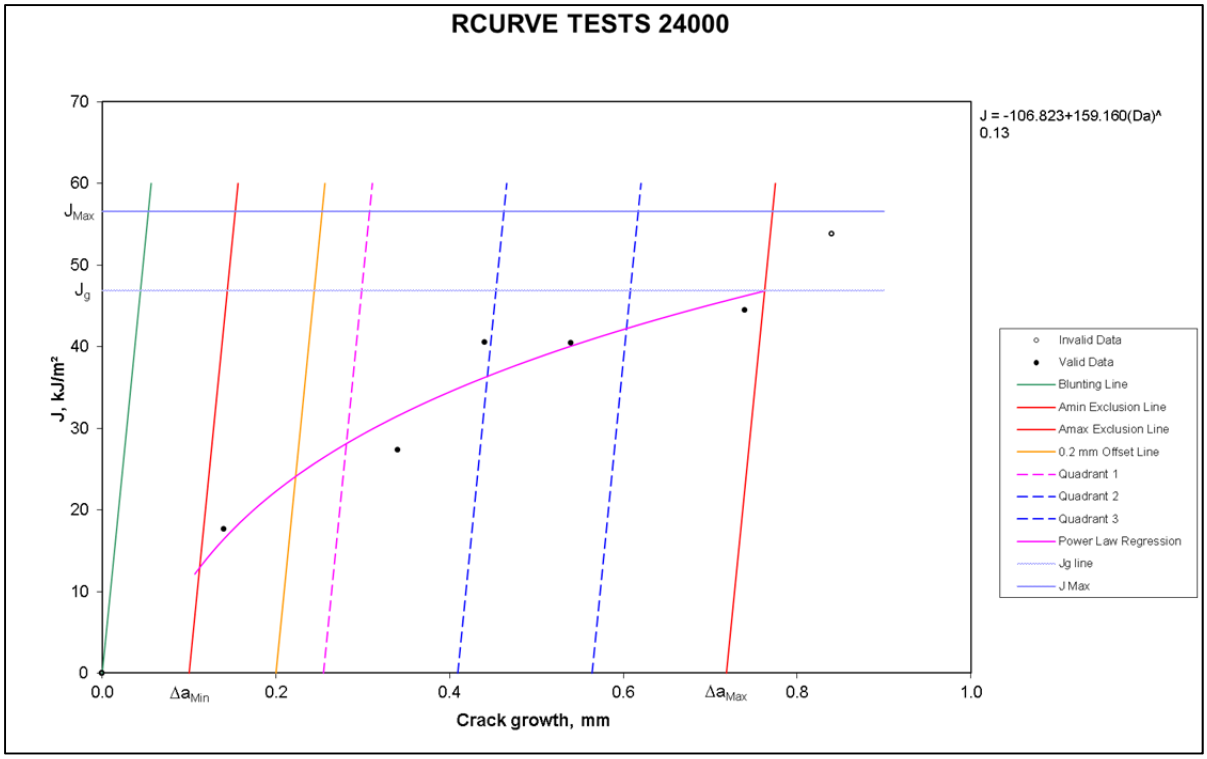

Figure H1 J R-Curve tearing resistance test result.